PMVictoriaESPPEm Resource

From: Jessie, Janelle
Sent: Thursday, May 13, 2010 10:57 AM
To: 'david.distel@exeloncorp.com'
Attachments: clinton SER.pdf

Janelle B. Jessie
Project Manager
U.S. Nuclear Regulatory Commission
Office of New Reactors
Division of New Reactor Licensing
NGE1 Projects Branch
301-415-6775
janelle.jessie@nrc.gov

God makes three requests of his children: Do the best you can, where you are, with what you have, now. Do not worry about tomorrow; for tomorrow will care for itself. Each day has enough trouble of its own.
----------African-American folklore

Hearing Identifier: Victoria_ESP_Public
Email Number: 71

Mail Envelope Properties (88EDD64608FA36499C5AED7AC8B78FB4CA7E37DDE0)

Subject:
Sent Date: 5/13/2010 10:56:56 AM
Received Date: 5/13/2010 10:56:00 AM
From: Jessie, Janelle

Created By: Janelle.Jessie@nrc.gov

Recipients:
"'david.distel@exeloncorp.com'" <david.distel@exeloncorp.com>
Tracking Status: None

Post Office: HQCLSTR01.nrc.gov

Files	**Size**	**Date & Time**
MESSAGE	543	5/13/2010 10:56:00 AM
clinton SER.pdf	8679405	

Options
Priority: Standard
Return Notification: No
Reply Requested: No
Sensitivity: Normal
Expiration Date:
Recipients Received:

2.5 Geology, Seismology, and Geotechnical Engineering

In Section 2.5, "Geology, Seismology, and Geotechnical Engineering," of the site safety analysis report (SSAR), the applicant described the geological, seismological, and geotechnical engineering properties of the early site permit (ESP) site. SSAR Section 2.5.1, "Site and Regional Geology," describes the basic geological and seismological data for the site and region surrounding the site. SSAR Section 2.5.2, "Vibratory Ground Motions," describes the vibratory ground motion for the ESP site through a probabilistic seismic hazard analysis (PSHA) and develops the safe-shutdown earthquake (SSE) ground motion. SSAR Section 2.5.3, "Surface Faulting," describes the potential for surface faulting at or near the surface of the ESP site. SSAR Section 2.5.4, "Stability of Subsurface Materials and Foundations," presents information on the stability of the ESP site's subsurface materials. SSAR Section 2.5.5, "Stability of Slopes," defers the analysis of slope stability to the combined license (COL) application. Similarly, SSAR Section 2.5.6, "Embankments and Dams," defers the reanalyses of the Clinton Power Station (CPS) ultimate heat sink (UHS) under the updated SSE to the COL application. Appendices A, "Geotechnical Report for the [Exelon Generation Company, LLC (EGC)] ESP," and B, "Seismic Hazard Report for the EGC ESP," to the SSAR provide further detail in support of each of the above sections.

Since the ESP site is located within 700 feet (ft) of the CPS site, the applicant stated in SSAR Section 2.5 that its starting point for the characterization of the geology, seismology, and engineering properties of the ESP site was the previous site investigations for the CPS site. As such, the material in Section 2.5 of the ESP application focuses on any newly published information since the publication of the CPS updated safety analysis report (USAR) in the 1970s, as well as recent geological, seismological, geophysical, and geotechnical investigations performed for the ESP site.

The applicant also used the seismic source and ground motion models published by the Electric Power Research Institute (EPRI) for the central and eastern United States (CEUS), "Seismic Hazard Methodology for the Central and Eastern United States," issued in 1986. As such, SSAR Section 2.5 focuses on those data developed since publication of the 1986 EPRI report. Regulatory Guide (RG) 1.165, "Identification and Characterization of Seismic Sources and Determination of Safe Shutdown Earthquake Ground Motion," issued March 1997, indicates that applicants may use the seismic source interpretations developed by Lawrence Livermore National Laboratory (LLNL) in the "Eastern Seismic Hazard Characterization Update," published in 1993, or the EPRI document as inputs for a site-specific analysis.

2.5.1 Site and Regional Geology

SSAR Section 2.5.1 describes the regional and site geology for the ESP site. The geologic settings of the region and the site are presented in Section 2.5.1.1, "Regional Geology," and in Section 2.5.1.2, "Site Geology," of the application, respectively. Additional descriptions of the regional and site geology are presented in Chapters 2 and 5 of SSAR Appendices A and B.

2.5.1.1 Technical Information in the Application

2.5.1.1.1 Regional Geology

SSAR Section 2.5.1.1 summarizes the regional geologic history and structural geology, with an emphasis on the Quaternary Period. Section 2.2 of SSAR Appendix A provides additional detail on the regional (1) physiography, (2) stratigraphy, and (3) structural geology. In addition, Section 2.1 of SSAR Appendix B provides a description of the regional (1) tectonic setting, (2) tectonic features, (3) prehistoric earthquakes, and (4) seismic sources. Finally, Attachment 1 to SSAR Appendix B describes the applicant's regional paleoliquefaction investigations. The applicant concluded that the ESP site is one of the most geologically stable areas in the United States and that the geologic conditions at the ESP site are the same as those at the CPS site.

Regional Physiography. The applicant described the regional physiography in Section 2.2.1 of SSAR Appendix A. The ESP site is located in the Till Plains section of the Central Lowland physiographic province. The terrain in central Illinois is typical of the province and consists of undulating, low-relief topography formed by the glacial drift cover, which ranges in thickness from a few tens of feet to several hundreds of feet. The applicant stated that much of the Till Plains section is characterized by landforms of low, commonly arcuate ridges, called moraines, interspersed with relatively flat intermorainal areas. The development of postglacial streams has led to the dissection of the glacial drift mantle and in some areas bedrock is exposed; however, there are no bedrock exposures near the site area.

Regional Geologic History and Stratigraphy. The applicant described the Quaternary geologic history and stratigraphy in SSAR Section 2.5.1.1 and Section 2.2.2 of SSAR Appendix A. During the Quaternary (mainly Pleistocene time), continental glaciation left widespread glacial deposits in the regional area. There were four major episodes of glaciation in the region, which from the youngest to the oldest are the Wisconsinan, Illinoian, Kansan, and Nebraskan. Wisconsinan deposits are found throughout the ESP site, and Illinoian deposits are present beyond the limit of Wisconsinan deposits in northern and central Illinois. Kansan- and Nebraskan-age glacial deposits are present at the surface and in the subsurface in areas of Iowa, Missouri, and part of western and east-central Illinois. These Quaternary deposits consist predominantly of glacial or glacial-derived sediments of glacial till, outwash, loess (a windblown silt), and glacialacustrine deposits, as well as alluvium.

Regional Structural Geology. The applicant described the structural geology in SSAR Section 2.5.1.1 and Section 2.2.3 of SSAR Appendix A. The Quaternary glacial deposits in the region are underlain by thick sequences of gently dipping Paleozoic sedimentary rocks. The bedrock surface throughout Illinois is of Paleozoic age, and the Paleozoic rocks are relatively thicker at the centers of the structural basins, such as the Illinois basin. During Paleozoic sedimentation, several discontinuations of regional importance occurred because of the widespread advances and retreats of the Paleozoic seas across the interior of North America. At a depth of about 2,000 to 13,000 ft below the ground surface, the basement complex of the Precambrian igneous and metamorphic rocks underlies the Paleozoic rocks. Throughout the Paleozoic era, the area underwent intermittent slow subsidence and gentle uplift, which resulted in broad regional geologic basins of gently dipping sedimentary rocks and intervening broad arches or highs. Locally, folds and faults are superimposed on this pattern.

Regional Tectonic Setting. The applicant described the tectonic setting in Section 2.1.1 of SSAR Appendix B. The ESP site is located within the Illinois basin in the stable continental region (SCR) of the North American craton. The Illinois basin is a spoon-shaped depression, covering parts of Illinois, Indiana, and Kentucky. The basin is bounded on the north by the Wisconsin arch, on the east by the Kankakee and Cincinnati arches, on the south by the Mississippi embayment, and on the west by the Ozark dome and Mississippi River arch. The east-west-trending Rough Creek-Shawneetown fault system divides the Illinois basin into two unequal parts. The northern part of the Illinois basin is larger but shallower, a typical cratonic depression with basement elevations ranging from approximately 2,950 ft below sea level in the northern part of the basin to 14,100 ft below sea level in southeastern Indiana. In the northern part of the basin, Paleozoic sedimentary strata overlie the Proterozoic-age basement rocks of the Eastern Granite-Rhyolite Province. The southern part of the Illinois basin is relatively smaller but deeper, with about 23,000 ft of Paleozoic sedimentary rocks. The southern part of the basin is underlain by portions of the Reelfoot rift and Rough Creek graben, which is a rift system that formed during late Precambrian to middle Cambrian time (800 to 500 million years ago (mya)).

The applicant stated that the ESP site lies within a compressive midplate stress province characterized by a relatively uniform compressive stress field with a maximum horizontal stress oriented northeast to east-northeast. However, within this relatively uniform stress field, the applicant cited recent studies that show a geographic shift from an east-west maximum horizontal compressive stress at the latitude of the New Madrid seismic zone (NMSZ) to a stress that trends just north of east in southern Illinois and Indiana.

Regional Tectonic Features. Section 2.1.2 of SSAR Appendix B describes the major geologic structures (folds, faults, and lineaments) in the region surrounding the ESP site as follows:

- folds
  - La Salle anticlinorium
  - Peru monocline
  - Du Quoin monocline
  - Louden anticline
  - Waterloo-Dupo anticline
  - Farmington anticline-Avon block
  - Peoria folds
- faults
  - Sandwich fault zone
  - Plum River fault zone
  - Centralia fault zone
  - Rend Lake fault zone
  - Cap au Gres faulted flexure
  - St. Louis fault
  - Eureka-House Springs structure
  - Ste Genevieve fault zone
  - Simms Mountain fault system
  - Bodenschatz-Lick fault system

- Cape Girardeau fault system
- Wabash Valley fault system (WVFS)
- Fluorspar Area fault complex (FAFC)
- Rough Creek graben faults
- Cottage Grove fault system

• lineaments

- Commerce geophysical lineament (CGL)
- St. Charles lineament
- South-Central magnetic lineament

Among the above-mentioned geologic features, the structures discussed below are described by the applicant as either (1) coinciding with recorded earthquake trends, (2) characterized by Quaternary deformation, or (3) attributed as potential sources of paleoliquefaction during the Quaternary. Many of these geologic features are shown below in Figure 2.5.1-1, reproduced from Figure 2.1-3 in Appendix B to the SSAR.

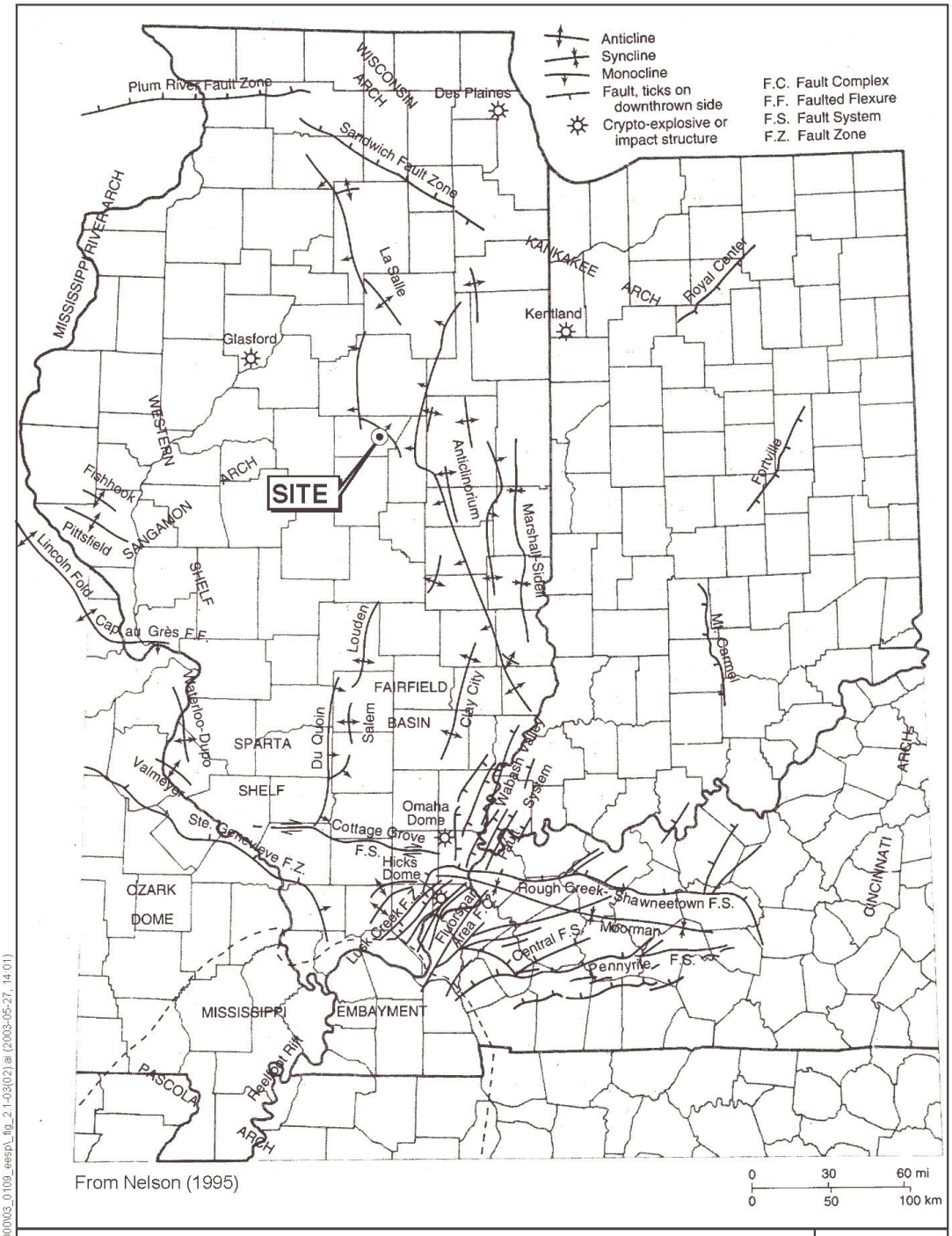

Seismic Hazards Report for the EGC ESP Site

Major Structural Features in Illinois and Neighboring States

Figure **2.1-3**

s:\7900\793557935.000\003_0109_eesp_fig_2.1-03(02).ai (2003-05-27, 14:01)

Figure 2.5.1-1 Major structural features in Illinois and neighboring States

Folds

The regional folds that the applicant considered to be potential Quaternary features are the (1) Peru monocline, (2) Du Quoin monocline, (3) Waterloo-Dupo anticline, and (4) Farmington anticline-Avon block.

The Peru monocline is a 65-mile-long northwest trending fold belt in which the rocks dip steeply to the southwest into the Illinois basin. The distance between the Peru monocline and the ESP site is about 50 to 55 miles. Three earthquakes occurring in September 1972 (body wave magnitude (m_b) 4.6), September 1999 (m_b 3.5), and possibly May 1881 (magnitude unknown) are assumed to be related to this structure, and, as such, the applicant concluded that the Peru monocline may be a reactivated Paleozoic structure.

The Du Quoin monocline, which is located about 90 to 100 miles south of the ESP site, is a north-south trending structure, which warps Paleozoic strata downwards on its eastern flank. Normal faults of the Dowell and Centralia fault zones are coincident with the dipping flank of the Du Quoin monocline. The applicant cited research that postulates that the Centralia fault zone represents extensional activation of the basement structure beneath the Du Quoin monocline, and these two structures may connect at depth. The Du Quoin monocline and related Centralia fault zone are considered as a potential source for an earthquake that produced middle Holocene paleoliquefaction features in southwestern Illinois and southeastern Missouri.

The Waterloo-Dupo anticline, which is located about 130 miles southwest of the ESP site, is a north-northwest-trending, asymmetrical anticline that may be a southern continuation of the Cap au Gres faulted monocline, located in Missouri and Illinois. The applicant stated that the Waterloo-Dupo anticline may be the seismic source for the paleoliquefaction features in eastern Missouri.

The Farmington anticline-Avon block is a broad (as much as 12 miles wide), northwest-trending, low-relief structure. Weak to moderate seismicity is clustered around this structure, which is located about 170 miles south of the ESP site.

Faults

The regional faults and fault zones that the applicant considered to be potential Quaternary features are the (1) Centralia fault zone, (2) St. Louis fault, (3) Ste Genevieve fault zone, (4) WVFS, and (5) FAFC.

The Centralia fault zone is a north-trending structure zone, composed of normal faults that dip 70° to 75° toward the west, with a consistent displacement of 100 to 160 ft for strata from the upper Mississippian to Ordovician periods. The fault zone is located about 100 miles south of the ESP site. The applicant stated that earthquakes with strike-slip focal mechanisms located near the structural axis of the Centralia fault are probably associated with the Du Quoin monocline.

The St. Louis fault, which is located about 130 miles from the ESP site, is a northeast-trending fault located along the border between Missouri and Illinois. The applicant cited recent studies which show that the St. Louis fault (1) appears to offset the Waterloo-Dupo anticline in the right-

lateral sense, and (2) is considered as a possible candidate for the paleoearthquake features found in eastern Missouri.

The Ste Genevieve fault zone, which is located about 165 miles south of the ESP site, extends for approximately 120 miles along strike from southeast Missouri into southwest Illinois. The fault zone consists of numerous en echelon strands (separate faults having parallel but steplike trends) and braided segments with variable deformation styles and a complex history of reactivation. Diffuse seismicity occurs in the block between the Ste Genevieve fault zone and Simms Mountain fault system, located in southeast Missouri, but the applicant stated that no documented evidence for Quaternary deformation or paleoliquefaction has been observed in the area.

The WVFS is a major zone of northeast-trending, high-angle normal and strike-slip faulting bordering Illinois, Kentucky, and Indiana. The fault system is about 55 to 60 miles long and as much as 30 miles wide; the closest point of the fault system is about 130 miles from the ESP site. The predominant normal movement along the fault system is post-Late Pennsylvanian with a vertical offset of about 480 ft. The applicant cited studies that suggest that the WVFS most likely developed in the early Permian by reactivation of a Precambrian rift zone that was the northern extension of Reelfoot rift. The WVFS is located inside the Wabash Valley/Southern Illinois seismic zone (WVSZ), a potential source for abundant paleoliquefaction features in the region.

The FAFC includes the faults that bound the grabens and horsts within the Fluorspar mining district. The nearest point of the fault complex is about 175 miles from the ESP site. The FAFC is predominately a normal fault with dip-slip as much as 2460 ft. The applicant cited the results of shallow drilling, trenching, outcrop mapping, and seismic reflection acquisition in southern Illinois that show evidence for Quaternary-age faulting on the FAFC in the northern Mississippi embayment.

Lineaments

Of the three regional lineaments, the applicant only considered the CGL to be a potential Quaternary feature.

The CGL is a northeast-trending basement magnetic and gravity anomaly that extends from northeast Arkansas to at least Vincennes, Indiana (more than 240 miles). The CGL is a significant, continental-scale linear feature that is apparent in topography, geophysical data, and remote sensory imagery. Quaternary deformation and paleoliquefaction have been associated with the CGL at several sites. These sites are all located inside the WVSZ, which is described below. Well-developed northeast- to north-northeast-trending strike-slip faults, which have a long-lived tectonic history, including Pleistocene and Holocene, occur over the lineament. In addition, the applicant noted that about 16 earthquakes with magnitudes of m_b 3.0 to 5.5 have occurred on or near the lineament.

<u>Regional Seismic Sources</u>. Section 2.1.5 of SSAR Appendix B describes the regional seismic sources. Rather than characterizing the seismic potential of each of the above regional tectonic features, the applicant used the EPRI-Seismicity Owners Group (SOG) seismic hazard study, which groups these potential sources into large areal seismic source zones. Within a 200-mile radius of the site (or just beyond), the three major sources of potential earthquakes are (1) the

NMSZ, (2) the WVSZ in southern Illinois and southern Indiana, and (3) the central Illinois basin/background source. A summary of each of these three seismic source zones is presented below.

New Madrid Seismic Zone

The New Madrid region was the location of three earthquakes in 1811–1812, which are the largest historical earthquakes in the CEUS. Estimates of the magnitudes of these three events generally range between 7.3 and 8.3. The northern boundary of the source region for New Madrid earthquakes is generally considered to lie at or just beyond the 200-mile radius of the ESP site. The NMSZ extends about 150 miles from northeastern Arkansas into western Tennessee and southwestern Kentucky. The applicant summarized the results of several geological, geophysical, and seismological studies, which have been conducted to characterize the location and extent of the likely causative faults of each of these earthquakes and to assess the maximum magnitude and recurrence of earthquakes in this region. Figure 2.5.1-2, reproduced from Figure 2.1-21 in Appendix B to the SSAR, shows a schematic diagram of the NMSZ, including areas of modern seismicity and the locations of liquefaction features.

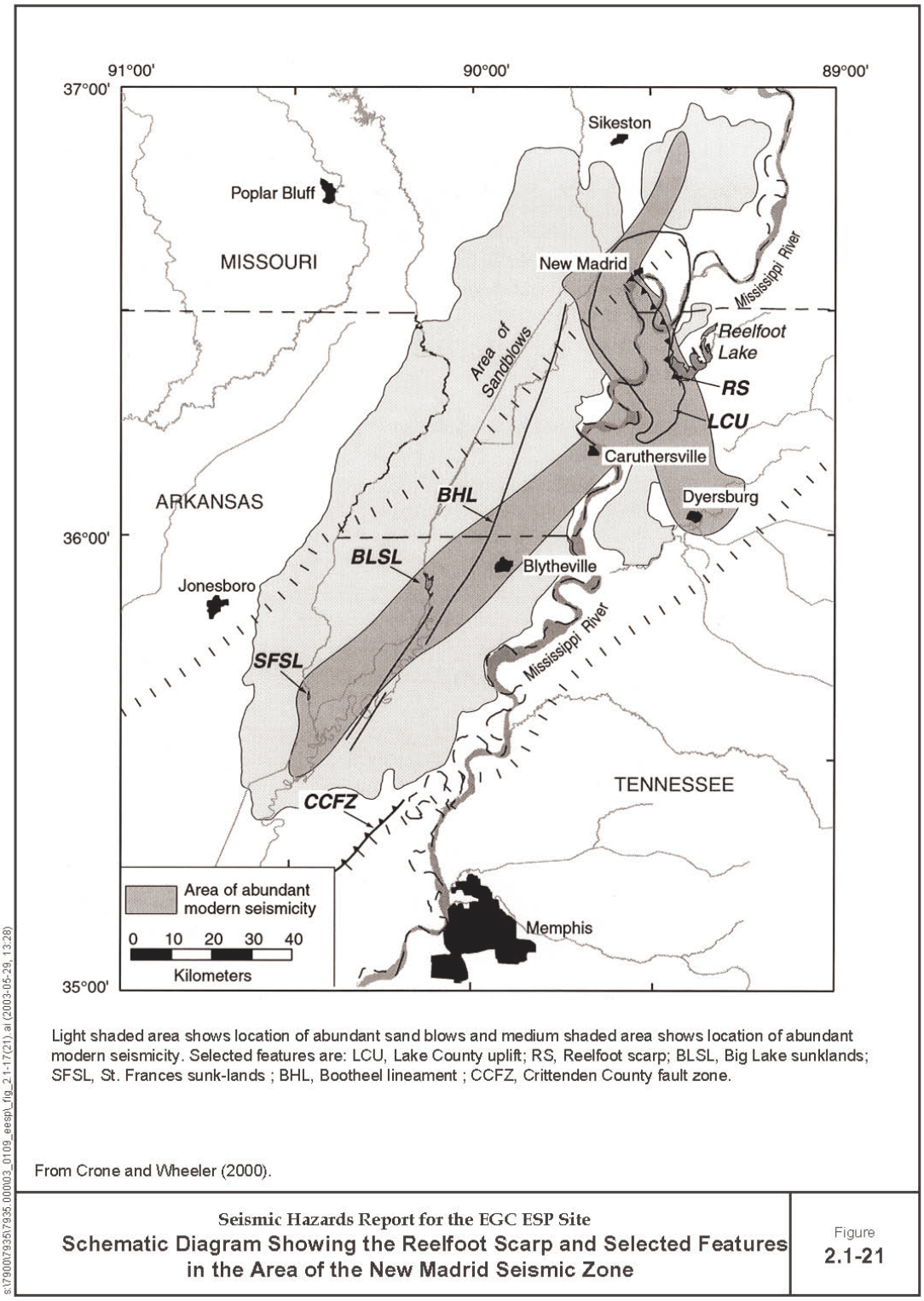

Light shaded area shows location of abundant sand blows and medium shaded area shows location of abundant modern seismicity. Selected features are: LCU, Lake County uplift; RS, Reelfoot scarp; BLSL, Big Lake sunklands; SFSL, St. Frances sunk-lands ; BHL, Bootheel lineament ; CCFZ, Crittenden County fault zone.

From Crone and Wheeler (2000).

Seismic Hazards Report for the EGC ESP Site
Schematic Diagram Showing the Reelfoot Scarp and Selected Features in the Area of the New Madrid Seismic Zone

Figure 2.1-21

s:\7900\7935\7935.000\03_0109_eesp_f\q_2.1-17(21).ai (2003-05-29, 13:28)

Figure 2.5.1-2 Schematic diagram showing the Reelfoot scarp and selected features in the area of the NMSZ

In Request for Additional Information (RAI) 2.5.1-1, the staff asked the applicant to clarify its magnitude estimates for the three 1811–1812 New Madrid earthquakes. In response, the applicant updated its magnitude estimates to include the latest research findings. Section 2.5.1.3.1 of this safety evaluation report (SER) provides further detail on the applicant's response to RAI 2.5.1-1 and the staff's evaluation of the applicant's response.

Seismicity within the New Madrid region is generally located along the Reelfoot rift, which is an ancient failed rift zone that has its long axis oriented to the northeast and runs parallel to the CGL. The applicant cited research which postulates a time-dependent model for the generation of repeated intraplate earthquakes that incorporates a weak lower crustal zone within an elastic lithosphere. According to this model, relaxation of this weak zone in the lower crust after tectonic perturbations (i.e., the recession of glacial ice sheets from central North America 14,000 years ago) transfers stress to the upper crust, triggering slip on overlying faults and generating a sequence of earthquakes that continues until the weak zone reaches its fully relaxed state. Coseismic slip, in turn, partially reloads the lower crust, causing cyclic stress transfer, which prolongs the relaxation process. The applicant stated that this source model is consistent with earthquake magnitude, coseismic slip, recurrence intervals, and surface deformation rates in the NMSZ. The applicant stated that this model is also supported by studies that show that the removal of the Laurentide ice sheet approximately 20,000 years ago changed the stress field in the vicinity of New Madrid, causing seismic strain rates to increase by about three orders of magnitude. This modeling predicts that the high rate of seismic energy release observed during the late Holocene time is likely to continue for the next few thousand years.

The principal seismic activity within the upper Mississippi embayment is interior to the Reelfoot rift along the NMSZ. The NMSZ consists of three principal trends of seismicity—two northeast-trending arms with a connecting northwest-trending arm. The NMSZ is considered to be a northeast-trending, right-lateral strike-slip fault system with a compressional left-stepover zone. Earthquakes in the NMSZ are produced by a network of intersecting faults. The applicant identified the following fault segments within the NMSZ:

- Blytheville arch (BA)
- Blytheville fault zone
- Bootheel lineament
- New Madrid west
- New Madrid north (NN)
- Reelfoot fault (RF)
- Reelfoot south

Each of these fault segments is shown in Figure 2.1-22 of SSAR Appendix B and reproduced below as SER Figure 2.5.1-3.

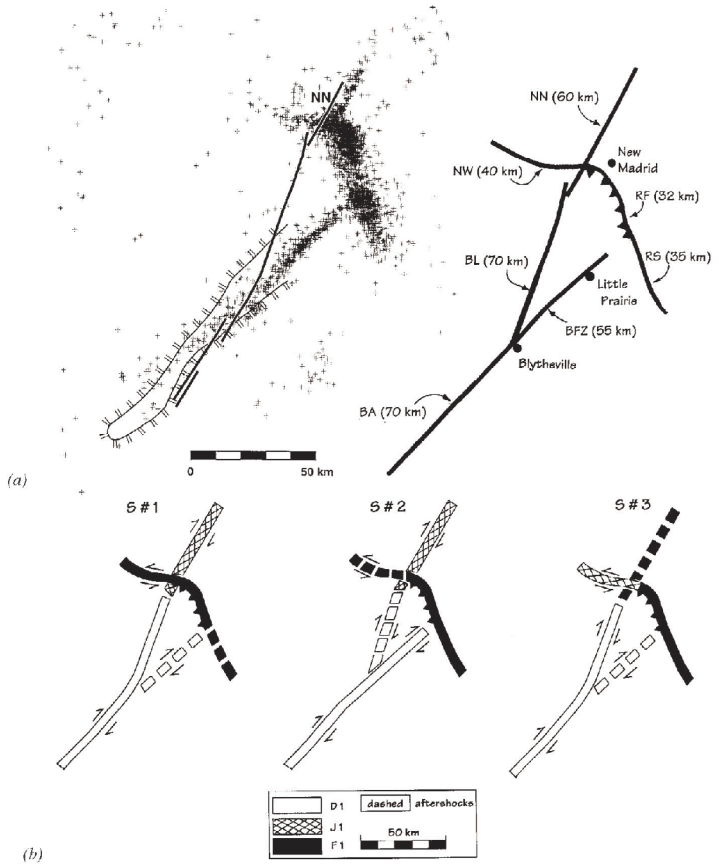

(*a*) Fault segmentation of the NMSZ. Seismicity of the NMSZ, the Blytheville arch, and the Bootheel lineament/NN fault (*left*) yield the seven segments (*right*) identified as: BA, Blytheville arch; BFZ, Blytheville fault zone; BL, Bootheel lineament; NW, New Madrid west; NN, New Madrid north; RF, Reelfoot fault; RS, Reelfoot south. Segments NW and RS are defined solely from seismicity.

(*b*) Possible fault rupture scenarios (S#1, S#2, S#3) for the 1811-1812 D1, J1, and F1 earthquake sequences, using the seven fault segments of (*a*). Based on historical and physical constraints, the D1 principal event must rupture BA, and the F1 principal event must rupture RF in all scenarios. S#1 is the favored scenario.

From Johnston and Schweig (1996)

s:\7900\7935\7935.000\03_0109_eess_fig_2.1-16.ai (2003-05-29, 13:29)

Seismic Hazards Report for the EGC ESP Site
Central Fault System of New Madrid Seismic Zone

Figure
2.1-22

Figure 2.5.1-3 Central fault system of NMSZ

Based on historical accounts and geologic evidence, geologists have postulated that the December 16, 1811, earthquake occurred primarily along the BA, which is the southernmost fault segment. Similarly, geologists have concluded that the causative fault for the January 23, 1812, earthquake is along the NN fault segment, and the February 7, 1812, earthquake occurred on the RF, which connects the two other fault zones through the stepover region.

Geologists have determined the maximum earthquake potential of the NMSZ based largely on the analysis of damage-intensity data and liquefaction features from the 1811–1812 earthquake sequence. The applicant found that recent analyses favor lower magnitudes (7.5 to 8.0) for the NMSZ, suggesting that site effects and population distribution biased earlier interpretations, which postulated higher magnitudes (7.8 to 8.4). To determine the recurrence interval for the maximum earthquakes in the NMSZ, geologists have used paleoliquefaction studies and the evaluation of fault-related deformation along the Reelfoot scarp. The applicant cited paleoliquefaction events with dates of AD 1450 ± 150, AD 900 ± 100, AD 490 ± 50, AD 300 ± 200, and BC 1370 ± 970, based on its review of the literature. As such, the applicant concluded that the occurrence interval of a New Madrid-type earthquake may have been as short as 200 years or as long as 800 years, with an average of about 500 years.

Wabash Valley/Southern Illinois Seismic Zone

The WVSZ is located in southeastern Illinois and southwestern Indiana to the northeast of the NMSZ. The WVSZ is a zone of moderate seismicity, with the strongest event (moment magnitude (M_w) 5.4) occurring in 1968 in southern Illinois. Other notable recent events occurring in the WVSZ include a magnitude 5.0 earthquake near Lawrenceville, Illinois, in 1987 and a magnitude 4.5 earthquake in 2002 near Evansville, Indiana. Much larger earthquakes have occurred in the WVSZ during the past 10,000 years. The applicant cited research that demonstrates, based on paleoliquefaction data, the existence of repeated large-magnitude (M_w 7.0 to 7.8) earthquakes in the Wabash Valley region. The applicant stated that the causative structure for these earthquakes may be basement thrust faults beneath the Illinois basin that coincide with an area of broad flexure in the CGL. The location of the 1968 M_w 5.4 earthquake in southern Illinois supports this hypothesis. Figure 2.5.1-4, reproduced from Figure 2.1-14 in SSAR Appendix B, shows the historical seismicity and estimated centers of the large prehistoric earthquakes in the WVSZ.

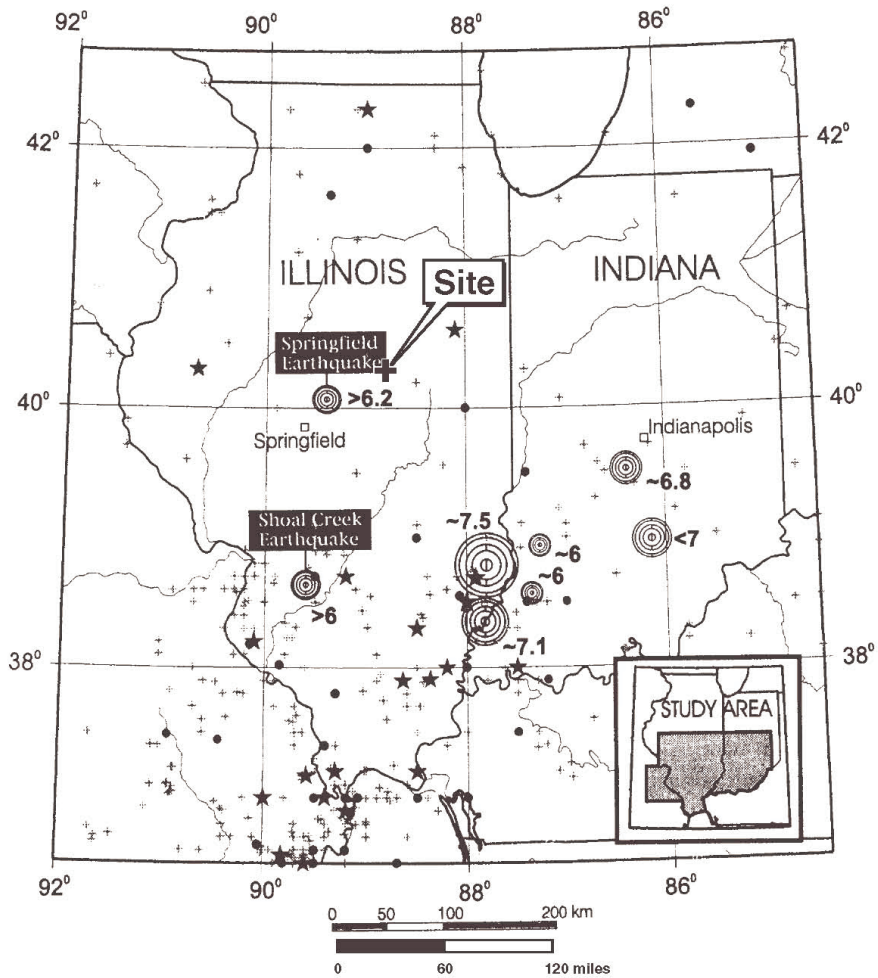

A star represents a magnitude of 5 or higher. A solid circle represents a magnitude between 4.5 and 5. A plus sign represents a magnitude between about 2.3 and 4.5. Historical earthquake data are from USGS/NEIC Global Hypocenter Data Base CD-ROM (Version 3.0). Concentric circles show estimated energy centers of large prehistoric earthquakes. The estimated moment magnitude, M, for a prehistoric earthquake is located near the circle.

Note:
Epicenters of historical earthquakes are shown for the time period 1804-1992

From McNulty and Obermeier (1999)

S:\7900\7935\7935.000\03_0109_eesp_fig_2.1-10(02).ai

Seismic Hazards Report for the EGC ESP Site
Historical Seismicity and Estimated Centers of Large Prehistoric Earthquakes in Site Region

Figure
2.1-14

Figure 2.5.1-4 Historical seismicity and estimated centers of large prehistoric earthquakes in site region

The applicant stated that the maximum-magnitude distribution for the WVSZ is based on the analysis of paleoliquefaction features in the vicinity of the lower Wabash Valley of southern Illinois and Indiana. The applicant cited research showing that the largest paleoearthquake occurred 6101 ± 200 years ago with an estimated M_w range between 7.0 to 7.5. The next largest earthquake occurred 12,000 ± 1,000 years ago with an estimated magnitude between 7.1 to 7.3. Both of these earthquakes occurred close to one another in the lower Wabash Valley of Indiana and Illinois.

Central Illinois Basin/Background Source

In addition to the NMSZ and WVSZ, evidence from recent paleoliquefaction studies and seismic reflection data show that significant earthquakes may occur in parts of the central Illinois basin where there are no obvious folds or faults at the surface. The applicant stated that the location, size, and recurrence of such events are not well constrained by available data. However, because of the paleoliquefaction evidence, the applicant has developed a background source zone for this region. The central Illinois basin/background source covers the area to the west and north of the WVSZ and encompasses the ESP site. The applicant stated that one or two prehistoric earthquakes may have occurred near Springfield, Illinois, approximately 35 miles southwest of the ESP site (see SER Figure 2.5.1-4 above) between about 5900 to 7400 years ago. These earthquakes were apparently large enough to generate liquefaction features, with magnitude estimates ranging between 6.2 and 6.8. The applicant was unable to associate the Springfield earthquakes with any known geologic structure or local seismic activity. In addition to the Springfield events, the applicant stated that additional liquefaction features were discovered further south near the confluence of the Shoal Creek and Kaskaskia River. The estimated magnitude and date for this event is about 6.0 and 5700 before present (BP).

To further characterize the seismic potential of the central Illinois basin/background source, the applicant investigated the banks of several streams (Sangamon River, Salt Creek, North Fork of Salt Creek, and the Mackinaw River) near the ESP site for evidence of liquefaction features resulting from strong ground motion. These paleoliquefaction investigations are described in Attachment 1 to SSAR Appendix B. Figure 2.5.1-5, reproduced from Figure B-1-6 in Attachment 1 to SSAR Appendix B, shows the streams that the applicant surveyed during its paleoliquefaction reconnaissance.

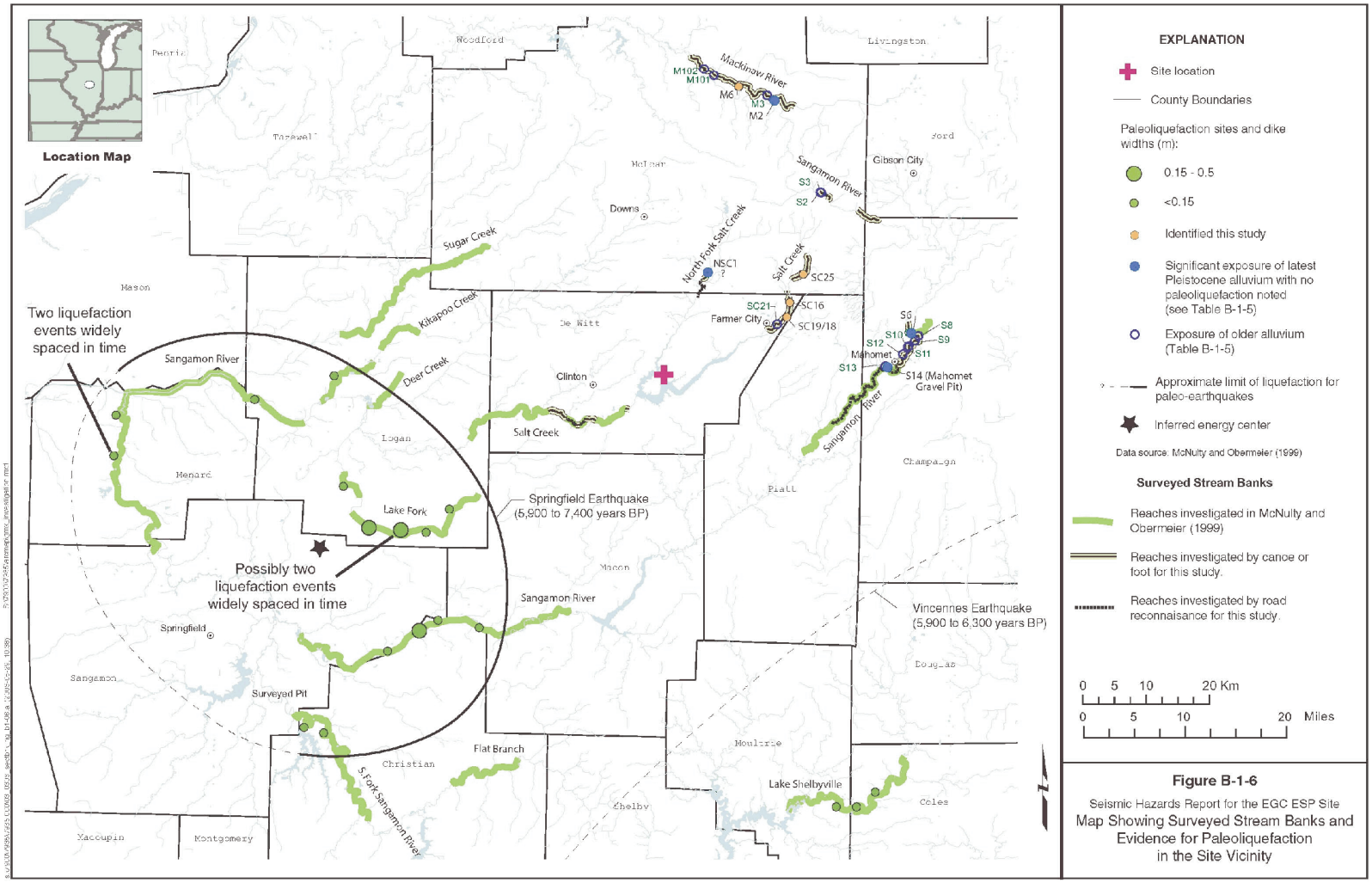

Figure 2.5.1-5 Map showing surveyed stream banks and evidence for paleoliquefaction in the site vicinity

Although the applicant discovered some small liquefaction features, which suggest possible local seismic sources, the applicant stated that these features could also be related to more distant sources, such as the WVSZ or NMSZ. The applicant concluded by stating the following:

> Given the low rate of historical seismicity in this region, the apparent long recurrence between events suggested by the paleoliquefaction data, and the lack of clearly defined seismogenic structures close to the inferred energy centers, it is unlikely that distinct seismic sources can be defined for these paleoliquefaction events.

For the central Illinois basin/background source, the applicant stated that the results of its paleoliquefaction investigations show that there have not been repeated moderate to large events, comparable to the magnitude (M) 6.2 to 6.8 Springfield earthquake in the vicinity of the ESP site, in the late Holocene time (approximately 6 to 7 thousand years). However, because of the uncertainty in the paleoliquefaction data, the applicant stated that the range in maximum magnitude assigned to a random earthquake in the background source should include events comparable to that estimated for the Springfield earthquake.

In RAI 2.5.2-6, the staff asked the applicant to explain its selected paleoliquefaction study area along the streams near the ESP site. Specifically, the staff asked the applicant why it did not examine the streams northwest and southeast of the site as part of its study. In response, the applicant stated that it selected its study area to supplement previous liquefaction studies along portions of the Sangamon River, portions of Salt Creek, and similar drainages west and northwest of the site. SER Section 2.5.1.3.1 provides further detail on the applicant's response to RAI 2.5.2-6 and the staff's evaluation of the applicant's response.

In RAI 2.5.1-4, the staff asked the applicant to provide better annotated photographs of the liquefaction features found along the Salt Creek. In response, the applicant provided photographs that clearly indicate the locations of the sand dikes. In RAI 2.5.1-5, the staff asked the applicant to substantiate the reliability of its methods to determine the size and location of paleoearthquakes based on liquefaction features. In response, the applicant demonstrated how it used the paleoliquefaction data and analyses to characterize the regional and local seismic potential of these paleoearthquake centers. SER Section 2.5.1.3.1 provides further detail on the applicant's response to RAIs 2.5.1-4 and 2.5.1-5 as well as the staff's evaluation of these responses.

2.5.1.1.2 Site Geology

SSAR Section 2.5.1.2 summarizes the local geologic history and structural geology, with an emphasis on the Quaternary Period. Section 2.2 of SSAR Appendix A provides additional detail on the local (1) physiography, (2) stratigraphy, and (3) structural geology. In addition, Chapter 5 of SSAR Appendix A provides a description of the site ground water conditions and other geologic considerations, such as potential topographic depressions caused by karst terrain and mine subsidence. Chapter 5 of SSAR Appendix A also describes regional natural gas production and oil fields, ground water springs, landslides, and the overall geologic suitability.

<u>Site Physiography</u>. The ESP site lies within the Bloomington Ridged Plain physiographic subsection of the Till Plains physiographic section in Central Illinois. The site is located in an

upland area ground moraine that is dissected by the Salt Creek and the North Fork of the Salt Creek. The local relief of the uplands is about 10 ft, except near the drainage ways, and the average elevation of the uplands is approximately 740 ft above mean sea level (msl). The applicant concluded that the physiography of the ESP site is the same as that of the CPS site.

Site Stratigraphy. The ESP site is located a few miles inside the extent of the Wisconsinan glaciation. The surface deposits in the upland site area consist of a thin layer of loess (silt with some fine sand) over glacial till. Other stratigraphic units beneath the glacial till include organic silt, under which lie glacial till deposits of the Illinoian Stage and pre-Illinoian Stage. Bedrock in the vicinity of the ESP site is from the Bond and Modesto formations, which generally consist of alternating bands of limestone, shale, siltstone, sandstone, and some coal seams. At the base of the Bond formation is a layer of limestone, which corresponds to the top of the Modesto formation (495 ft above msl). The applicant concluded that the site stratigraphy across the ESP and CPS sites is very similar in terms of soil consistency and layering. The primary difference between the two sites is that the depth to bedrock is approximately 50 ft deeper at the ESP site than at the CPS site.

Site Structural Geology. The ESP site is located in a tectonically stable area of North America. The applicant stated that although the ESP site is within several miles of structural features, there is no evidence of surface faulting at the site or the area surrounding the site within a 25-mile radius. In addition, the applicant stated that no evidence of faulting was observed based on interpretations of borehole data at the ESP and CPS sites, excavations for CPS, or during geologic reconnaissance for this study. The applicant found that although differences in bedrock unit elevations can be attributed to structural deformation, the relatively flat-lying and undeformed Pleistocene drift overlying the bedrock demonstrates that the stresses that would have been responsible for the deformation have been inactive since at least Illinoian time (~ 185 to 128 ka). The applicant concluded that its understanding of the CPS and ESP site structural geology and geologic history has not changed since the geology work done for the CPS site.

Site Ground Water Conditions. The applicant found that the ground water elevations at the ESP site are consistent with those of the CPS site. As indicated by the ESP site piezometers, the ground water generally exists in a perched water table condition a few feet below the ground surface in the shallow Wisconsinan till soils. A downward gradient of about 20 ft in the ground water elevation was observed by the applicant across the ESP site. SSAR Section 2.4.13.2, “Sources,” presents a detailed discussion of the hydrogeologic conditions at the ESP site.

Other Geologic Conditions. Chapter 5 of SSAR Appendix A covers additional geologic conditions that the applicant investigated as part of its ESP application. These additional geologic conditions include (1) karst terrain, (2) mine subsidence, (3) natural gas production and oil fields, (4) ground water springs, (5) landslides, and (6) overall geologic suitability.

Karst terrain includes topographic depressions (sinkholes), caves, large springs, fluted rocks, blind valleys, and swallow holes that develop in areas of high rock solubility and permeability. These features have the potential to affect the foundation support for buildings and other structures. The applicant stated that the Illinois State Geologic Survey (ISGS) identified some areas in Illinois that are susceptible to karst development; however, the ISGS assessment of DeWitt County found no susceptibility.

Mine subsidence is the sinking of the ground surface after the collapse of an underground mine, which can damage overlying structures. Although ISGS has identified areas susceptible to mine subsidence in Illinois, the applicant found no historic mines in DeWitt County. As such, the applicant concluded that there is no potential for mine subsidence at the ESP site.

Natural gas production from organic matter in deep valleys filled with glacial material has occurred in Illinois since the early 1900s. Five gas-producing wells are located in the western part of DeWitt County; however, the applicant did not identify any wells near the ESP or CPS sites and concluded that the occurrence of gas-producing strata is not a concern. The applicant did note the locations of two oil-well fields, more than 4 miles northeast of the CPS site, and concluded that they do not pose a hazard to the ESP site.

The Weldon Springs State Recreation Area is located about 5 miles southwest of the ESP site. This spring originates in the near-surface Wisconsinan silty sands and gravels and discharges to a small lake in the recreation area. The applicant stated that the recreation area will not be impacted by ground water extraction activities in the ESP site because the ground water springs are hydraulically separated from the ESP site by Clinton Lake and Salt Creek.

The applicant used the ISGS landslide potential map for Illinois to determine that the landslide potential for DeWitt County is low. The only slopes near the ESP site are those associated with Clinton Lake. These slopes are located approximately 800 ft northwest of the ESP site. The applicant stated that they have been very stable for the past 30 years, and therefore landsliding does not pose a hazard. In addition, the applicant concluded that the distance between the ESP site and the slopes is such that, if landsliding were to occur, it would not extend to the ESP site. The applicant stated that further slope stability studies may be necessary during the COL stage in the area of the outfall pipe, if a new outfall is constructed. At the ESP stage, the applicant stated that it has not yet determined the need for an outfall.

Regarding the overall geologic suitability, the applicant stated that the surficial materials present few serious problems to construction. The most common problem is poor drainage caused by the relatively flat, dense glacial deposits.

2.5.1.2 Regulatory Evaluation

SSAR Section 2.5.1 presents information on the geological characteristics of the ESP site region and area. The applicant stated that SSAR Section 2.5.1 addresses Title 10 of the *Code of Federal Regulations* (10 CFR), Part 52, “Early Site Permits; Standard Design Certifications; and Combined Licenses for Nuclear Power Plants,” and 10 CFR Part 100, “Reactor Site Criteria.” SSAR Sections 3.4.1 and 3.4.2 describe the applicant’s compliance with the geological and seismological requirements of 10 CFR 100.21, “Non-seismic Siting Criteria,” and 10 CFR 100.23, “Geologic and Seismic Siting Criteria,” respectively. In addition, in response to RAI 1.5-1, the applicant stated that it complied with all of the regulations listed in Review Standard (RS)-002, “Processing Applications for Early Site Permits,” for each of the pertinent SSAR sections. This statement by the applicant implies that SSAR Section 2.5.1 conforms with the requirements of General Design Criterion (GDC) 2, “Design Bases for Protection Against Natural Phenomena,” in Appendix A, “General Design Criteria,” to 10 CFR Part 50, “Domestic Licensing of Production and Utilization Facilities.” In SSAR Section 1.5, “USNRC Regulatory Guides,” the applicant provided a list of the RGs that it used in developing each of the SSAR sections. For SSAR Section 2.5.1, the applicant listed RG 1.132, “Site Investigations for

Foundations of Nuclear Power Plants," and RG 1.165. The staff reviewed this portion of the application for conformance with the regulatory requirements and guidance applicable to the geological and seismological characterization of the proposed site, as identified below. The staff notes that GDC 2 applies to this portion of the review of an ESP application only with regard to consideration of the most severe natural phenomena reported for the site (in this case earthquakes), including margin.

In reviewing the SSAR, the staff considered the regulations at 10 CFR 52.17(a)(1)(vi) and 10 CFR 100.23(c), which require that the applicant for an ESP describe the seismic and geologic characteristics of the proposed site. In particular, 10 CFR 100.23(c) requires that an ESP applicant investigate the geological, seismological, and engineering characteristics of the proposed site and its environs with sufficient scope and detail to support evaluations to estimate the SSE ground motion and to permit adequate engineering solutions to actual or potential geologic and seismic effects at the site. Section 2.5.1 of NUREG-0800, "Standard Review Plan" (SRP), issued 1997; RG 1.165; and Section 2.5 of RG 1.70, "Standard Format and Content of Safety Analysis Reports for Nuclear Power Plants," Revision 3, issued November 1978, provide specific guidance concerning the evaluation of information characterizing the geology and seismology of the proposed site.

2.5.1.3 Technical Evaluation

This section of the SER provides the staff's evaluation of the geological and seismological information submitted by the applicant in SSAR Section 2.5.1. The technical information presented in SSAR Section 2.5.1 resulted from the applicant's surface and subsurface geological, seismological, and geotechnical investigations performed in progressively greater detail as they moved closer to the site. Through its review, the staff determined whether the applicant had complied with the applicable regulations and conducted its investigations with an appropriate level of thoroughness in accordance with the four areas designated in RG 1.165, which are based on various distances from the site (i.e., 320 km (200 mi), 40 km (25 mi), 8 km (5 mi), and 1 km (0.6 mi)).

SSAR Section 2.5.1 contains the geologic and seismic information gathered by the applicant in support of the vibratory ground motion analysis and site SSE spectrum provided in SSAR Section 2.5.2. According to RG 1.165, applicants may develop the vibratory design ground motion for a new nuclear power plant using either the EPRI or LLNL seismic source models for the CEUS. However, RG 1.165 recommends that applicants update the geological, seismological, and geophysical database and evaluate any new data to determine whether revisions to the EPRI or LLNL seismic source models are necessary. As a result, the staff focused its review on geologic and seismic data published since the late 1980s that could indicate a need for changes to the EPRI or LLNL seismic source models.

To thoroughly evaluate the geological and seismological information presented by the applicant, the staff obtained the assistance of the U.S. Geological Survey (USGS). The staff and its USGS advisors visited the ESP site to confirm the interpretations, assumptions, and conclusions presented by the applicant concerning potential geologic and seismic hazards. The staff's review of SSAR Section 2.5.1 focused on (1) tectonic or seismic information, (2) nontectonic deformation information, and (3) conditions caused by human activities, with respect to both the regional geology and site geology.

2.5.1.3.1 Regional Geology

The staff focused its review of SSAR Section 2.5.1.1 on the applicant's description of the regional tectonics, with emphasis on the Quaternary Period, structural geology, seismology, paleoseismology, physiography, geomorphology, stratigraphy, and geologic history within a distance of 200 miles from the site. The applicant provided additional detail, beyond that presented in SSAR Section 2.5.1.1, in Section 2.2 of SSAR Appendix A and Section 2.1 of SSAR Appendix B. In addition, Attachment 1 to SSAR Appendix B describes the applicant's regional paleoliquefaction investigations.

In SSAR Section 2.5.1.1 and Appendices A and B, the applicant described the regional physiography, the Quaternary geologic history and stratigraphy, structural geology, and regional tectonic setting and features. The applicant concluded that the ESP site is one of the most geologically stable areas in the United States, and the geologic conditions at the ESP site are the same as those at the CPS site. Based on its review of SSAR Section 2.5.1.1 and the pertinent portions of Appendices A and B, the staff concludes that the applicant provided a thorough and accurate description of these geologic features and characteristics in support of the ESP application. In addition, SSAR Section 2.5.1.1 and Appendices A and B describe well-documented geologic information, and the staff concludes that the applicant's description fulfills the requirements of 10 CFR 52.17, "Contents of Applications," and 10 CFR 100.23.

In Section 2.1.5 of SSAR Appendix B, the applicant described the regional seismic sources. Rather than characterizing the seismic potential of each of the regional tectonic features (folds, faults, lineaments), the applicant used the EPRI-SOG seismic hazard study, which groups these potential seismic sources into large areal seismic source zones. Within a 200-mile radius of the site (or just beyond), the three major sources of potential earthquakes are (1) the NMSZ, (2) the WVSZ in southern Illinois and Indiana, and (3) the central Illinois basin/background source. For each of these three seismic source zones, the applicant updated the original EPRI-SOG seismic hazard characterization. These updates are described in SSAR Section 2.5.2 and evaluated by the staff in Section 2.5.2 of this SER.

The New Madrid region was the location of three large earthquakes in 1811–1812, which the applicant estimated (based on its review of the geologic literature) to be between 7.0 and 8.0. The NMSZ consists of three principal trends of seismicity—two northeast-trending arms with a connecting northwest-trending arm. These seismicity trends coincide with what researchers believe to be the causative faults for the three 1811–1812 earthquakes, as well as previous earthquake sequences occurring around AD 1450 ± 150, AD 900 ± 100, AD 490 ± 50, AD 300 ± 200, and BC 1370 ± 970. These three causative faults are the RF, NN fault, and New Madrid south (NS) fault. In addition, the applicant modeled the large seismic events within the NMSZ as characteristic earthquakes, which means that these three faults repeatedly generated earthquakes of similar size during each of the previous earthquake sequences. In RAI 2.5.1-1, the staff asked the applicant to evaluate the publication of Bakun and Hooper (2004), which estimates the magnitudes of the New Madrid earthquake sequence to be M 7.6, 7.5, and 7.8. The applicant used the preliminary magnitude estimates by Bakun and Hooper (2003, in press), which were M 7.2, 7.1, and 7.4. In its response to RAI 2.5.1-1, the applicant stated that its review of the recent literature as well as discussion with researchers indicated that "there still remains uncertainty and differing views within the research community regarding the size and location of the 1811–12 earthquakes." Based on its review of the recent literature concerning the magnitudes for New Madrid earthquake sequences, the applicant added two new models

(rupture sets) and revised its previous model based on the Bakun and Hooper (2003, in press) magnitude estimates. The applicant stated that these revisions to the magnitude distributions for characteristic New Madrid earthquakes produced approximately 3 to 4 percent higher ground motions at the mean 10^{-4} and mean 10^{-5} hazard levels. Table 2.5.1-1, reproduced from the applicant's response to RAI 2.5.1-1, provides the six different models (rupture sets) for the New Madrid characteristic earthquakes.

Table 2.5.1-1 Updated Magnitude Distributions for Characteristic New Madrid Earthquakes

Rupture Set	NS Magnitude	Reelfoot Magnitude	NN Magnitude	Weight
1	7.8	7.7	7.5	0.1667
2	7.9	7.8	7.6	0.1667
3	7.6	7.8	7.5	0.2500
4	7.2	7.4	7.2	0.0833
5	7.2	7.4	7.0	0.1667
6	7.3	7.5	7.0	0.1667

The staff considers the applicant's response to RAI 2.5.1-1 to be an adequate assessment of the latest geologic literature concerning the magnitudes for New Madrid characteristic earthquakes. The applicant revised its magnitudes for rupture set number 3 to reflect the changes made by Bakun and Hooper (2004). In addition, the applicant added two new models based on its review of the latest literature and communications with researchers. The applicant assessed the impact of these additions and revisions by reevaluating its PSHA and found an increase (3 to 4 percent) in the 1 Hertz (Hz) ground motion hazard curve at the mean 10^{-4} and mean 10^{-5} hazard levels. However, the applicant did not incorporate this new information into its PSHA or subsequent SSE ground motion spectrum and indicated that the ESP application did not need to be updated as a result of its response to RAI 2.5.1-1. In Open Item 2.5.1-1, the staff asked the applicant to incorporate this information into its PSHA or SSE and to update the SSAR to reflect the corrected magnitude estimates. In response, the applicant updated its source characterization of the New Madrid earthquakes including the final published assessments of Bakun and Hooper (2004). These changes have been incorporated into the ESP application. Therefore, the staff considers Open Item 2.5.1-1 to be resolved.

In RAIs 2.5.1-3 and 2.5.1-4, the staff asked the applicant to provide an improved regional seismicity map and better annotated photographs of the regional liquefaction features, respectively. In response, the applicant revised Figure 2.1-13 in SSAR Appendix B and Figures B-1-13, B-1-14, and B-1-15 in Attachment 1 to SSAR Appendix B. The staff reviewed these revised SSAR figures and concludes that they provide more detail and support for the applicant's characterization of the regional seismic sources.

In RAI 2.5.1-5, the staff asked the applicant to describe, given the heterogeneous nature of the glacial till deposits, how it used the size of paleoliquefaction features (i.e., dike width) to estimate the locations and magnitudes of paleoearthquakes in the Wabash Valley region and

within the Illinois basin. In addition, the staff asked the applicant to account for possible differences in the ground water level, compaction, and overburden pressures between the time of the paleoearthquakes and the present. In response, the applicant stated that the width of dikes provides information that can be used to estimate the level of shaking at the specific site. The applicant used this information in conjunction with regional data on the spatial pattern and distribution of dike size to estimate the location and magnitude of the prehistoric earthquakes. Concerning the uniformity and quantity of susceptible sediments in the study region, the applicant stated that deposits of latest Pleistocene and Holocene age, which have been laid down by moderate to large streams in the CEUS, are generally moderately susceptible. Finally, regarding how potential differences in the geoenvironment are accounted for in determining the size of paleoearthquakes, the applicant stated that researchers have developed recommendations for accounting for uncertainties related to these factors in analyses to back calculate the strength of the earthquake shaking at individual sites.

The staff notes that the applicant acknowledged the uncertainties of using paleoliquefaction analyses to determine the size and location of prehistoric earthquakes by its characterization of these regional seismic sources. Rather than specifically using the inferred locations and magnitudes of paleoearthquake sources, the applicant characterized the Wabash Valley and Illinois basin/background seismic zones as large areal source zones that encompass all of the paleoearthquake locations. In addition, the applicant assumed that the earthquakes within these source zones can occur over large areas as part of its PSHA. The applicant also assumed a conservative range of maximum magnitudes for both source zones. As such, the staff concludes that the applicant has effectively used the paleoliquefaction data and analyses to characterize the regional and local seismic potential of the Wabash Valley and Illinois basin/background source zones.

In RAI 2.5.2-6, the staff asked the applicant to explain its selected paleoliquefaction study area along the streams near the ESP site. Specifically, the staff asked the applicant why it did not examine the streams northwest and southeast of the ESP site as part of the paleoliquefaction study. In addition, the staff asked the applicant if it used other locations besides river bank exposures to confirm the absence of liquefaction features in the vicinity of the ESP site. In response, the applicant stated that it did not conduct reconnaissance investigations in the areas to the northwest and southeast for both logistical and technical reasons. The applicant stated that it selected locations along the Salt Creek, North Fork of the Salt Creek, Sangamon River, and Mackinaw River to supplement previous liquefaction studies in this area. The applicant determined that the Mackinaw River, in the northern part of the study area, was a good candidate to evaluate the evidence for paleoearthquakes because of an abundance of accessible exposures. In addition, McNulty and Obermeier (1999) previously surveyed portions of the Sangamon River. Concerning reconnaissance of regions southeast and northwest of the ESP site, the applicant stated that it considered coverage of these areas to be unnecessary because of the absence of liquefaction-susceptible deposits as well as difficulties in accessing the drainage areas. The applicant provided the following technical rationale for its selected study area:

> Although there are regions to the northwest and southeast of the site within 25 miles of the site that have not been examined, the coverage provided by the previous mapping and the mapping done as part of this study provides sufficient coverage to support the conclusion that paleoearthquakes comparable to the postulated Springfield event have not occurred within a radius of approximately

25 miles of the site post-hypsithermic time (post-6-7 ka). A moderate to large event located within the 25-mile radius to the southeast of the site likely would have been recorded along the examined reaches of Salt Creek and the Sangamon River. A moderate to large event within the 25-mile radius northwest of the site also likely would have been recorded along the examined reaches of the Mackinaw River, Salt Creek, or Sugar Creek.

Regarding the confirmation of the absence of liquefaction features in the vicinity of the ESP site at locations other than riverbank exposures, the applicant stated that it examined gravel pits in the region southwest of the ESP site. However, the applicant stated that there are more abundant exposures along riverbanks, and searching along riverbanks provides for a more efficient method for covering an extensive area.

Based on its review of the applicant's response to RAI 2.5.2-6, the staff concludes that the applicant adequately surveyed the site area for liquefaction features. The staff concurs with the applicant's conclusion that the few liquefaction features indicate that there has not been a paleoearthquake comparable to the Springfield earthquake in the site area during the past 6000 to 7000 years. An earthquake of this size (M 6.2 to 6.8) would most likely have produced liquefaction features along many of the stream banks in the site area that were examined by the applicant. In addition, the staff finds that the applicant has conservatively modeled the seismic potential of the site area by defining a broad areal seismic source zone (Illinois basin/background) as part of its PSHA.

Based upon its review of SSAR Section 2.5.1.1 and the supporting appendices and attachments, as set forth above, the staff concludes that the applicant has provided a complete and accurate description of the regional geology, as required by 10 CFR 52.17 and 10 CFR 100.23.

2.5.1.3.2 Site Geology

The staff focused its review of SSAR Section 2.5.1.2 on the applicant's description of the site-related geologic features and structure, as well as conditions caused by human activities. In addition to SSAR Section 2.5.1.2, the staff reviewed Chapters 2 and 5 of SSAR Appendix A, which provides supporting information on the local geologic features. Based on its review of SSAR Section 2.5.1.2, described below, the staff concludes that the applicant has provided a thorough and accurate description of the local geology in support of the ESP application.

In SSAR Section 2.5.1.2 and Chapters 2 and 5 of SSAR Appendix A, the applicant described the site physiography, stratigraphy, structural geology, ground water conditions, and other geologic conditions. The ESP site is located in an upland area with a local relief of about 10 ft that is dissected by the Salt Creek and the North Fork of the Salt Creek. The site is located within the extent of the Wisconsinan glaciation with surface deposits consisting of a thin layer of loess over glacial till. The top of bedrock is about 300 ft below the ground surface. The ESP site is located in a tectonically stable area of North America, and there is no evidence of surface faulting at the site or in the local site area. The ESP site area is part of the Illinois/basin background seismic source zone, which includes the presumed epicenter of the Springfield earthquake (M 6.2 to 6.8) in central Illinois as well as the few liquefaction features that the applicant discovered to the northeast of the site. The ground water at the ESP site exists in a perched water table condition a few feet below the ground surface in the shallow Wisconsinan

till soils. Concerning other geologic conditions, the ESP site is not susceptible to karst development or mine subsidence, and the landslide potential is low.

Based on its review of SSAR Section 2.5.1.2 and Chapters 2 and 5 of SSAR Appendix A, the staff concludes that the applicant has provided an accurate and thorough description of the local site geology as required by 10 CFR 52.17 and 10 CFR 100.23. SSAR Section 2.5.1.2 and Chapter 2 of SSAR Appendix A accurately describe readily observable local geologic features, and Chapter 5 of SSAR Appendix A provides an adequate description of the local site conditions. Because of limited ground water withdrawal, the distance of any mining activity from the site, and the absence of karst terrain, the staff concludes that there is no potential for the effects of human activity, such as subsidence or collapse, that could compromise the safety of the site.

2.5.1.4 Conclusions

As set forth above, the staff reviewed the geological and seismological information submitted by the applicant in SSAR Section 2.5.1. On the basis of its review, the staff finds that the applicant provided a thorough characterization of the geological and seismological characteristics of the site, as required by 10 CFR 100.23. These results provide an adequate basis to conclude that no capable tectonic sources exist in the plant site area that have the potential to cause near-surface fault displacement. In addition, the staff concludes, as described above, that the applicant has identified and appropriately characterized the seismic sources significant to determining the SSE for the ESP site, in accordance with RG 1.165 and SRP Section 2.5.1, and therefore satisfied 10 CFR 100.23(c) and GDC 2 in this respect. Based on the applicant's geological investigations of the site vicinity and the site area, the staff concludes that the applicant has properly characterized the site lithology, stratigraphy, geologic history, and structural geology. The staff also concludes that there is no potential for the effects of human activities (i.e., ground water withdrawal or mining activity) to compromise the safety of the site. Therefore, the staff concludes that the proposed ESP site is acceptable from a geological and seismological standpoint and meets the requirements of 10 CFR 100.23.

2.5.2 Vibratory Ground Motions

SSAR Section 2.5.2 describes the applicant's determination of the SSE ground motion at the ESP site from possible earthquakes in the site area and region. SSAR Section 2.5.2.1, "Seismicity," describes the earthquake catalog used for the ESP site; SSAR Section 2.5.2.2, "Geologic Structure and Tectonic Activity," summarizes the geologic structure and tectonic activity that could potentially result in ground motion at the ESP site; and SSAR Section 2.5.2.3, "Correlation of Earthquake Activity with Geologic Structure or Tectonic Province," describes the correlation of earthquake activity with geologic structures or tectonic provinces. SSAR Section 2.5.2.4, "Maximum Earthquake Potential," describes the maximum earthquake potential for seismic sources in the region surrounding the ESP site; SSAR Section 2.5.2.5, "Seismic Wave Transmission Characteristics of the Site," describes the seismic wave transmission characteristics of the site; SSAR Section 2.5.2.6, "Safe Shutdown Earthquake," provides the SSE ground motion spectrum; and SSAR Section 2.5.2.7, "Operating Basis Earthquake," provides the operating-basis earthquake (OBE) ground motion spectrum.

The applicant stated that the information provided in SSAR Section 2.5.2 of the ESP application uses the procedures recommended in RG 1.165 with certain exceptions. In addition, the applicant has decided to use the EPRI-SOG seismic source model for the CEUS as an input for its seismic ground motion calculations. RG 1.165 indicates that applicants may use the seismic source interpretations developed by LLNL (1993) or EPRI as inputs for a site-specific analysis. RG 1.165 also recommends a review and update, if necessary, of both the seismic source and ground motion models used to develop the SSE ground motion for the ESP site.

To determine if an update of the 1989 EPRI-SOG seismic source and ground motion models was necessary, the applicant reviewed the literature published since the mid-to-late 1980s. This literature review identified the need for changes in some of the seismic source characterization parameters, such as maximum magnitudes and recurrence intervals. In addition, the applicant determined that the ground motion modeling used for the 1989 EPRI-SOG seismic study needed to be updated. To assess the impact of each of these updates on the site hazard, the applicant performed sensitivity studies.

2.5.2.1 Technical Information in the Application

2.5.2.1.1 Seismicity

SSAR Section 2.5.2.1 describes the development of a current earthquake catalog for the ESP site. The applicant started with the original EPRI-SOG earthquake catalog, which covers the time period from 1777 to the beginning of 1985. To update the earthquake catalog, the applicant used information from the (1) National Center for Earthquake Engineering Research (NCEER), (2) USGS, and (3) Advanced National Seismic System (ANSS), formerly the Council of the National Seismic System. Of these three catalogs, the applicant primarily used the USGS National Hazard Mapping Catalog for the period of 1985 through 1995 (Frankel, et al., 2002) and the ANSS catalog for 1995 through June 2002. As shown in Figure 2.5.2-1, reproduced from Figure 2.1-11 of SSAR Appendix B, a comparison of the geographic distribution of earthquakes contained in the EPRI-SOG earthquake catalog (1777–1985) and the earthquakes contained in the updated catalog (1985–2002) shows a very similar spatial distribution.

s:\7900\7935\7935.000\03_0109_eesp_fig_2.1-07(31).ai (2003-05-29, 16:32)

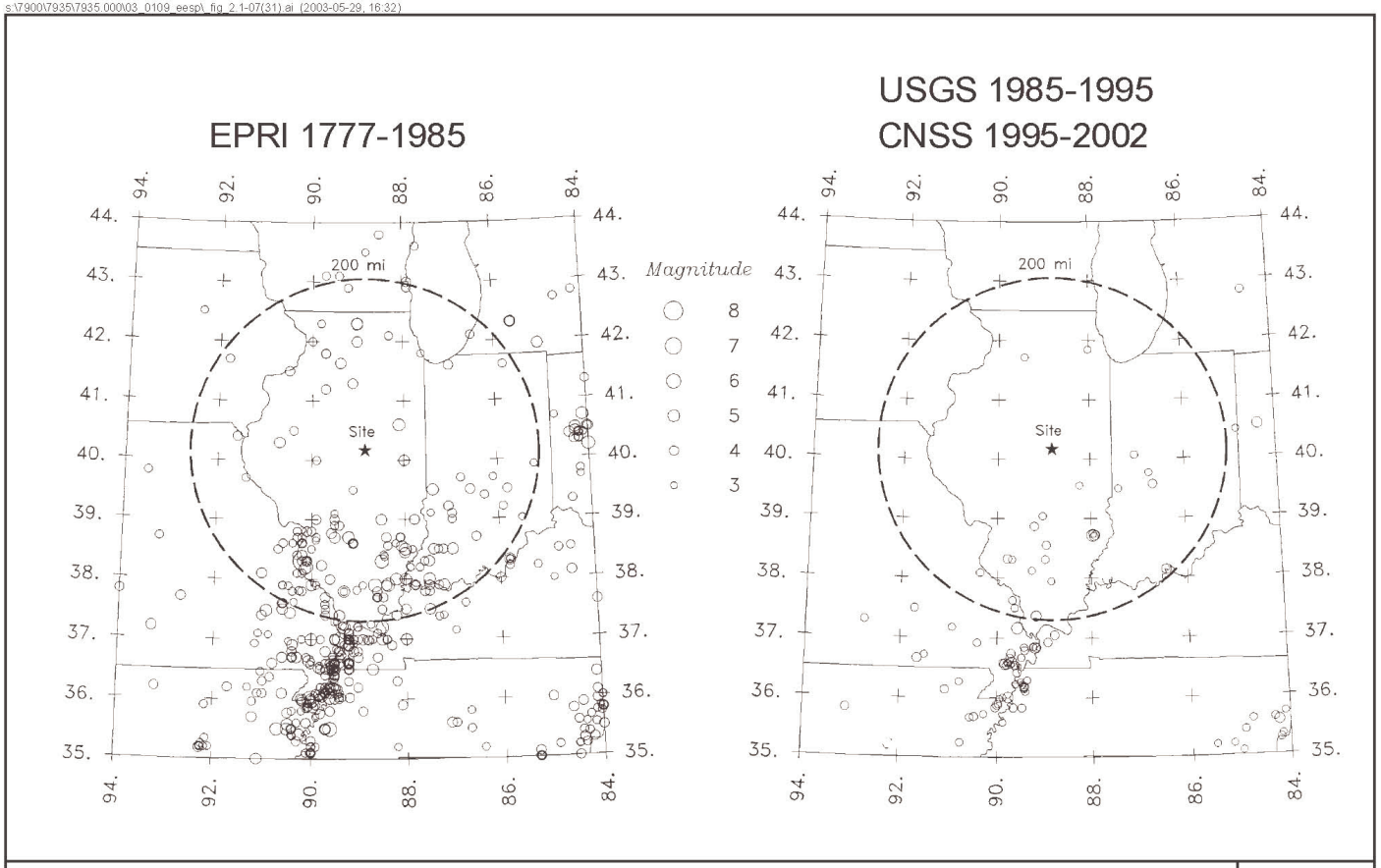

Seismic Hazards Report for the EGC ESP Site
Updates to Seismicity Catalog

Figure
2.1-11

Figure 2.5.2-1 Updates to seismicity catalog

Significant additions to the original EPRI-SOG earthquake catalog include prehistoric earthquakes inferred from evaluation of prehistoric liquefaction information in the ESP site region. Paleoliquefaction features are generally identified along the cut banks of streams and include features such as sand boils or blows, dikes, and sills that intrude into an overlying layer of silt. By establishing the date and geographical distribution of these features, the applicant was able to estimate the earthquake magnitude that caused the paleoliquefaction features. Previous investigations of paleoliquefaction features at sites in the southern Illinois basin and parts of Indiana, Illinois, and Missouri have identified a number of episodes of paleoliquefaction that have been interpreted to have been caused by Holocene and latest Pleistocene earthquakes with estimated M_w of 6 to 7.8. The applicant stated that one set of these paleoliquefaction features was discovered approximately 30 miles southwest of the ESP site. These features are from an earthquake centered in the Springfield, Illinois, area that occurred between 5900 and 7400 years ago with an estimated magnitude range of 6.2 to 6.8.

To augment the paleoliquefaction studies covering the site region, the applicant performed additional field reconnaissance to search for additional paleoliquefaction features within a 25–30-mile radius of the ESP site. After analyzing the field reconnaissance results, the applicant concluded that evidence for an earthquake comparable to the postulated Springfield earthquake had not been observed in the study area. However, isolated features of mid-Holocene and latest Pleistocene age were observed in the study area and interpreted to be seismically induced. These features were discovered 11–13 miles from the ESP site; however, the small scale of the features and lack of evidence for similar features elsewhere in the study area led the applicant to conclude that they arose from a distant source or from a low-magnitude event. Additional older paleoliquefaction features were discovered 17 miles from the ESP site. In RAI 2.5.2-6, the staff asked the applicant to explain its selected paleoliquefaction study area along the streams near the ESP site. In response, the applicant stated that it selected locations along the Salt Creek, Sangamon River, and Mackinaw River to supplement previous liquefaction studies in this area. Further details of the applicant's field reconnaissance for paleoliquefaction features near the ESP site are provided in Section 2.1.4 and Attachment 1 to Appendix B to the ESP application.

As a result of the recent discoveries of prehistoric earthquakes in the site region and two recent earthquakes in the study region (M 5.0 in 1987 east of Olney, Illinois, and M 4.5 in 2002 in southern Indiana), the applicant determined that the range of maximum magnitudes assigned to the site region should be increased to include events comparable to the Springfield earthquake (M 6.2 to 6.8).

2.5.2.1.2 Geologic Structure and Tectonic Activity

SSAR Section 2.5.2.2 describes the geologic structure and activity that could result in seismically induced vibratory ground motions at the ESP site. The applicant's evaluation of the geologic structure and tectonic activity for the ESP site included a detailed update of the structural features (folds and faults) within the site region. The applicant indicated that the results of the information update on the structural features showed that the general structural picture remains the same. Table 2.1-1 in Chapter 2 of SSAR Appendix B provides a list of the status for each of the folds in the ESP site region. Similarly, Table 2.1-2 in Chapter 2 of SSAR Appendix B provides a list of the status for each of the faults in the ESP site region. In addition, each of the folds and faults are described by the applicant in Section 2.1.2 of SSAR Appendix B. Rather than attempting to characterize the seismic potential of each of these folds

and faults, the applicant defined broad seismic source zones that encompass many of these structural features. These broad seismic source zones are termed areal source zones. The staff's detailed evaluation of the seismogenic potential of the structural features is presented in Section 2.5.1.1.1 of this SER.

Within a 200-mile radius of the site (or just beyond), the two major sources of potential earthquakes are the NMSZ and the WVSZ in southern Illinois and southern Indiana. The New Madrid region was the location of three earthquakes in 1811–1812, which are the largest earthquakes recorded in the CEUS. The Wabash Valley region is a zone of elevated seismicity in which a number of paleoearthquakes have been identified. In addition to the NMSZ and WVSZ, evidence from recent paleoliquefaction studies and seismic reflection data show that significant earthquakes may occur in parts of the central Illinois basin where there are no obvious folds or faults at the surface. The applicant stated that the location, size, and recurrence of such events are not well constrained by available data. However, because of the paleoliquefaction evidence, the applicant developed a background source zone for this region, referred to as the central Illinois basin background source zone.

Since the EPRI-SOG seismic study for the CEUS, several studies have focused on the NMSZ and WVSZ. These studies include extensive paleoliquefaction investigations, acquisition and reprocessing of shallow seismic reflection data, paleoseismic trenching and mapping investigations, and seismological studies. These studies have used a variety of techniques to characterize the location, magnitudes, and seismic activity rates of the NMSZ and WVSZ. A complete description of the NMSZ and WVSZ is provided in Section 2.1 of SSAR Appendix B. In addition, the applicant's incorporation of the new information on the NMSZ and WVSZ into its PSHA is provided in Section 3.0 of SSAR Appendix B. The staff's evaluation of the applicant's characterization of the NMSZ and WVSZ is contained in Section 2.5.1.1.1 of this SER; the applicant's incorporation of the new information on these two source zones is provided below in Section 2.5.2.1.3 of this SER.

The ESP site is located within the Illinois basin in the SCR of the North American craton, which is characterized by low rates of historical seismicity. The Illinois basin is a spoon-shaped depression covering parts of Illinois, Indiana, and Kentucky. The Illinois basin is bounded on the north by the Wisconsin arch, on the east by the Kankakee and Cincinnati arches, on the south by the Mississippi embayment, and on the west by the Ozark dome and Mississippi River arch. Basement elevation ranges from approximately -2,950 ft in the northern end of the Illinois basin to -14,100 ft in southeastern Indiana.

The ESP site lies within a compressive midplate stress province characterized by a relatively uniform compressive stress field with the maximum horizontal stress oriented northeast to east-northeast. The applicant reported that preliminary results from a global positioning system (GPS) network in the southern Illinois basin provide evidence for present-day tectonic strain in the WVSZ. However, given the current level of error in individual GPS observations, an extended period of time will be required before these observations can fully characterize the strain field and confirm the postulated tectonic motions. Recent geodetic measurements in the NMSZ indicate that the rate of strain accumulation is below the current detection threshold. However, the applicant concluded that these observations are not inconsistent with a model of seismicity in intraplate regions as a transient phenomenon localized along weak zones in the crust.

2.5.2.1.3 Correlation of Earthquake Activity with Geologic Structure or Tectonic Province

SSAR Section 2.5.2.3 describes the evaluation of recent geological and seismological information and how this information was used to perform a new PSHA. Chapter 3 of SSAR Appendix B provides a more detailed account of the incorporation of new information for the ESP PSHA.

The original EPRI-SOG PSHA indicated that the most significant contributors to the seismic hazard at the ESP site are the NMSZ, the WVSZ, and the random background event in the local source zone (central Illinois basin background source zone). SER Section 2.5.1.1.1 provides a description of each of these three seismic source zones. After evaluating recent information on these three source zones, other potential sources in the site region, and ground motion estimation, the applicant made the following determinations regarding (1) earthquake recurrence rates, (2) maximum magnitudes, and (3) ground motion attenuation.

Earthquake Recurrence Rates. The applicant focused on the recurrence rates for the NMSZ, WVSZ, and central Illinois basin background source zone since these three source zones are the main contributors to the total seismic hazard at the ESP site. Comparing the updated catalog (with an additional 17 years of earthquake data) to the original EPRI-SOG catalog, the applicant concluded that the recurrence rates used for the EPRI-SOG study are still valid. In addition to the smaller recorded events over the past 17 years, the applicant also included the additional prehistoric events that have occurred in the three source zones as revealed by paleoliquefaction studies. The applicant found that for the central Illinois basin and the Wabash Valley source zones, the fit of the earthquake recurrence relationships to the recorded seismicity envelops the rates of larger earthquakes estimated from paleoliquefaction data. However, for the NMSZ, the applicant found that recent paleoliquefaction data provide evidence that large-magnitude earthquakes have occurred on the NMSZ faults more frequently than the seismicity rates specified in the EPRI-SOG source characterizations for the NMSZ.

New Madrid Seismic Zone Characteristic Earthquake Modeling

Recent seismologic, geologic, and geophysical studies have associated faults within the NMSZ with the three large-magnitude historical earthquakes (NM1, NM2, and NM3) that occurred during the 1811–1812 sequence. These three faults are (1) the NS fault, (2) the NN fault, and (3) the RF. These faults are also believed to be the causative faults for previous NMSZ earthquake sequences occurring around AD 1450 ± 150, AD 900 ± 100, AD 490 ± 50, AD 300 ± 200, and BC 1370 ± 970. The applicant modeled these large seismic events within the NMSZ as characteristic earthquakes, which means that these three faults repeatedly generated earthquakes of similar size during each of the previous earthquake sequences. The applicant found that these similarly sized characteristic earthquakes occur more frequently than would be implied by extrapolation of the recurrence of low-magnitude events in the NMSZ. As such, the applicant focused on the characterization of these characteristic large-magnitude events within the NMSZ. The key source parameters considered by the applicant for the NMSZ are (1) the fault source geometry, (2) characteristic earthquake magnitude, and (3) characteristic earthquake recurrence.

The three fault sources included in the updated characterization of the central fault system of the NMSZ are the NS, NN, and RF. The applicant characterized the uncertainty regarding the location and extent or length of the causative faults that ruptured during the 1811–1812 and

other characteristic earthquake sequences by weighting alternative fault source geometries for each of the three fault sources of the NMSZ central fault system. These alternative geometries affect the distance from the earthquake rupture to the ESP site. The weights assigned to each of the alternative source geometries are based on recently published studies of the NMSZ.

Next, the applicant considered the magnitude for the characteristic earthquakes on the three New Madrid fault sources. The uncertainty in the magnitude estimates for the 1811–1812 earthquakes is largely caused by the subjective nature of interpretations of historical accounts, the lack of historical accounts in many areas (especially to the west of the NMSZ), and the lack of large recent earthquakes in the eastern United States that could be used to calibrate the intensity values from eyewitness accounts to actual ground motion values. For the ESP application, the applicant assigned weights for the characteristic earthquake magnitudes to each of the major faults within the central NMSZ. The magnitude estimates are weighted based on consideration of the published values estimated from intensity data and from estimates of rupture area for individual fault segments. For the NS fault, which is thought to be the source for NM1, the probability distribution for the characteristic magnitude is M 7.3 (0.4), M 7.7 (0.5), and M 8.1 (0.1). For the NN fault, which is thought to be the source for NM2, the probability distribution for the characteristic magnitude is M 7.0 (0.45), M 7.4 (0.45), and M 7.8 (0.1). Finally, for the RF, thought to be the source of NM3, the probability distribution for the characteristic magnitude is M 7.2 (0.2), M 7.4 (0.4), M 7.6 (0.3), and M 8.0 (0.1). For the earlier NMSZ characteristic earthquake sequences (pre-1811–1812), the applicant also assumed that these sequences consisted of multiple, large-magnitude earthquakes. As such, the applicant considered each characteristic earthquake to be the rupture of multiple (two to three) of the NMSZ fault sources.

In RAI 2.5.2-5, the staff asked the applicant to justify its modeling of the relative frequency of event sequences in the NMSZ. Specifically, the staff noted that Tuttle et al. (2002) concluded that all three sources (RF, NN, and NS) ruptured in each of the three sequences, but that one-third of the time the NN rupture may have been smaller than for the 1811–12 sequence, and one-third of the time NS may have been smaller than in 1811–1812. Tuttle et al. (2002) also concluded that these smaller earthquakes are at least magnitude M 7 events. This result differs from the event sequence modeling used by the applicant for NMSZ, which does not include NN or NS for some of the event sequences. The applicant responded to RAI 2.5.2-5 by stating that if the size of the 1811–1812 ruptures on these faults were in the low-magnitude M 7 range (e.g., values estimated by Bakun and Hooper (2003)), then the size of previous ruptures would have been below magnitude M 7. These smaller ruptures, which would be considered dependent events, were not included in the hazard calculations as characteristic earthquakes. SER Section 2.5.2.3.3 provides further detail on the applicant's response to RAI 2.5.2-5 as well as the staff's evaluation of the applicant's response.

After consideration of the magnitudes for characteristic earthquakes from the NMSZ, the applicant examined recently published studies dealing with the recurrence of the characteristic events. The best constraints on recurrence of characteristic NMSZ events are from paleoliquefaction studies throughout the New Madrid region and paleoseismic investigations of the RF scarp and associated fold. Paleoseismic studies of the NMSZ have found that the fault system responsible for the New Madrid seismicity generated temporally clustered, very large earthquakes in AD 900 ± 100 and AD 1450 ± 150, as well as during 1811–1812. In addition, these studies have found evidence for prehistoric sand blows that are compound structures, resulting from multiple earthquakes closely clustered in time (i.e., earthquake sequences)

occurring around AD 490 ± 50, AD 300 ± 200, and BC 1370 ± 970. The applicant fit the time intervals between these dates with two recurrence models, a Poissonian model and a lognormal model. The applicant weighted each model equally. Figure 4.1-1 in SSAR Appendix B shows a logic tree with the different recurrence models and the intervals between NMSZ characteristic events. For example, the time intervals and weights for the Poisson model are 187 years (0.10), 294 years (0.24), 443 years (0.31), 704 years (0.24), and 1389 years (0.10).

As stated above, the applicant concluded, based on its review of the literature, that the RF has ruptured in each of the previous three characteristic earthquake sequences, but the NN and NS sources may not have produced large earthquakes in all three sequences. The applicant used these observations to set the relative frequency of event sequences in the NMSZ as (1) rupture of all three sources (NN, RF, and NS) one-third of the time, (2) rupture of NN and RF one-third of the time, and (3) rupture of NS and RF one-third of the time.

Maximum Magnitudes. The applicant focused on the maximum magnitude values for the NMSZ, WVSZ, and central Illinois basin background seismic source zone, since these three source zones are the main contributors to the total seismic hazard at the ESP site. For the NMSZ, the applicant compared the maximum magnitude range used for the EPRI-SOG study, which is 7.2 to 8.8, with the maximum magnitudes that have been published recently, which range from 7.4 to 8.2. As a result, the applicant concluded that the recent maximum magnitudes for the NMSZ are consistent with the EPRI-SOG experts' assessments. For the WVSZ, the maximum magnitudes used for the EPRI-SOG study range from 5.0 to 8.0, while recently published maximum magnitudes range from 7.0 to 7.8. Similarly, for the central Illinois background source zone, the maximum magnitudes used for the EPRI-SOG study range from 4.3 to 7.6, while recently published maximum magnitudes range from 6.0 to 7.0. As a result, the applicant concluded, as described below, that the maximum magnitude values for both the WVSZ and the central Illinois background source zone need to be increased to reflect the magnitudes implied by the new paleoliquefaction data.

Wabash Valley-Southern Illinois Source Zone—Maximum Magnitude Distribution

The applicant stated that the updated maximum magnitude distribution for the Wabash Valley-Southern Illinois source zone is based on recent analysis of paleoliquefaction features in the vicinity of the lower Wabash Valley of southern Illinois and Indiana. The magnitude of the largest paleoearthquake in the lower Wabash Valley (the Vincennes-Bridgeport earthquake), which occurred 6011 ± 200 years BP, was estimated to be between 7.2 to 7.8. The next largest earthquake occurred 12,000 ± 1,000 years BP. This earthquake is estimated to be an M 7.1 to 7.2. Both of these earthquakes were in proximity to one another and took place in the general vicinity of the more recent and strongest historical earthquakes (M 4 to 5.5) in the lower Wabash Valley. Based on the above information, the applicant used the following maximum magnitude range for earthquakes in the Wabash Valley region—M 7.0 (0.1), M 7.3 (0.4), M 7.5 (0.4), and M 7.8 (0.1). The highest weight is given to the range from M 7.3 to 7.5 where most of the magnitude estimates lie.

Central Illinois Basin/Background Source Zone—Maximum Magnitude Distribution

The applicant stated that evidence from recent paleoliquefaction studies suggests that significant earthquakes may occur in parts of the central Illinois basin where there are no obvious surface faults or folds. The location, size, and recurrence of these earthquakes are not

well constrained by available data. One known earthquake is the M 6.2 to 6.8 prehistoric Springfield earthquake, located approximately 30 miles to the southwest of the ESP site. At present, the moderate-size prehistoric earthquakes in the central Illinois basin cannot be associated clearly with any known geologic structure, and no seismicity trends have been observed for this region. The applicant stated that paleoliquefaction evidence suggests that there may have been additional moderate-magnitude events in central and southern Illinois, such as the Shoal Creek earthquake which occurred about 5700 years BP. In addition to a literature review, the applicant conducted its own field reconnaissance north and east of the ESP site. Some paleoliquefaction features were discovered, but the applicant stated that the data are too limited to provide a basis for estimating the size or location of the event or events. The applicant also concluded that there have not been repeated moderate to large events (comparable to the Springfield earthquake) in the vicinity of the ESP site in the latest Pleistocene to Holocene time (6,000 to 7,000 years BP). A study of earthquakes in SCRs conducted by EPRI in 1994 (Johnston, et al., 1994) specifically addresses the problem of defining a maximum magnitude for regions that are characterized by the rare occurrence of maximum earthquakes and the lack of recognized surface expression or well-defined seismicity patterns associated with seismic sources, typical conditions over much of the CEUS. The 1994 EPRI study developed worldwide databases that could be used for assessments of maximum magnitudes for seismic sources in the CEUS. Using the database and method found in the 1994 EPRI study, the applicant developed the following maximum magnitude range for earthquakes in the central Illinois basin background source—M 6.2 (0.4), M 6.4 (0.3), M 6.6 (0.2), and M 6.8 (0.1).

In RAI 2.5.2-4, the staff asked the applicant to provide further detail and justification regarding its use of the 1994 EPRI study and accompanying worldwide database of earthquakes. Specifically, the staff requested the applicant to explain why its maximum magnitude for central Illinois should not be set at 6.8 since the two largest SCR earthquakes from nonextended crust are the Accra, Ghana, earthquake of 1862 (M 6.75 ± 0.35) and the Meeberrie, Western Australia, earthquake of 1941 (M 6.78 ± 0.25). In its response to RAI 2.5.2-4, the applicant stated that the method developed by the 1994 EPRI study does not start from the assumption that all SCR domains have the same maximum magnitude potential. Instead it assumes that there are characteristics that control the maximum size of an earthquake that can occur in an individual SCR domain, and these characteristics vary from domain to domain. SER Section 2.5.2.3.3 provides further detail on the applicant's response to RAI 2.5.2-4 as well as the staff's evaluation of the applicant's response.

<u>Ground Motion Attenuation</u>. The original EPRI-SOG study used three attenuation relationships, developed in the mid-1980s. Since the completion of the EPRI-SOG study, estimating ground motions in the CEUS has been the focus of considerable research. Following the guidance provided in NUREG/CR-6372, "Recommendations for Probabilistic Seismic Hazard Analysis: Guidance on Uncertainty and Use of Experts," prepared by the Senior Seismic Hazard Analysis Committee, EPRI completed in 2003 a study to characterize the distribution of ground motion prediction in the CEUS (EPRI 1008910, "CEUS Ground Motion Project: Model Development and Results"). For the EPRI study, a panel of six ground motion experts was assembled, and, during a series of workshops, the experts provided advice on the available CEUS ground motion attenuation relationships. In addition, the experts provided information on the appropriate criteria for evaluating the ground motion attenuation relationships. The product of the EPRI study is a suite of ground motion relationships and associated relative weights that represent the uncertainty in predicting median levels of ground motion. The EPRI study

grouped the selected ground motion attenuation relationships into four clusters, in which each cluster represents a group of models based on a similar approach for ground motion modeling. After comparing the three attenuation models used for the EPRI-SOG study with the new EPRI ground motion study, the applicant concluded that the recent median ground motion models are generally consistent with two of the three older models. However, the estimates of uncertainty or variability about the median ground motion predictions are considerably higher for the recent ground motion attenuation relationships compiled by the recent EPRI study compared to the uncertainty in the ground motion used for the original EPRI-SOG study.

In RAI 2.5.2-3, the staff asked the applicant to describe how the recent EPRI ground motion study converted the distance measure used for each of the attenuation relationships to a common measure. Specifically, the 13 CEUS attenuation relationships selected by the EPRI ground motion experts each use one of two different distance measures. In response to RAI 2.5.2-3, the applicant provided a description of the method it used to convert the "point-source" distance measure to the more commonly used "Joyner-Boore" distance measure. SER Section 2.5.2.3.3 provides further detail on the applicant's response to RAI 2.5.2-3 as well as the staff's evaluation of the applicant's response.

In summary, from the data obtained after the original EPRI-SOG study, the applicant concluded the following:

> (1) there are no additional specific seismic sources in the site region, (2) with the exception of large [characteristic] earthquakes occurring on the central faults in the NMSZ, the EPRI-SOG recurrence parameters provide a good estimate of the current rate of seismicity in the study region, (3) the maximum magnitude distributions for the central Illinois and Wabash Valley/Southern Illinois source zones developed by the EPRI-SOG expert teams likely underestimate what would be assessed give the present state-of-knowledge, and (4) current ground motion models for the CEUS are generally consistent with the median models used in the EPRI-SOG study. However, the aleatory variability about the median ground motions used in the EPRI-SOG study is generally lower than current estimates.

As a result of the above conclusions, the applicant made the following adjustments to the source parameters and ground motion relationships as part of sensitivity tests for the seismic hazard characterization of the ESP site:

- Set the mean return period for large characteristic earthquakes on the central faults of the NMSZ to 500–1000 years.
- Increase the maximum magnitude distributions of the WVSZ and central Illinois sources.
- Use updated attenuation models.

After implementing the above adjustments to the seismic source characterizations and ground motion models, the applicant concluded that the resulting seismic hazard curves are generally higher for the ESP site. The applicant implemented each of the above adjustments individually and then made comparisons with the earlier EPRI-SOG hazard curves for the ESP site. In addition, the applicant implemented each of the above adjustments simultaneously and made

similar comparisons. For both cases, the applicant considered the change in the seismic hazard levels to be significant enough to perform an updated PSHA for the ESP site.

2.5.2.1.4 Maximum Earthquake Potential

SSAR Section 2.5.2.4 presents the maximum earthquake potential for the ESP site in terms of the controlling earthquake magnitudes and distances. The applicant determined the low- and high-frequency controlling earthquakes by deaggregating the PSHA results at selected probability levels. Before determining the controlling earthquakes, the applicant updated the original EPRI-SOG PSHA using the seismic source zone adjustments and new ground motion modeling described above in the previous SER subsection.

PSHA Results. The applicant performed the PSHA by combining the hazard from the EPRI-SOG seismic sources (with updated maximum magnitude distributions) with the hazard from the New Madrid characteristic earthquake sources. The applicant assumed that the characteristic earthquake ruptures on the New Madrid faults rupture along the entire length of the fault, and the closest approach of the fault to the ESP site was used as the distance to the rupture. In addition, the applicant assumed that the characteristic earthquakes occurring on the central New Madrid faults rupture as clustered events or as a sequence within a short time period relative to the return period for the events.

The applicant performed PSHA calculations for peak ground acceleration (PGA) and spectral acceleration at frequencies of 25, 10, 5, 2.5, 1, and 0.5 Hz. Following the guidance provided in RG 1.165, the PSHA calculations were performed assuming generic hard rock site conditions (i.e., a shear- (S-) wave velocity of 9200 ft/s). The actual local site characteristics are incorporated in the calculation of the SSE spectrum, which uses the hard rock PSHA hazard results as the starting point. To compare the relative contribution of each of the dominant seismic source zones to the total hazard, the applicant computed PSHA results for the central Illinois basin background source, Wabash Valley, and New Madrid individually. At low ground motion levels, the distant Wabash Valley and New Madrid characteristic earthquakes produce the highest hazard. As the ground motion level increases, the local central Illinois background source becomes the dominant contributor to the hazard for high-frequency ground motions.

Controlling Earthquakes. To determine the low- and high-frequency controlling earthquakes for the ESP site, the applicant followed the procedure outlined in Appendix C to RG 1.165. This procedure involves the deaggregation of the PSHA results at a target probability level to determine the controlling earthquake in terms of a magnitude and source-to-site distance. The applicant chose to perform the deaggregation of the mean 10^{-4} and 10^{-5} PSHA hazard results. The low- and high-frequency controlling earthquakes are shown below in Table 2.5.2-1.

Table 2.5.2-1 High- and Low-Frequency Controlling Earthquakes

Hazard	Magnitude (m_b)	Distance
Mean 10^{-4} High Frequency (5 and 10 Hz)	6.5	83 km (52 mi)
Mean 10^{-4} Low Frequency (1 and 2.5 Hz)	7.2	320 km (199 mi)
Mean 10^{-5} High Frequency (5 and 10 Hz)	6.2	24 km (15 mi)
Mean 10^{-5} Low Frequency (1 and 2.5 Hz)	7.2	320 km (199 mi)

For the high-frequency mean 10^{-4} hazard, the controlling earthquake is a magnitude 6.5 event occurring at a distance of 83 km (52 mi), corresponding to an earthquake from the Wabash Valley-southern Illinois source zone. In contrast, for the high-frequency 10^{-5} hazard, the controlling earthquake has a magnitude of 6.2 at a distance of only 24 km (15 mi). This controlling earthquake is from the nearby central Illinois background source zone. For the low-frequency mean 10^{-4} and 10^{-5} hazard, the controlling earthquake has a magnitude of 7.2 at a distance of 320 km (199 mi). This earthquake corresponds to an event in the NMSZ. The ground motion response spectra for these controlling earthquakes are shown below in Figure 2.5.2-2, which is reproduced from Figure 4.2-19 in SSAR Appendix B. The applicant used the EPRI 2003 ground motion relationships to estimate the ground motion response spectra for the controlling earthquakes.

Non-GDS

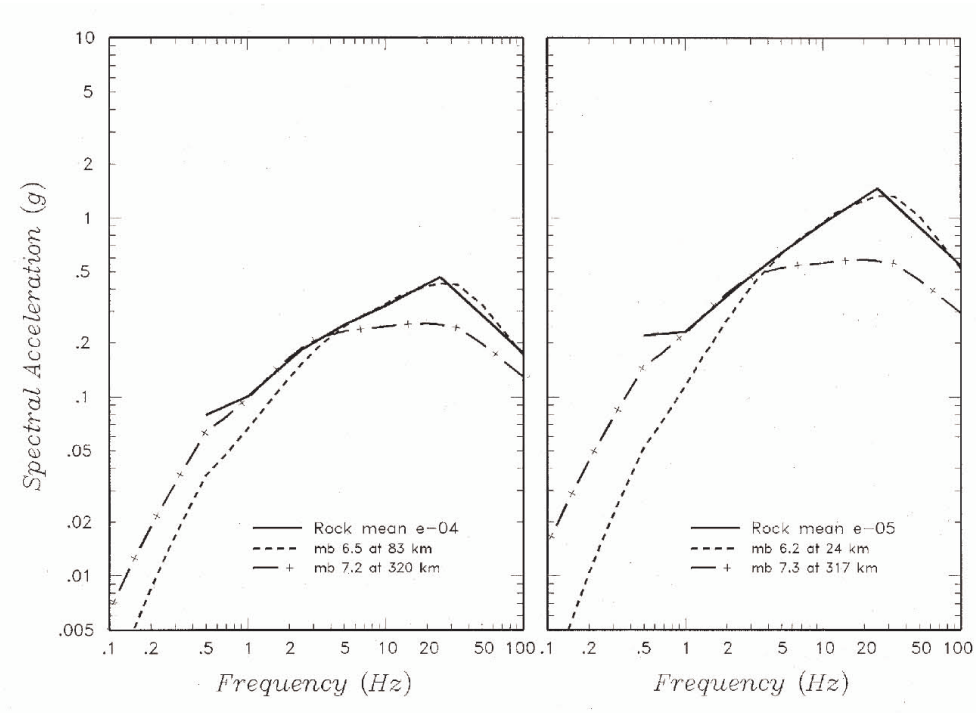

Seismic Hazards Report for the EGC ESP Site

Reference Earthquake (RE) Response Spectra for Mean 10^{-4} and Mean 10^{-5} Hazard

Figure **4.2-19**

Figure 2.5.2-2 Reference earthquake response spectra for mean 10^{-4} and mean 10^{-5} hazard

2.5.2.1.5 Seismic Wave Transmission Characteristics of the Site

SSAR Section 2.5.2.5 describes the method used by the applicant to develop the site free-field ground motion spectrum. The hazard curves from the PSHA are defined for generic hard rock conditions. According to the applicant, these hard rock conditions exist at the ESP site at a depth of several thousand feet or more below the ground surface. To determine the free-field ground motion, the applicant (1) developed soil/rock profile models for the ESP site, (2) selected seed earthquake time histories, and (3) performed the final site response analysis.

ESP Profile Model. The soil profile model used by the applicant for its site response analysis is shown in SSAR Figure 2.5-3. The profile consists of a thin layer of loess underlain by interbedded glacial tills and lacustrine (lake) deposits of Quaternary age to a depth of nearly 300 ft. For the 310-ft soil column at the ESP site, the applicant used the S-wave velocity (V_s) values from its ESP geophysical surveys, which are described in SER Section 2.5.4.1.4. SER Figure 2.5.4-5 shows the compressional- (P-) wave velocity (V_p) and V_s for each of the different soil layers to a depth of about 300 ft below the ground surface. As described in SER Section 2.5.4.1.2, the applicant conducted cyclic testing of the ESP site soils to determine the variation in soil shear strain modulus and material damping ratio with shearing strain amplitude. Based on the dynamic test results, the applicant selected appropriate shear modulus and damping curves for the ESP site.

As a result of the large range in S-wave velocities for some of the soil layers (Table 5-2 in SSAR Appendix A) and the differences in standard penetration test (SPT) blowcount values for ESP borings B1 and B4 compared to those of B2 and B3, the staff in RAI 2.5.4-4 requested that the applicant justify the appropriateness of using a single “average” soil column for the site response analyses rather than including a number of different base-case soil columns. In response to RAI 2.5.4-4, the applicant stated that it modeled the variations in S-wave velocity and SPT blowcounts by statistically creating a large number of profiles, or realizations, and conducting the site response analyses using these profiles. SER Section 2.5.2.3.5 provides further detail on the applicant’s response to RAI 2.5.4-4 as well as the staff’s evaluation of the applicant’s response.

At a depth of approximately 300 ft is the top of the bedrock, which consists of limestone, shale, sandstone, siltstone, and a single 1-ft-thick interval of coal. The bedrock is of Pennsylvanian age. The applicant characterized the dynamic properties of this soil/bedrock profile during field and laboratory testing. These dynamic properties consisted of S-wave velocity data to a depth of 310 ft and a set of shear modulus reduction and damping data obtained from samples taken from boreholes drilled at the ESP site. Since the V_s at a depth of 310 ft below the ESP site is about 4000 ft/s, the applicant used nearby deep borehole V_p measurements to estimate the bedrock V_s profile. The applicant assumed V_p/V_s ratios of 1.73 and 2, which correspond to depths of 1900 ft and 3000 ft to reach the hard rock value of V_s = 9200 ft/s. In addition, for the sedimentary rocks below a depth of 310 ft, the applicant assumed a linear behavior during earthquake shaking. The damping values used by the applicant for the sedimentary rocks vary from 3.3 percent at depths ranging from 310 to 400 ft to 1.8 percent for rocks at a depth of 1200 to 1900 ft.

Once the applicant determined the appropriate soil and rock dynamic properties, it modeled the variability present in the site data by randomizing the soil and rock S-wave velocity profiles, soil

shear modulus and damping relationships, and rock damping values. The applicant generated 60 soil/rock profiles to account for variability in the site properties.

To account for the variability in soil shear strain modulus and material damping ratio with shearing strain amplitude, the applicant randomized the shear modulus and damping curves used for the site response analysis. In RAI 2.5.4-7, the staff asked the applicant to explain how these curves were used in the randomization process with respect to both the different depth ranges and the soil types occurring within those depth ranges. In response to RAI 2.5.4-7, the applicant stated that the computation performed for the EGC ESP project resulted in 60 modulus reduction curves and 60 material damping curves for each of the depth intervals. The range represented by each of the 60 sets of curves is intended to cover the uncertainties in the shape and absolute value of the modulus reduction and material damping ratio curves resulting from a number of different effects, including the particular soil type, the stress history for the soil, sample disturbance associated with the laboratory testing of soil samples, and random variability that is typically observed in laboratory testing programs. SER Section 2.5.2.3.5 provides further detail on the applicant's response to RAI 2.5.4-7 as well as the staff's evaluation of the applicant's response.

Earthquake Time Histories. Using the controlling earthquake (low- and high-frequency) magnitudes and distances listed above in Table 2.5.2-1, the applicant developed hard rock site response spectra using the EPRI (2003) ground motion models and then scaled these spectra to match the ESP site rock spectral accelerations at 1 and 2.5 Hz (low frequency) and 5 and 10 Hz (high frequency). However, instead of using these two rock response spectra to develop the ESP site response, the applicant determined an additional three "deaggregation earthquakes" for each controlling earthquake. These three deaggregation earthquakes represent a more complete range of the earthquakes that contribute to the low-frequency (1 and 2.5 Hz) and high-frequency (5 and 10 Hz) hazard than just a single controlling earthquake. To illustrate, Figure 2.5.2-3, reproduced from Figure 4.1-20 in SSAR Appendix B, shows the deaggregation results for the mean 10^{-4} hazard. The high-frequency controlling earthquake has a magnitude of 6.5 and distance of 83 km (52 mi). The three high-frequency deaggregation earthquakes at the mean 10^{-4} hazard level and their weights are m_b = 5.7 at 15 km (0.377), m_b = 6.7 at 153 km (0.322), and m_b = 7.2 at 375 km (0.301). As shown below in Table 2.5.2-2, there are three deaggregation earthquakes for each controlling earthquake.

Non-GDS

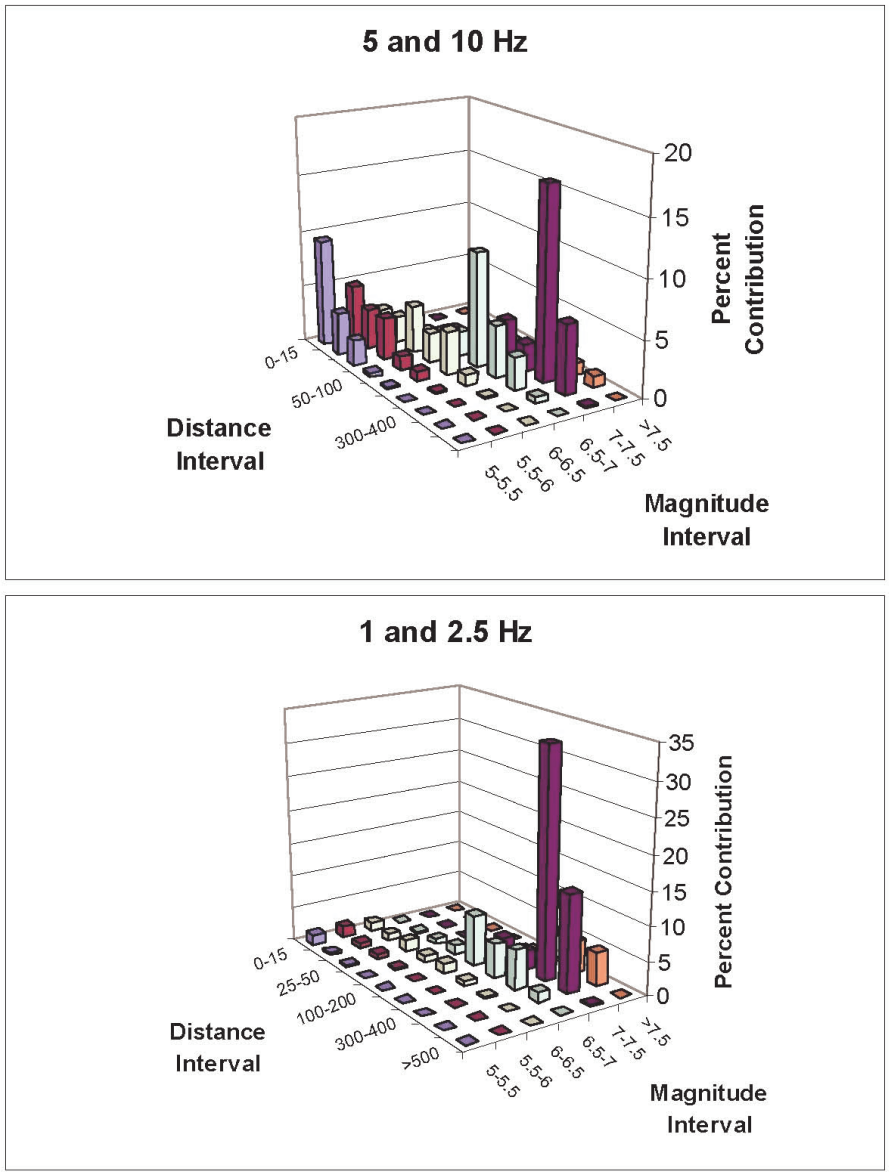

Seismic Hazards Report for the EGC ESP Site

Deaggregation Results for Mean 10^{-4} Hazard

Figure **4.1-20**

Figure 2.5.2-3 Deaggregation results for mean 10^{-4} hazard

Table 2.5.2-2 Controlling and Deaggregation Earthquakes

Hazard	Controlling Earthquake		Deaggregation Earthquakes		
	Magnitude (m_b)	Distance	Magnitude (m_b)	Distance	Weight
mean 10^{-4} 5 and 10 Hz	6.5	83 km (52 mi)	5.7 6.7 7.2	15 km (9 mi) 153 km (95 mi) 375 km (233 mi)	0.377 0.322 0.301
mean 10^{-4} 1 and 2.5 Hz	7.2	320 km (199 mi)	5.9 6.8 7.3	15 km (9 mi) 166 km (103 mi) 379 km (236 mi)	0.093 0.240 0.667
mean 10^{-5} 5 and 10 Hz	6.2	24 km (15 mi)	5.8 6.8 7.4	11 km (7 mi) 140 km (87 mi) 380 km (236 mi)	0.733 0.149 0.118
mean 10^{-5} 1 and 2.5 Hz	7.2	320 km (199 mi)	6.0 6.9 7.4	12 km (7 mi) 155 km (96 mi) 381 km (237 mi)	0.212 0.220 0.568

To determine the ESP dynamic site response, the applicant developed appropriate ground motion or earthquake time histories for each of the 12 deaggregation earthquakes. The applicant selected these earthquake time histories from the CEUS time history library provided with NUREG/CR-6728, "Technical Basis for Revision of Regulatory Guidance on Design Ground Motions: Hazard and Risk Consistent Ground Motion Spectral Guidelines." This library contains recordings divided into magnitude and distance ranges, each containing 30 time histories. The applicant scaled each of the 30 time histories to match the response spectrum for the corresponding deaggregation earthquake.

Site Response Analysis. To determine the final site response, the applicant used the program SHAKE to compute the site amplification function for each deaggregation earthquake. The applicant paired the 60 randomized velocity profiles with the 60 sets of randomized shear modulus and damping curves (i.e., one velocity profile with one set of modulus reduction and damping curves). To obtain a site amplification function, the applicant divided the response spectrum from the computed surface motion by the response spectrum from the input hard rock motion. The applicant then computed the arithmetic mean of these 60 individual response spectral ratios to define the mean amplification function for each deaggregation earthquake. Figure 2.5.2-4, reproduced from Figure 4.2-23 in SSAR Appendix B, shows the computed high- and low-frequency average site amplification functions for the mean 10^{-4} hazard level deaggregation earthquakes. As shown in Figure 2.5.2-4, the ESP site subsurface amplifies the input hard rock motion over the fairly wide frequency range of 0.5 to 10 Hz, with the maximum amplification of 3.3 at a frequency of 1.7 Hz. The thick line shown in Figure 2.5.2-4 is the final site amplification function for each controlling earthquake and represents the weighted average of the amplification functions for the associated deaggregation earthquakes. The weights, listed above in Table 2.5.2-2, represent the relative contribution of earthquakes represented by

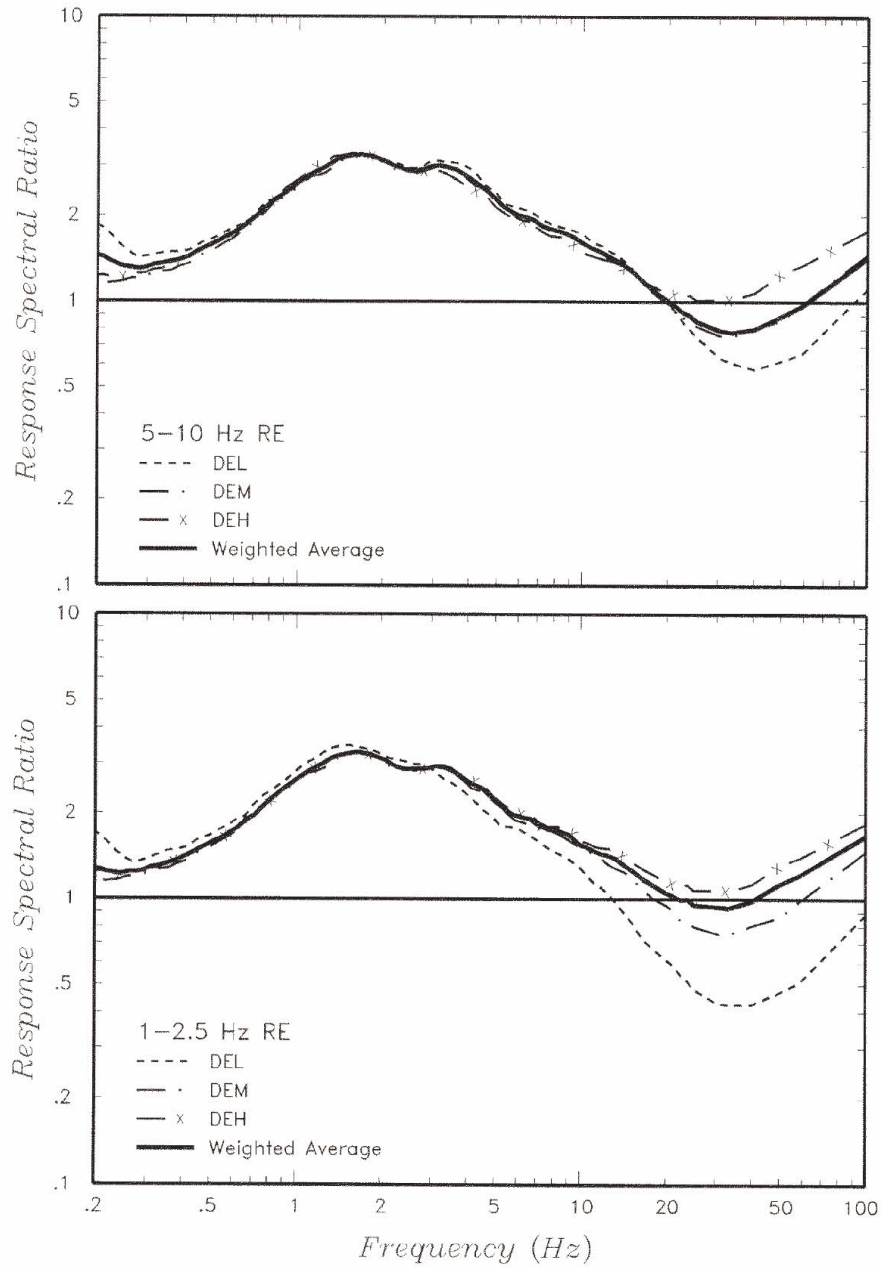

Seismic Hazards Report for the EGC ESP Site Mean Site Amplification Functions for Deaggregation Earthquakes and Weighted Average Site Amplification Functions for Reference Earthquakes for Mean 10^{-4} Hazard	Figure **4.2-23**

Figure 2.5.2-4 Mean site amplification functions for deaggregation earthquakes and weighted average site amplification functions for reference earthquakes for mean 10^{-4} hazard

the deaggregation earthquakes to the hazard at the appropriate spectral frequency and hazard level.

The applicant determined the final soil surface spectra for the ESP site by scaling the rock-controlling earthquake spectra by the mean site amplification functions. These spectra are shown below in Figure 2.5.2-5, reproduced from Figure 4.2-26 in SSAR Appendix B. The applicant enveloped the low- and high-frequency soil surface spectra with smooth envelope spectra, as shown in Figure 2.5.2-5.

Non-GDS

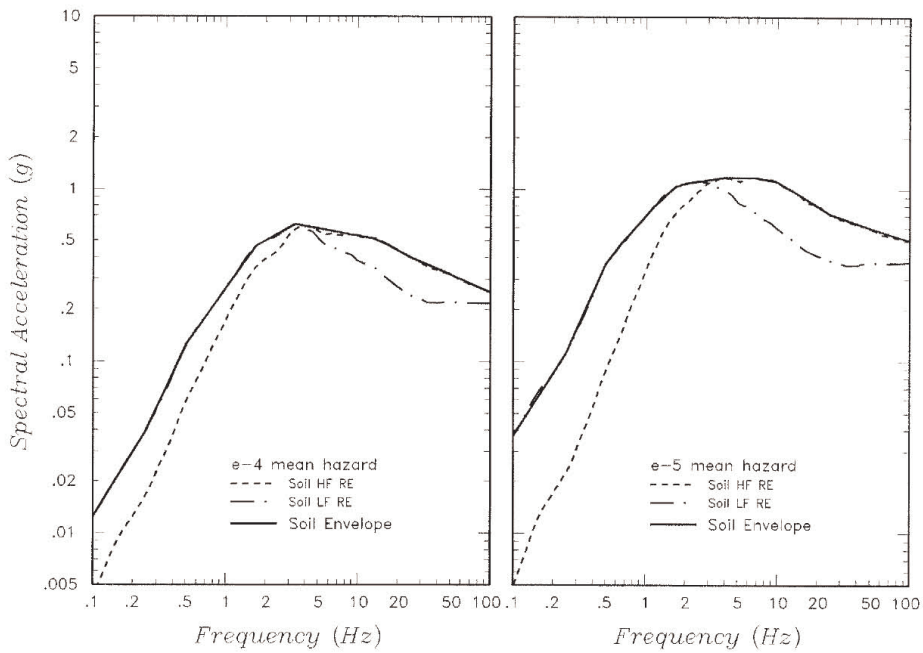

Seismic Hazards Report for the EGC ESP Site **Rock Reference Earthquake Spectra Scaled by Weighted Average Site Amplification Functions and Soil Envelope Spectra**	Figure **4.2-26**

Figure 2.5.2-5 Rock reference earthquake spectra scaled by weighted average site amplification functions and soil envelope spectra

2.5.2.1.6 Safe-Shutdown Earthquake

The method for determining the SSE for a site, as described in RG 1.165, is based on the use of a reference probability (R_p). The basis for the procedure in RG 1.165 and the determination of the reference probability is that existing nuclear power plants do not represent an undue risk to the health and safety of the public. As such, using existing plants as a reference, RG 1.165 recommends a procedure to determine the seismic design basis for future plants. The reference probability is the average probability of exceeding the SSE ground motion at 5 and 10 Hz using either the 1993 LLNL PSHA or the 1989 EPRI PSHA. A reference probability level was calculated for 29 nuclear power plant sites in the CEUS, and the median reference probability for these 29 sites, using median hazard results, is 10^{-5} per year. A similar value was obtained using both the 1993 LLNL and 1989 EPRI PSHAs; therefore, RG 1.165 endorses both the LLNL and EPRI PSHA results as being suitable for seismic hazard estimation for future siting. Concerning the R_p value, in SSAR Section 2.5.4.9, "Earthquake Design Basis," the applicant stated the following:

> These probabilities [Rp] were computed using ground motion models developed in the mid-to-late 1980's. As discussed in Regulatory Position 3 in Regulatory Guide 1.165, significant changes to the overall database for assessing seismic hazard in the CEUS warrants a change in the reference probability. The availability of the recently developed EPRI ground motion characterization for the CEUS (EPRI, 2003) represents a significant advancement in the seismic hazard database for the CEUS. Appendix B of Regulatory Guide 1.165 discusses that selection of another reference probability may be appropriate, such as one founded on risk-based considerations. That is the approach taken for developing the EGC ESP SSE design ground motions.

Rather than updating R_p and using the methodology described in RG 1.165 to determine the SSE ground motion, the applicant chose to use a different approach, which is described in the American Society of Civil Engineers (ASCE)/Structural Engineering Institute (SEI) Standard 43-05, "Seismic Design Criteria for Structures, Systems, and Components in Nuclear Facilities and Commentary." This new approach is referred to as a "performance-based" approach. The performance-based approach sets a goal or target of a mean annual frequency of 10^{-5} of unacceptable performance of nuclear structures, systems, and components (SSCs) as a result of seismically initiated events. Specifically, the performance-based approach is intended to achieve a mean 10^{-5} risk per year of core damage caused by seismic initiators. This safety performance goal is based on assuming a target 10^{-4} mean annual risk of core damage caused by all accident initiators and the assumption that seismic initiators contribute about 10 percent of the risk of core damage posed by all accident initiators.

To determine the SSE that achieves the annual performance goal of 10^{-5}, the performance-based approach scales the site-specific mean 10^{-4} uniform hazard response spectrum (UHRS), shown above in Figure 2.5.2-5, by a design factor (DF):

$$SSE = UHRS_{10^{-4}} \times DF \qquad (2.5.2\text{-}1)$$

where

$$DF = \mathbf{Max}(DF_1, DF_2)$$

and

$$DF_1 = 1.0$$

$$DF_2 = 0.6(A_R)^{0.8}$$

The amplitude ratio, A_R, is given by the ratio of 10^{-5} UHRS and 10^{-4} UHRS spectral accelerations for each spectral frequency. As shown in the above equations, the minimum value of DF for each spectral frequency is 1.0, which implies that the SSE will be equivalent to the 10^{-4} UHRS or higher, depending on the amplitude ratio. Table 2.5.2-3 shows the applicant's computation of the horizontal SSE using the two UHRS spectra and the DF for a select number of spectral frequency values.

Table 2.5.2-3 Computation of the Horizontal SSE Spectrum for the ESP Site

Spectral Frequency (Hz)	10^{-4} Mean UHRS (g)	10^{-5} Mean UHRS (g)	DF_2	DF	Horiz. SSE (g)
0.1	0.0129	0.0412	1.519	1.511	0.0196
0.5	0.1400	0.4160	1.434	1.434	0.2007
1.0	0.2970	0.8020	1.328	1.328	0.3945
2.5	0.6382	1.2561	1.031	1.031	0.6582
5.0	0.6570	1.2149	0.981	1.600	0.6570
10.0	0.5864	1.1065	0.997	1.079	0.6002
20.0	0.4599	0.7862	0.921	1.000	0.4599
50.0	0.3200	0.5791	0.914	1.000	0.3200
100.0 (PGA)	0.2660	0.4895	0.977	1.000	0.2660

Figure 2.5.2-6 shows the soil surface 10^{-4} (green line) and 10^{-5} (red line) mean UHRS and the applicant's performance-based SSE spectrum (black line). As shown in Figure 2.5.2-6 and above in Table 2.5.2-3, the final performance-based SSE is approximately equivalent to the 10^{-4} UHRS for spectral frequencies above 2.5 Hz.

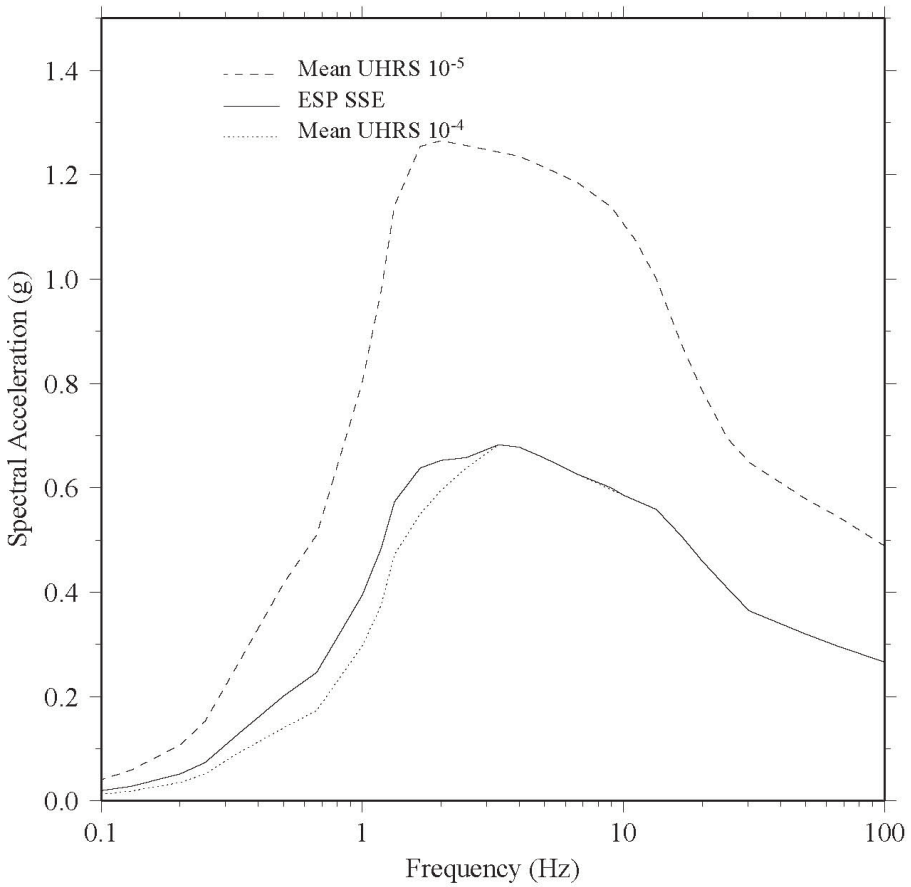

Figure 2.5.2-6 Comparison of performance-based SSE spectrum for the ESP site and the mean 10^{-4} and 10^{-5} UHRS

In RAI 2.5.2-1(a), the staff asked the applicant to justify the selection of the site-specific mean 10^{-4} UHRS as the appropriate starting point for determining the final SSE. In response to RAI 2.5.2-1(a), the applicant stated that the "design amplitude required to achieve the performance goal at each structural period can be calculated starting from the mean 10^{-4} annual probability level of the seismic hazard spectrum in the free field at the ground surface, or from the 10^{-5} annual probability level, or from any intermediate probability level." The applicant explained that it selected a 10^{-4} annual probability level as the starting point based on the precedent set in ASCE/SEI Standard 43-05.

In RAI 2.5.2-1(b), the staff asked the applicant to demonstrate that the SSE envelops the site-specific response spectra from the controlling earthquakes at the reference probability level (median 10^{-5} per year) recommended by RG 1.165 or to justify why this approach was not used to determine the SSE. In response to RAI 2.5.2-1(b), the applicant stated that it did not rely on the site-specific response spectra from the controlling earthquakes at the hazard reference probability level of median 10^{-5} per year to determine the site-specific SSE. Instead, the applicant used the performance-based approach in ASCE/SEI Standard 43-05 to determine the site-specific SSE.

In RAI 2.5.2-1(c), the staff asked the applicant to justify using SSC seismic fragility information, before the selection of a reactor design, to determine the site SSE. In response to RAI 2.5.2-1(c), the applicant stated that the performance-based approach "combines a conservative characterization of equipment/structure performance with ground motion hazard to establish risk-consistent SSEs, rather than only hazard-consistent ground shaking, as occurs using the hazard reference probability approach in Appendix B of RG 1.165."

2.5.2.1.6.1 Derivation of Performance-Based Approach

In RAI 2.5.2-7(b), the staff asked the applicant to provide the derivation of the DF (Equation 2.5.2-1) used to achieve the target performance goal of mean 10^{-5} per year. Using the applicant's response to RAI 2.5.2-7(b), supplemented by a review of ASCE/SEI Standard 43-05, NUREG/CR-6728, and papers by R.P. Kennedy ("Overview of Methods for Seismic PRA and Margins Analysis Including Recent Innovations," dated August 1999, and "Establishing Seismic Design Criteria to Achieve an Acceptable Seismic Margin," dated August 1997), the staff derived the equations and assumptions underlying the performance-based approach. The following SER subsections describe this derivation.

Seismic Hazard Curves. In order to achieve a site SSE that meets the target performance level, the performance-based approach stipulates both the site seismic hazard characteristics as well as the fragility characteristics of nuclear SSCs. The site seismic hazard characteristics are quantified by the PSHA seismic hazard curves and UHRS that cover a broad range of natural frequencies. Figure 2.5.2-7 below shows the mean seismic hazard curves on a log-log scale for the frequencies of 1, 2.5, 5, and 10 Hz for the EGC ESP site. These four seismic hazard curves indicate the mean annual rate of exceedance for different values of spectral acceleration (S_a) for each of the four natural frequencies. Specifically, these curves show the annual probability that the S_a exceeds a particular acceleration value for each of the seismic sources surrounding the ESP site. The hazard curves are developed by identifying and characterizing each seismic source in terms of magnitude recurrence and location as well as determining the ground motion at the site resulting from each source. SER Section 2.5.2.1.4 provides a complete description of the applicant's PSHA results for the ESP site.

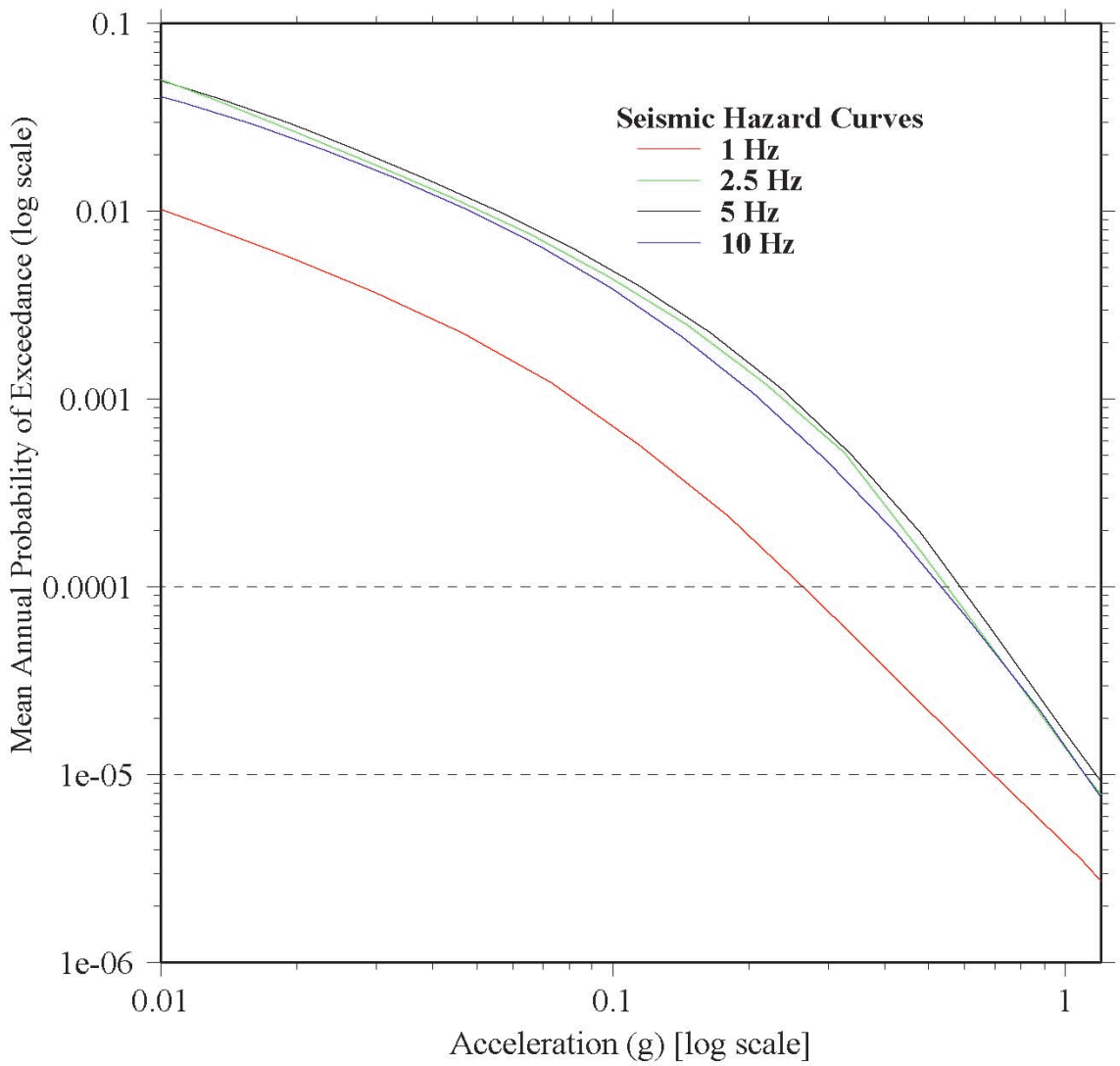

Figure 2.5.2-7 Four mean seismic hazard curves (1 Hz, 2.5 Hz, 5 Hz, and 10 Hz) for EGC ESP site plotted on a log-log scale. Dashed lines indicate annual probability of exceedance intervals of 10^{-4} per year and 10^{-5} per year.

Seismic Fragility. The performance-based approach uses the standard assumption that the seismic fragility of nuclear SSCs can be modeled using a lognormal distribution. The probability density function (PDF) for the lognormal distribution is given by

$$f_C(a;\mu,\sigma) = \frac{1}{\sqrt{2\pi}\sigma a}\exp\left\{-\frac{1}{2}\left[\frac{\ln a - \mu}{\sigma}\right]^2\right\}, a > 0 \qquad (2.5.2\text{-}2)$$

where μ and σ are the mean and standard deviation, respectively, of the related normal random variable $X = \ln(C)$. In the area of seismic fragility or capacity, β is used rather than σ to denote the standard deviation. Figure 2.5.2-8 shows lognormal probability density functions for a specified μ and four different β values from 0.3 to 0.6, which is the typical range of standard deviations for nuclear SSCs based on seismic probabilistic risk assessment (PRA) studies. The probability that a lognormally distributed random variable C is less than or equal to some specified value a is given by the cumulative distribution function (CDF)

$$P(C \le a) = F_C(a;\mu,\beta) = \Phi\left(\frac{\ln a - \mu}{\beta}\right) \qquad (2.5.2\text{-}3)$$

where Φ denotes the standardized normal distribution with a zero mean and standard deviation of one $F_Z(z; 0, 1)$. Seismic fragility curves are based on the lognormal CDF and express the probability of failure as a function of spectral acceleration or other ground motion parameter. Figure 2.5.2-9 shows seismic fragility curves for a specified μ and four different β values from 0.3 to 0.6. Important quantile values such as the median and lower and upper bounds are shown on the lognormal PDF and CDF curves, respectively, in Figures 2.5.2-10 and 2.5.2-11. The 1-percent quantile value is defined as the high-confidence-low-probability-of-failure (HCLPF) point and represents the seismic capacity corresponding to a 1-percent mean probability of failure. Quantile values (C_q) for the lognormal distribution are given by

$$C_q = \exp\left(\mu + Z_q\beta\right) \qquad (2.5.2\text{-}4)$$

where Z_q are quantile values from the standard normal distribution with a zero mean and standard deviation of one.

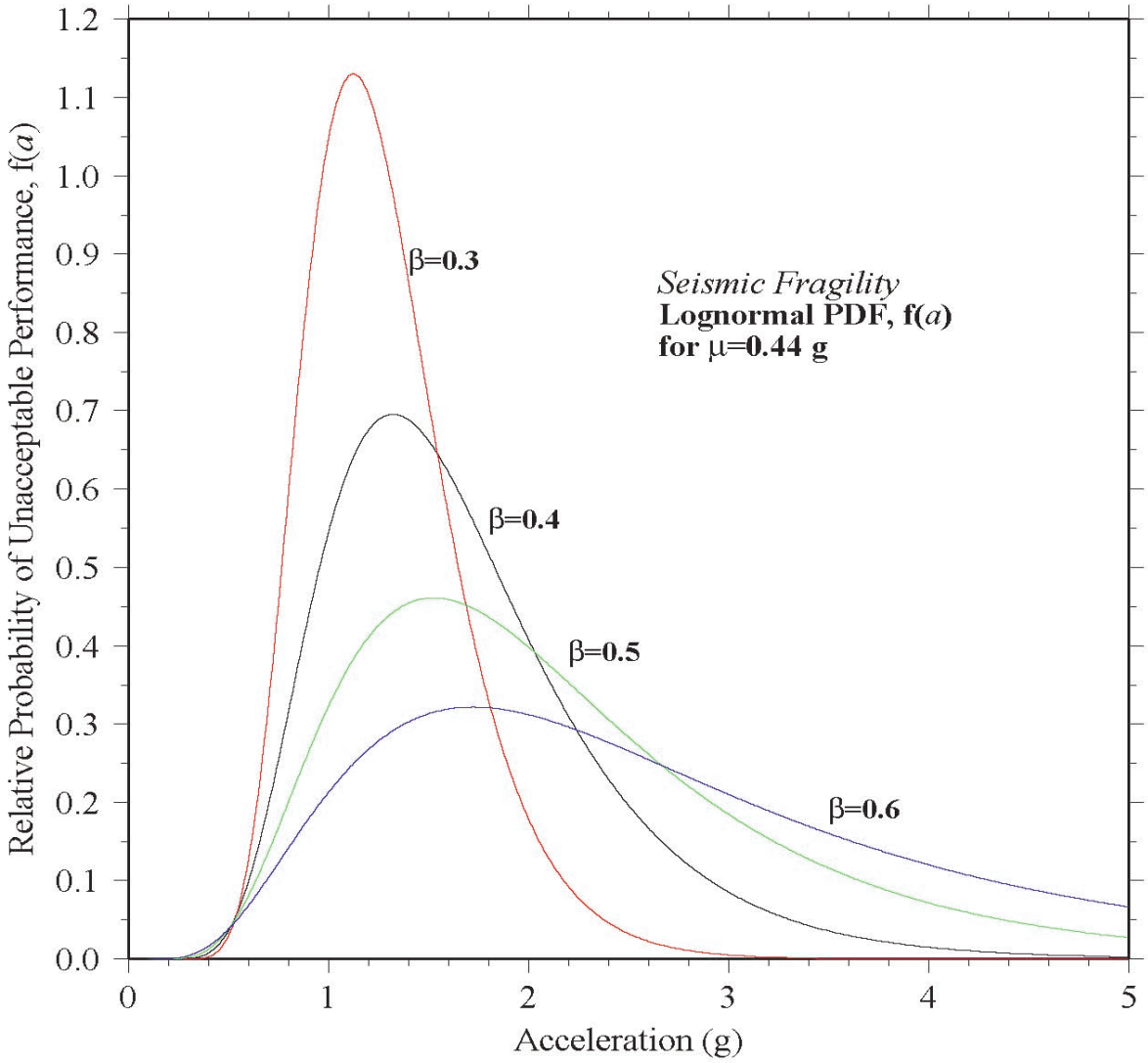

Figure 2.5.2-8 Lognormal PDF for different values of the lognormal standard deviation value, β

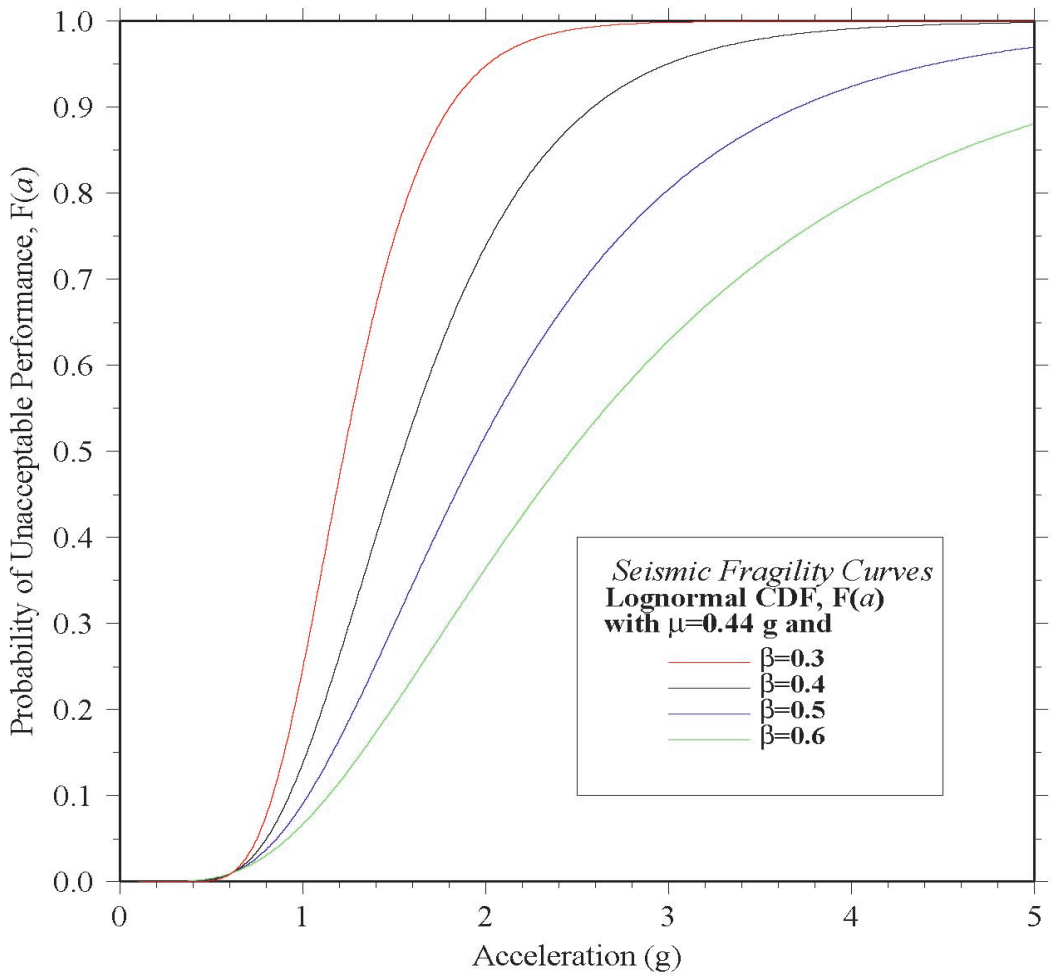

Figure 2.5.2-9 Lognormal CDF for different values of the lognormal standard deviation value, β. Lognormal CDF is used to model the seismic fragility of SSCs.

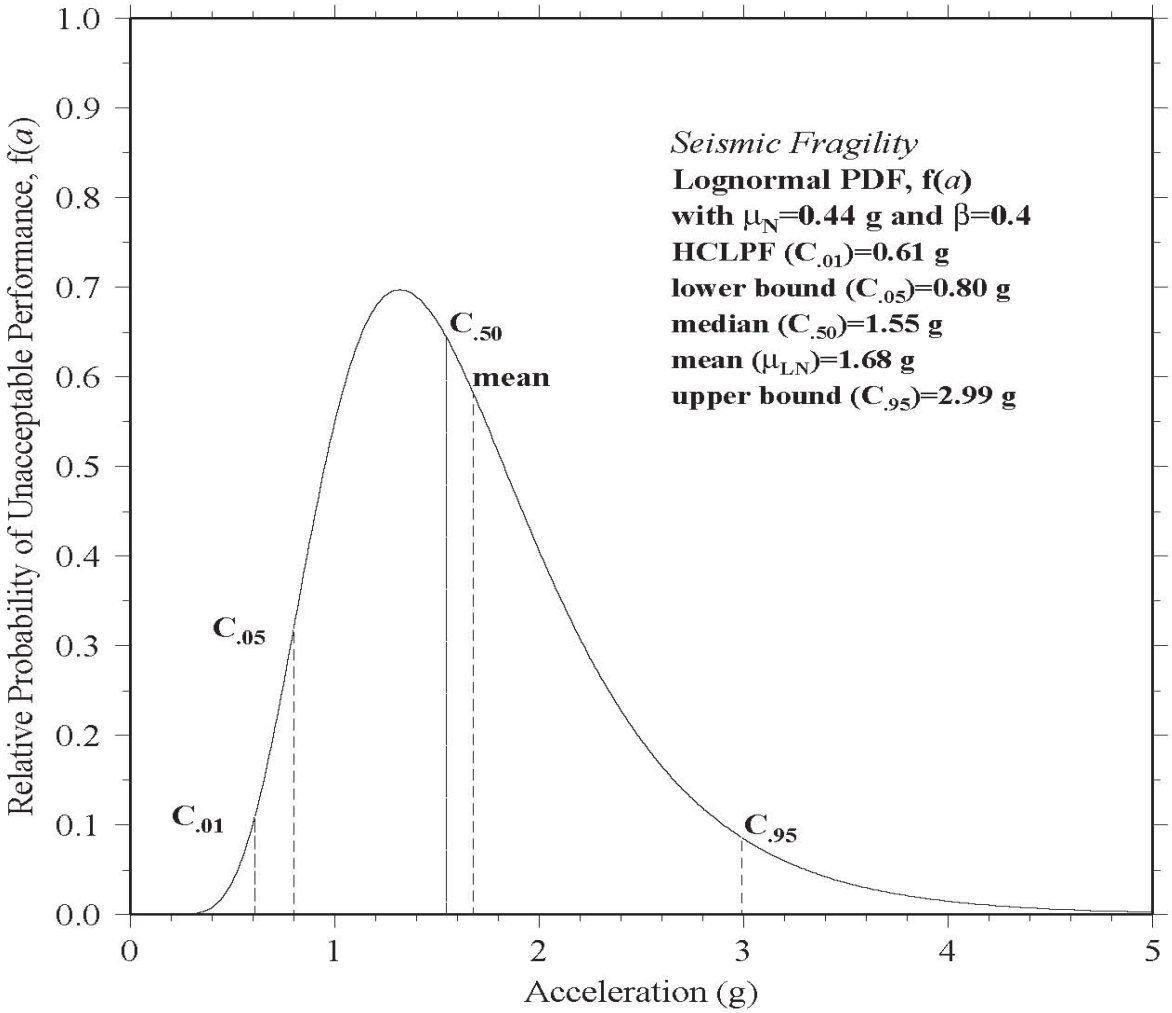

Figure 2.5.2-10 Significant parameter and quantile values for lognormal PDF, including the HCLPF value

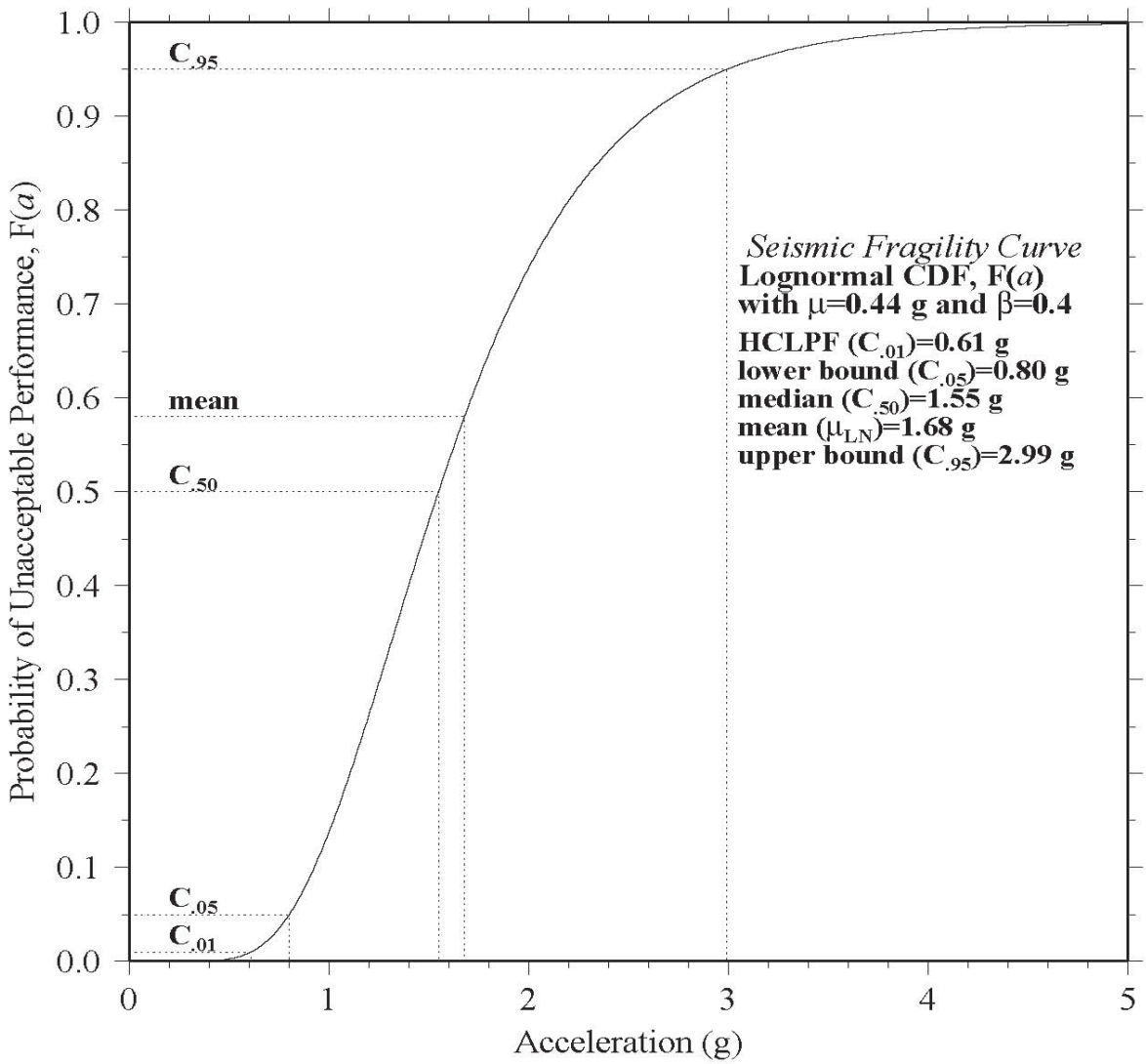

Figure 2.5.2-11 Significant parameter and quantile values for lognormal CDF, including the HCLPF value

Risk Integral. The starting point for the performance-based method is the risk integral, which is an application of the law of total probability:

$$P(B) = \sum_{i=1}^{n} P(B|A_i)P(A_i) \qquad (2.5.2\text{-}5)$$

where $P(B)$ and $P(A_i)$ denote the probabilities of events B and A_i, $P(B|A_i)$ denotes the conditional probability of event B given that event A_i has occurred, and n is the total number of possibilities for event A_i (the probabilities of which sum to unity).

When A is instead a continuous non-negative random variable, the law of total probability is expressed as

$$P(B) = \int_0^{\infty} P(B|A = a) f_A(a) da \qquad (2.5.2\text{-}6)$$

where $f_A(a)$ is the PDF for A.

Letting B denote failure (in a year), A denote the ground motion amplitude (demand), and C denote SSC seismic capacity (in terms of ground motion amplitude), the continuous expression of the law of total probability can also be expressed as

$$P(B) = \int_0^{\infty} P(B|C = a) f_C(a) da \qquad (2.5.2\text{-}7)$$

where $f_C(a)$ is the lognormal seismic capacity PDF given by Equation 2.5.2-2 above.

Recognizing that SSC failure (event B) can be expressed as event A greater than event C (i.e., demand greater than capacity), the conditional probability $P(B|C = a)$ can be rewritten as

$$P(B|C = a) = P(A > C|C = a) = P(A > a) = H(a) \qquad (2.5.2\text{-}8)$$

where $H(a)$ is the site seismic hazard curve. Combining the above two equations gives the risk integral, which forms the basis for the performance-based approach,

$$P_{FT} = \int_0^{\infty} H(a) f_C(a) da \qquad (2.5.2\text{-}9)$$

where *'a'* represents ground motion amplitude, P_{FT} is the target performance goal (10^{-5}), $H(a)$ is one of the mean seismic hazard curves for the site (see Figure 2.5.2-7) and $f_C(a)$ is the seismic SSC fragility curve expressed in terms of a lognormal PDF. In words, the risk integral states that the annual probability of failure P_{FT} is equal to the product of (1) the annual probability that the ground motion amplitude, or seismic demand, exceeds *'a'* and (2) the probability (within the

differential *da*) that the seismic fragility equals *'a'*, summed (or integrated) over all possible values of *'a'*.

To determine the SSE spectral acceleration value that achieves the target performance goal (P_{FT}) of 10^{-5}, the mean (μ) in the fragility lognormal PDF (Equation 2.5.2-2) can be written in terms of the *HCLPF* capacity using Equation 2.5.2-4 above:

$$\mu = \ln C_q - Z_q\beta = \ln C_{.01} - Z_{.01}\beta = \ln HCLPF + 2.326\,\beta \qquad (2.5.2\text{-}10)$$

Making this substitution provides an expression for the seismic fragility PDF in terms of the *HCLPF* capacity and the standard deviation, β. The *HCLPF* capacity can then be written in terms of the SSE by assuming that the *HCLPF* seismic capacity of SSCs will exceed the SSE ground motion by a seismic margin, M_s:

$$M_s = \frac{HCLPF}{SSE} \qquad (2.5.2\text{-}11)$$

The seismic fragility lognormal PDF then becomes:

$$f_C(a) = \frac{1}{\sqrt{2\pi}\beta a}\exp\left\{-\frac{1}{2}\left[\frac{\ln a - (\ln SSE \times M_s + 2.326\beta)}{\beta}\right]^2\right\} \qquad (2.5.2\text{-}12)$$

Substituting this expression for the fragility PDF into the risk integral (Equation 2.5.2-9) enables the determination of the SSE value that achieves the target performance goal of 10^{-5}. Figure 2.5.2-12 shows the EGC ESP seismic hazard curve for a natural frequency of 5 Hz along with the seismic fragility PDF, assuming specific values for the SSE, seismic margin (M_s), and standard deviation(β). Figure 2.5.2-13 shows the product of the seismic hazard and fragility curves. The spectral acceleration value that gives an area of 10^{-5} under the curve in Figure 2.5.2-13 is the value of the SSE for the natural frequency of 5 Hz.

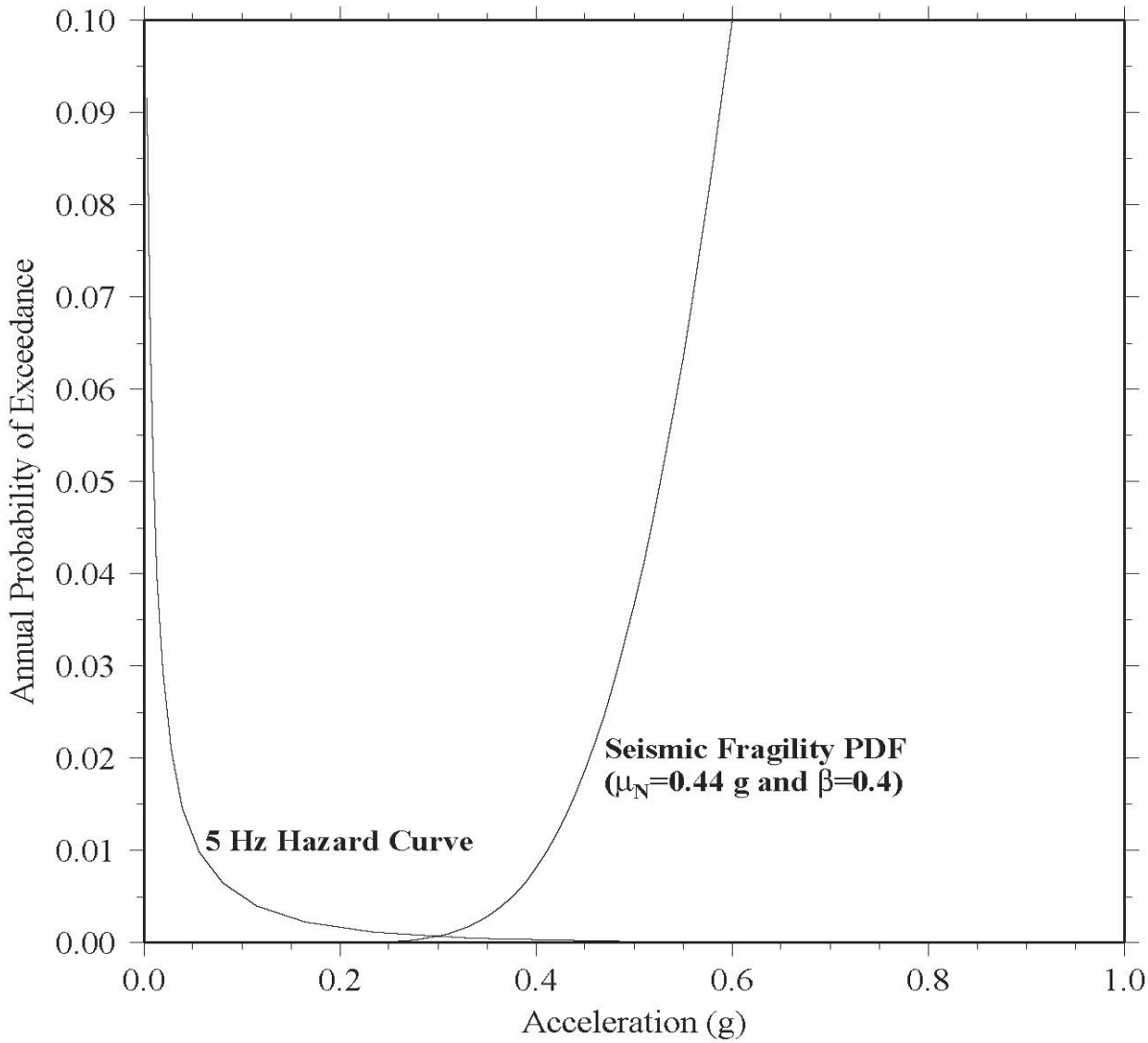

Figure 2.5.2-12 EGC ESP 5-Hz mean seismic hazard curve and seismic fragility curve in terms of the lognormal PDF

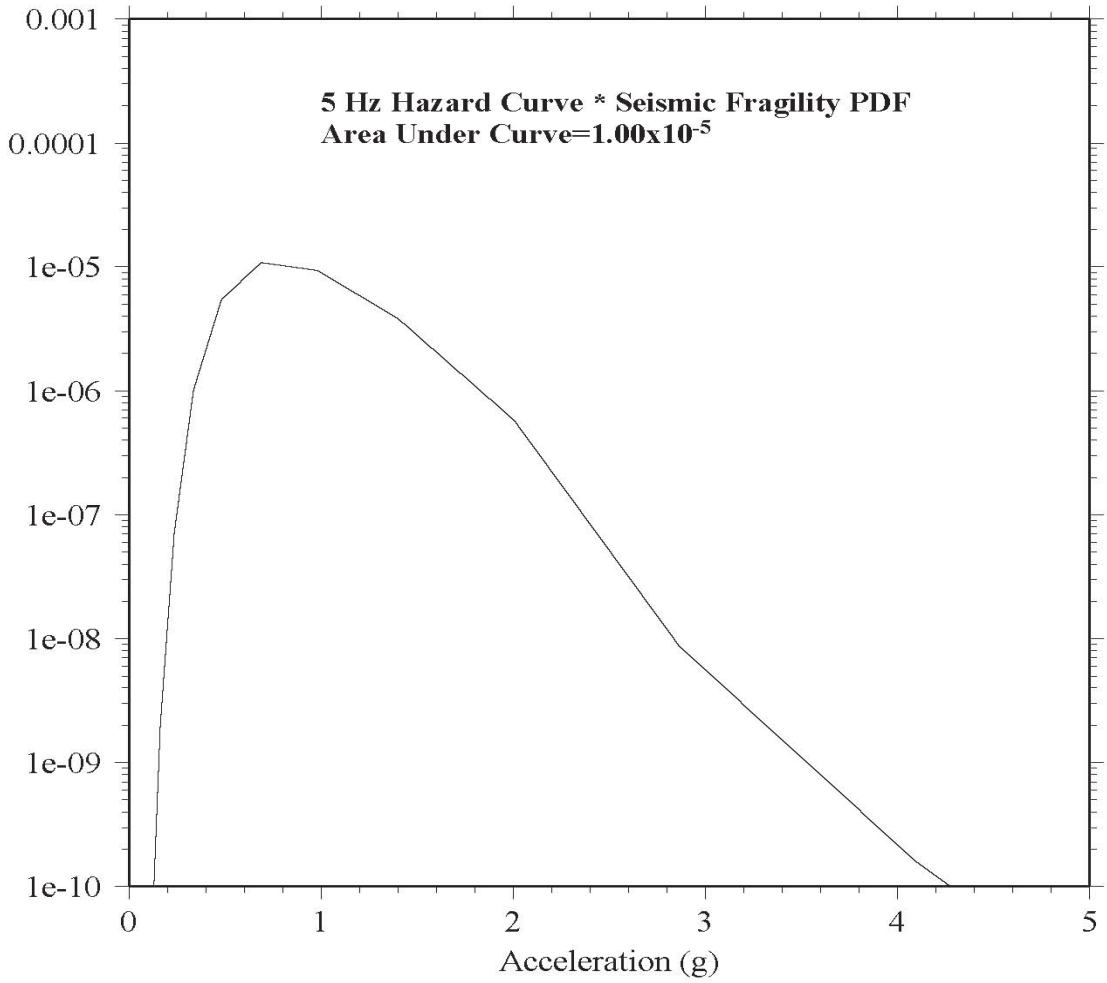

Figure 2.5.2-13 Product of EGC ESP 5-Hz mean seismic hazard curve and seismic fragility curve. Spectral acceleration value that gives an area of 10^{-5} under the curve is the SSE for 5 Hz.

Risk Equation. Rather than using the direct numerical integration approach, illustrated above, to determine the SSE that achieves the target performance goal for each natural frequency, the developers of the performance-based approach assume a functional form for the hazard curve, *H*(*a*). As shown previously in Figure 2.5.2-7, the seismic hazard curves are very close to linear in logarithmic space between the exceedance probabilities of 10^{-4} and 10^{-5}. Assuming a linear hazard curve in logarithmic space implies that the hazard curve can be expressed as

$$\log H(a) = b + m \log a \qquad (2.5.2\text{-}13)$$

where *b* and *m* are the intercept and slope, respectively, between the exceedance probabilities of 10^{-4} and 10^{-5} per year and the slope, *m*, as given by

$$m = \frac{\log 10^{-5} - \log 10^{-4}}{\log a_2 - \log a_1} = \frac{-1}{\log A_R} \qquad (2.5.2\text{-}14)$$

with $A_R = {}^{a_2}\!/_{a_1}$. The equation for the hazard curve, *H(a)*, is then given by

$$H(a) = 10^b a^{-1/\log A_R} = k a^{-1/\log A_R} \qquad (2.5.2\text{-}15)$$

with $k = 10^b$. Assuming this functional form for the hazard curve allows for a closed-form solution of the risk integral:

$$P_{FT} = \int_0^\infty \left\{ k a^{-1/\log A_R} \right\} \left(\frac{1}{\sqrt{2\pi} a \beta} \exp\left\{ -\frac{1}{2} \left[\frac{\ln a - \left(\ln SSE \times M_s + 2.326\beta \right)}{\beta} \right]^2 \right\} \right) da \qquad (2.5.2\text{-}16)$$

This closed-form solution is obtained by making the substitution $x = \ln a$, which reduces the risk integral to the form

$$\int_0^\infty Z(x) \exp(cx) dx \qquad (2.5.2\text{-}17)$$

where $c = {}^{-1}\!/_{\log A_R}$ is a constant and *Z(x)* is the PDF for a normal random variable with mean $\mu = \ln(SSE \times M_s) + 2.326\beta$ and standard deviation β. The solution to the risk integral is then given by

$$\exp\left\{ \mu c + \frac{1}{2} \beta^2 c^2 \right\} \qquad (2.5.2\text{-}18)$$

and solving for the SSE after substituting back in for μ and c gives

$$SSE = \frac{1}{M_s}\left[\frac{k \times g(\beta, A_R)}{P_{FT}}\right]^{\log A_R} \qquad (2.5.2\text{-}19)$$

where

$$g(\beta, A_R) = \exp\left\{\frac{-2.326\beta}{\log A_R} + \frac{1}{2}\left(\frac{\beta}{\log A_R}\right)^2\right\}$$

Since k and A_R are given by the intercept and slope of the hazard curve, respectively, only values for the seismic margin (M_s) and standard deviation of the seismic fragility (β) must be assumed. As shown above in Equation 2.5.2-15, the SSE decreases as the seismic margin increases. For this application of the performance-based approach, the seismic margin is assumed to be unity, and as such *HCLPF* = SSE for each SSC. A value for the standard deviation of the seismic fragility, β, must also be assumed in order to determine the SSE. Based on empirical evidence from past seismic PRA studies, the applicant stated that the range of anticipated β values is 0.3 to 0.6. For this application of the performance-based approach, β is assumed to be 0.4.

Rather than using Equation 2.5.2-19 above to determine the SSE value that achieves the target performance goal, the developers of the performance-based approach use the simpler expression given previously in Equation 2.5.2-1, which is repeated here for convenience:

$$SSE = UHRS_{10^{-4}} \times DF$$

where $UHRS_{10\text{-}4}$ is the uniform hazard spectral acceleration value for an exceedance probability of 10^{-4} per year and DF is the design factor. Substituting this expression for the SSE into Equation 2.5.2-19 above shows that DF is given by

$$DF = \frac{1}{M_s}\left[\frac{k \times UHRS_{10^{-4}}^{-1/\log A_R}}{P_{FT}}\, g(\beta, A_R)\right]^{\log A_R} \qquad (2.5.2\text{-}20)$$

Since the numerator of the ratio within the brackets is simply equal to P_{REF}, which is 10^{-4}, the DF becomes

$$DF = \frac{1}{M_s}\left[\frac{P_{REF}}{P_{FT}}\, g(\beta, A_R)\right]^{\log A_R} \qquad (2.5.2\text{-}21)$$

Substituting M_s = 1, P_{FT} = 10^{-5} and P_{REF} = 10^{-4} results in a function for *DF* that depends only on the amplitude ratio A_R and β. Rather than use this exact equation for *DF*, ASCE/SEI Standard 43-05 uses a close approximation given by Equation 2.5.2-1 above and repeated below for convenience:

$$DF = \max\left[0.6 \times \left(A_R\right)^{0.8}, 1.0\right]$$

Figure 2.5.2-14 shows a comparison between the "exact" *DF* (Equation 2.5.2-21) and the approximate *DF* (Equation 2.5.2-1). The approximate *DF* as a function of A_R is larger than the exact *DF*, which is a function of both A_R and β, except for β=0.3.

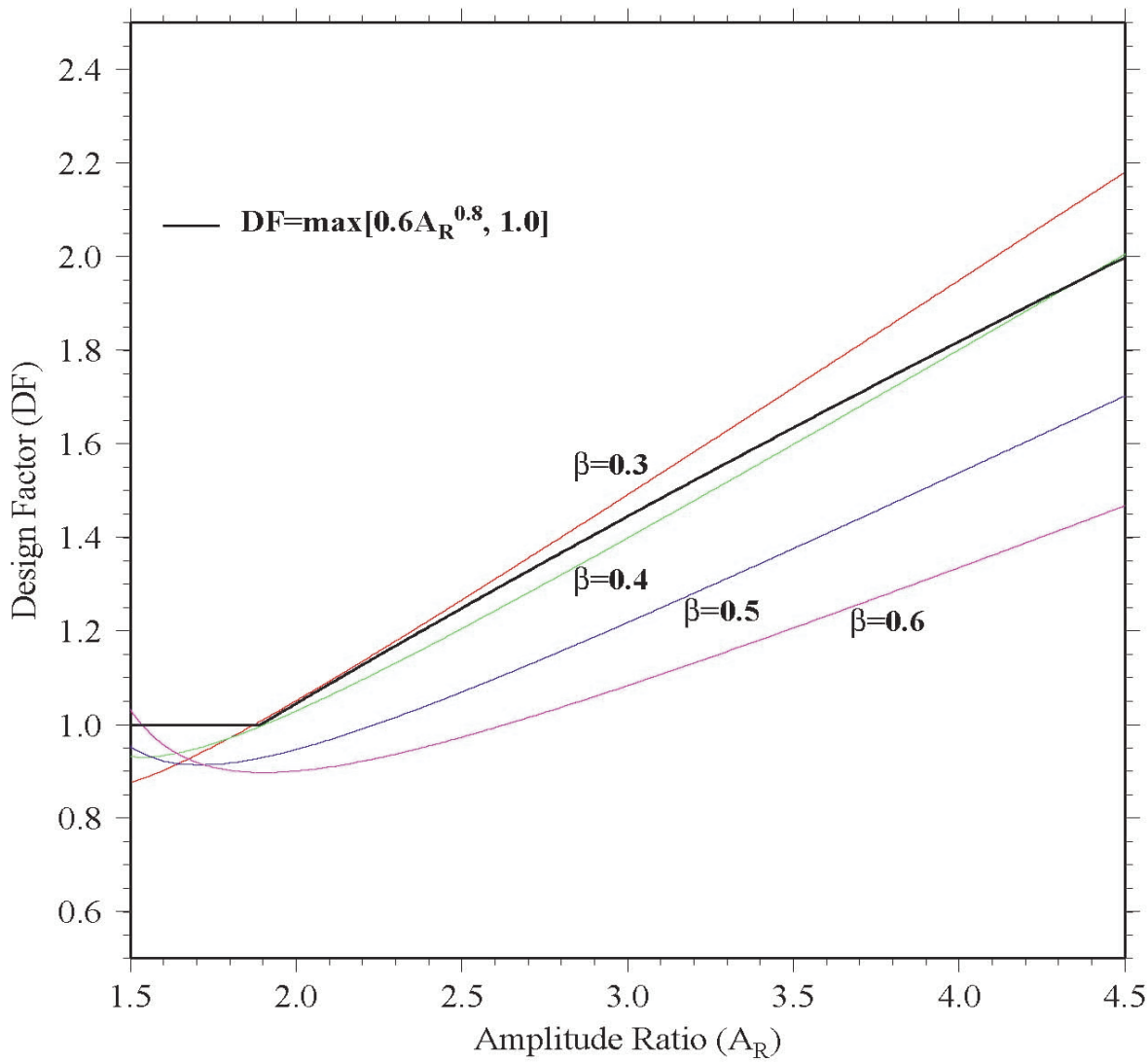

Figure 2.5.2-14 Comparison of exact and approximate *DF*. Exact *DF* varies with both A_R and β, while approximate *DF* depends only on A_R.

2.5.2.1.6.2 Target Annual Performance Goal

In RAI 2.5.2-7(a), the staff asked the applicant to justify the selection of the mean annual frequency of 10^{-5} as the safety performance target for the unacceptable performance of Category I SSCs as a result of seismically initiated events. In response to RAI 2.5.2-7(a), the applicant stated that the primary basis for the target 10^{-5} annual performance goal is from the results of seismic PRAs of 25 nuclear power plants (NUREG-1742, "Perspectives Gained from the IPEEE Program"), which show the median value for the mean seismic core damage frequency (SCDF) to be 1.2×10^{-5}. In addition, the applicant stated the following:

> The approach described in Section 2.5.2 of the EGC ESP SSAR is based on the recently approved ASCE/SEI Standard 43-05, *Seismic Design Criteria for Structures, Systems, and Components in Nuclear Facilities and Commentary*. This standard uses a mean 10^{-5} probability per year of "unacceptable performance of nuclear structures, systems, and components as a result of seismically initiated events" for nuclear power plants. As noted subsequently in this response, the quantitative goal of this performance-based approach is to achieve an annual frequency of seismically induced core damage frequency ([S]CDF) that is 10^{-5} or lower, when conservatively estimated by calculating the annual frequency of onset of significant inelastic deformation (FOSID) of structures, systems, and components (SSCs).
>
> Justification for the use of mean 10^{-5} per year as an appropriate performance goal is based on work that was published in 2002 as NUREG-1742, as summarized below.
>
> - The selection of mean 10^{-5} annual frequency of exceedance as an appropriate performance goal for generic models of SSCs is based on the results from seismic probabilistic risk assessments (PRA) that were performed for 25 operating nuclear facilities using an SSE ground motion spectrum. These PRAs achieved an annual mean [S]CDF of 10^{-5} or higher for seismic core damage for 50 percent of the operating power plants. The computed results were provided previously in the response to RAI 2.5.2-1. The summary table shows that a mean 10^{-5} annual frequency of core damage from seismic events corresponds to 50 percent of U.S. nuclear power plants where a full seismic PRA has been performed.
>
> - The annual frequency of onset of significant inelastic deformation (FOSID) of structures, systems and components is generally much less than failure of the SSC. Failure results in large inelastic deformations—leading to loss of containment or other unacceptable performance. As long as the SSCs remain essentially elastic in their performance—or have limited inelastic response—performance during the seismic event is considered acceptable. It is generally recognized that [seismic] core damage frequency ([S]CDF) is typically less than the highest SSC failure frequency—indicating that by using [S]CDF as a basis for design, the approach is conservative relative to other SSCs.

- By following the ASCE/SEI Standard 43-05 method, the target performance goal annual frequency is achieved so long as the seismic demand and structural capacity evaluations have sufficient conservatism to achieve both of the following:

  - Less than approximately a 1 percent probability of unacceptable performance for the SSE, and

  - Less than approximately a 10 percent probability of unacceptable performance for a ground motion equal to 150 percent of the SSE.

  Plants reviewed and approved using the USNRC Standard Review Plan guidelines have achieved at least these levels of conservatism.

- The mean 10^{-5} annual frequency of core damage represents a means for achieving safe plant design. Safe plant design is the underlying goal of developing the selected SSE spectrum as reflected in the first paragraph in 10 CFR 100.23:

  > *This section sets forth the principle geologic and seismic considerations that guide the Commission in its evaluations of the suitability of a proposed site and adequacy of the design bases established in consideration of the geologic and seismic characteristics of the proposed site, such that there is a reasonable assurance that a nuclear power plant can be constructed and operated at the proposed site without undue risk to the health and safety of the public ....*

  The requirement for no undue risk is met by determining an SSE spectrum that results in a plant that is as safe as the safest plants currently operating. The results of the seismic PRA analyses summarized above indicate that this objective is satisfied for a mean 10^{-5} frequency.

In summary, the applicant made four main points in response to RAI 2.5.2-7(a) in order to justify the value of mean 10^{-5} per year as an appropriate performance goal:

(1) The results from seismic PRAs, which were performed for 25 nuclear facilities, show an annual mean SCDF of 10^{-5} or higher for 50 percent of the operating power plants.

(2) Setting the performance goal of 10^{-5} to be equivalent to the annual FOSID of SSCs is conservative since the seismic demand resulting in the onset of significant inelastic deformation is less than that for failure of the SSC.

(3) The target 10^{-5} annual performance goal is achieved so long as seismic demand and structural capacity evaluations have sufficient conservatism, which is inherent for plants reviewed and approved using the SRP guidelines.

(4) The target 10^{-5} annual performance goal results in a plant that is as safe as the plants currently operating, as shown by the seismic PRAs.

The primary basis for the target 10^{-5} annual performance goal is from the results of seismic PRAs of 25 nuclear power plants (NUREG-1742), which show the median value for the mean SCDF to be 1.2×10^{-5}. Figure 2.5.2-15 below shows the results of the seismic PRAs from NUREG-1742 in terms of mean ground motion recurrence interval, which is the inverse of mean SCDF. Mean ground motion recurrence intervals for seismic core damage based on the seismic PRA results of 25 nuclear power plants vary from 4,000 to 5,263,158 years. In comparison, the FOSID value in terms of mean ground motion recurrence interval is set at 100,000 years for the performance-based approach.

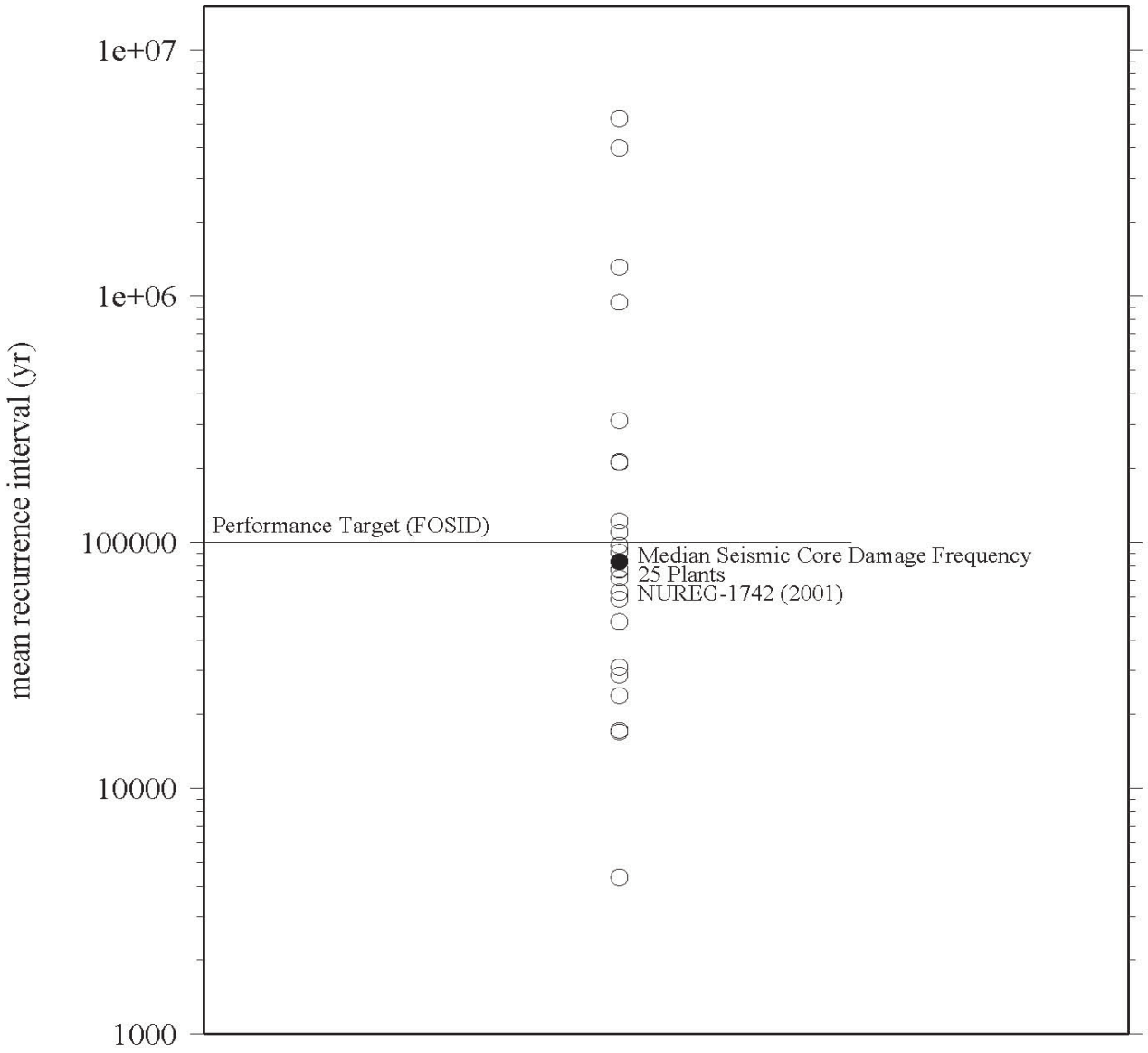

Figure 2.5.2-15 Seismic core damage in terms of mean ground motion recurrence interval for 25 nuclear power plants. For comparison, FOSID is also shown.

2.5.2.1.6.3 Vertical SSE

To compute the vertical SSE, the applicant used the vertical-to-horizontal (V/H) response spectral ratios provided in NUREG/CR-6728. The V/H response spectral ratios given in NUREG/CR-6728 are CEUS hard rock site conditions and depend on the PGA value of the horizontal SSE spectrum. For the ESP site, the V/H ratios used by the applicant are based on having a PGA less than 0.5g. The vertical SSE spectrum is given by multiplying the horizontal SSE spectrum by the V/H ratios. The applicant also considered the effects of the ESP site soil conditions on the vertical ground motions by using ground motion models that provide vertical motions for soil conditions. The applicant used a magnitude 6.4 earthquake at source-to-site distance of 15 km (9 mi) as input to the ground motion models. This magnitude and distance roughly correspond to the high-frequency controlling earthquake.

2.5.2.1.6.4 Design Response Spectrum

In SSAR Section 3.4.1.4.3, “Seismology,” the applicant compared the horizontal SSE for the ESP site with the RG 1.60, “Design Response Spectra for Seismic Design of Nuclear Power Plants,” design response spectrum (DRS) anchored to a PGA of 0.3g at 33 Hz, which is the DRS used by many of the current reactor designs. The applicant noted that the ESP SSE is lower than the RG 1.60 DRS except at frequencies between 16 and 50 Hz. The applicant stated that these exceedances are considered acceptable based on high-frequency evaluations discussed in a 1993 EPRI study, “Analysis of High-Frequency Seismic Effects.” The 1993 EPRI study recommends reduction factors for ground motion at 10 Hz and above because of the higher incoherence of high-frequency ground motion compared to low-frequency ground motion. These reduction factors are 10 percent for ground motion at a frequency of 10 Hz and increase to 20 percent for ground motion frequencies of 25 Hz and larger. The applicant stated that its ESP SSE, after applying the reduction factors, is completely enveloped by the RG 1.60 DRS. The applicant concluded by stating that the high-frequency exceedances of the RG 1.60 DRS by the ESP SSE are not significant, which indicates that the “EGC ESP site is suitable for any design based on the RG 1.60 DRS.” This is discussed further in SER Section 2.5.2.3.6.4. Figure 2.5.2-16 shows the horizontal and vertical SSEs as well as the RG 1.60 DRS anchored to a PGA of 0.3g.

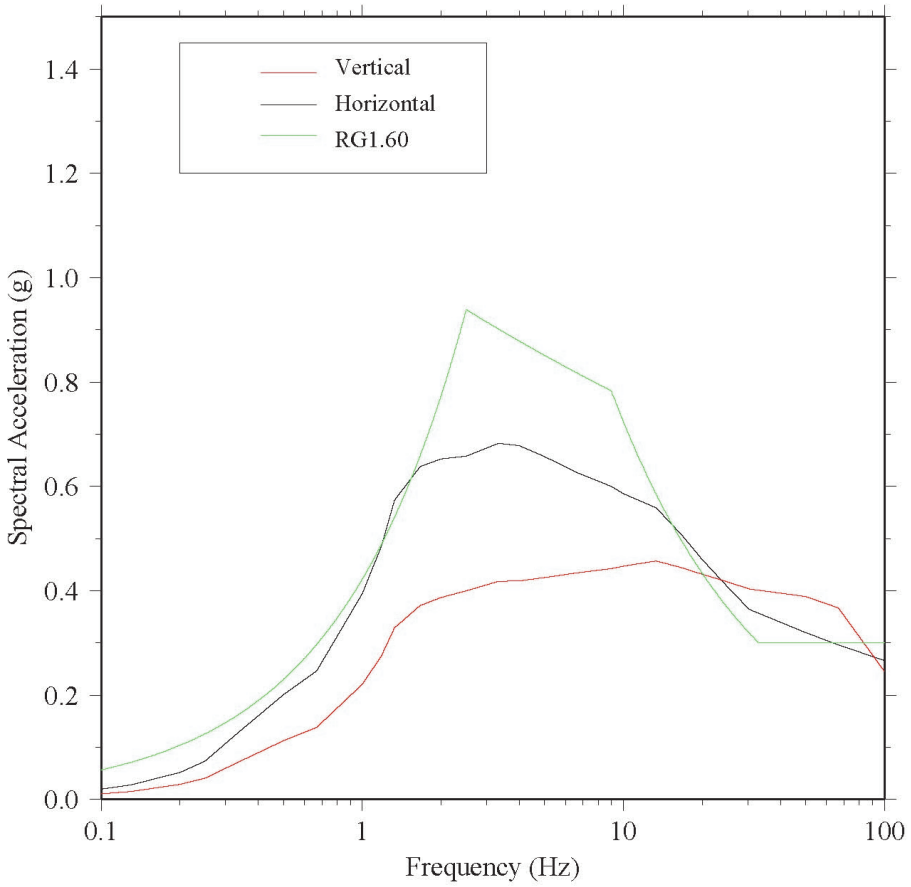

Figure 2.5.2-16 EGC ESP horizontal and vertical ESP SSE as well as the RG 1.60 DRS anchored at 0.3g

2.5.2.1.7 Operating-Basis Earthquake

SSAR Section 2.5.2.7 states that the applicant did not determine the OBE as part of the ESP application.

2.5.2.2 Regulatory Evaluation

SSAR Section 2.5.2 presents the applicant's determination of ground motion at the ESP site from possible earthquakes that might occur in the site region and beyond. In SSAR Section 1.5, the applicant stated that it developed the geological and seismological information used to determine the seismic hazard in accordance with regulations listed in Section 2.5.2 of RS-002, which include 10 CFR 50.34, "Content of Applications; Technical Information," Appendix S, "Earthquake Engineering Criteria for Nuclear Power Plants," to 10 CFR Part 50, and 10 CFR 100.23. The applicant further stated in SSAR Section 1.5 that it developed this information in accordance with the guidance presented in RG 1.165. The staff reviewed this portion of the application for conformance with the regulatory requirements and guidance applicable to the determination of the SSE ground motion for the ESP site, as identified below. The staff notes that the application of Appendix S to 10 CFR Part 50 in an ESP review, as referenced in 10 CFR 100.23(d)(1), is limited to defining the minimum SSE for design.

In its application review, the staff considered the regulatory requirements of 10 CFR 52.17(a)(1)(vi) and 10 CFR 100.23(c) and (d), which require that the applicant for an ESP describe the seismic and geologic characteristics of the proposed site. In particular, 10 CFR 100.23(c) requires that an ESP applicant investigate the geological, seismological, and engineering characteristics of the proposed site and its environs with sufficient scope and detail to support estimates of the SSE ground motion, and to permit adequate engineering solutions to actual or potential geologic and seismic effects at the proposed site. In addition, 10 CFR 100.23(d) states that the SSE ground motion for the site is characterized by both horizontal and vertical free-field ground motion response spectra at the free ground surface. Section 2.5.2 of RS-002 provides guidance concerning the evaluation of the proposed SSE ground motion, and RG 1.165 provides guidance regarding the use of PSHA to address the uncertainties inherent in the estimation of ground motion at the ESP site.

2.5.2.3 Technical Evaluation

This section of the SER provides the staff's evaluation of the seismological, geological, and geotechnical investigations the applicant conducted to determine the SSE ground motion for the ESP site. The technical information presented in SSAR Section 2.5.2 resulted from the applicant's surface and subsurface geological, seismological, and geotechnical investigations performed in progressively greater detail as they moved closer to the ESP site. The SSE is based upon a detailed evaluation of earthquake potential, taking into account regional and local geology, Quaternary tectonics, seismicity, and specific geotechnical characteristics of the site's subsurface materials.

SSAR Section 2.5.2 characterizes the ground motions at the ESP site from possible earthquakes that might occur in the site region and beyond to determine the site SSE spectrum. The SSE represents the design earthquake ground motion at the site and the vibratory ground motion for which certain nuclear power plant SSCs must be designed to remain functional. According to RG 1.165, applicants may develop the vibratory design ground motion for a new

nuclear power plant using either the EPRI or LLNL PSHAs for the CEUS. However, RG 1.165 recommends that applicants perform geological, seismological, and geophysical investigations and evaluate any relevant research to determine whether revisions to the EPRI or LLNL PSHA databases are necessary. As a result, the staff focused its review on geologic and seismic data published since the late 1980s that could indicate a need for changes to the EPRI or LLNL PSHAs.

2.5.2.3.1 Seismicity

The staff focused its review of SSAR Section 2.5.2.1 on the adequacy of the applicant's description of the historical record of earthquakes in the region. The earthquake catalog used in the original EPRI-SOG analysis is complete through 1984. To update the earthquake catalog, the applicant used information from NCEER, USGS, and ANSS. Next, the applicant compared the geographic distribution of earthquakes contained in the EPRI-SOG earthquake catalog (1777–1985) and the earthquakes in the updated catalog (1985–2002). The applicant stated that it found a very similar spatial distribution between the earthquake epicenters for the two time periods.

In addition to updating the EPRI-SOG earthquake catalog with more recent events, the applicant also added prehistoric earthquakes to the catalog, inferred from the evaluation of prehistoric liquefaction information in the ESP site region. These additions include earthquakes from the NMSZ, Wabash Valley-southern Illinois source zone, and the central Illinois basin/background source zone. The most notable addition to the catalog is the Springfield earthquake whose magnitude and location are inferred from paleoliquefaction features discovered approximately 30 miles southwest of the ESP site. These features are from an earthquake centered in the Springfield, Illinois, area that occurred between 5900 and 7400 years ago with an estimated magnitude range of 6.2 to 6.8.

The applicant also conducted paleoliquefaction studies to search for paleoliquefaction features within a 25–30-mile radius of the ESP site. After analyzing the field reconnaissance results, the applicant concluded that evidence for an earthquake comparable to the Springfield earthquake had not been observed in the study area. The applicant did discover some small-scale liquefaction features of probable mid-to-early Holocene age; however, these features were not widespread and likely resulted from a low-magnitude event. In RAI 2.5.2-6, the staff asked the applicant to explain its selected paleoliquefaction study area along the streams near the ESP site. In response, the applicant stated that it selected locations along the Salt Creek, Sangamon River, and Mackinaw River to supplement previous liquefaction studies in this area. SER Section 2.5.1.3.1 provides a complete description of RAI 2.5.2-6 and the staff's evaluation of the applicant's response.

Because the applicant used the EPRI-SOG seismicity catalog, which is part of the 1989 EPRI seismic hazard study that the NRC endorsed, the staff concludes that the seismicity catalog used by the applicant is complete and accurate for the time period 1777–1985. The staff compared the applicant's update of the regional seismicity catalog with its own listing of recent earthquakes and, as a result, concurs with the applicant's assertion that the rate of seismic activity has not increased in the ESP site region since 1985. In addition, the staff reviewed the paleoearthquakes that the applicant added to its earthquake catalog based on evidence from paleoliquefaction features discovered in the NMSZ, WVSZ, and central Illinois seismic zone.

The staff concludes that the earthquake catalog used by the applicant is complete and provides a conservative estimate of earthquake magnitudes and locations for the ESP site region.

2.5.2.3.2 Geologic Structure and Tectonic Activity

The staff focused its review of SSAR Section 2.5.2.2 on the applicant's characterization of potential seismic sources in the region surrounding the ESP site. As part of its evaluation of the geologic structure and tectonic activity for the ESP site, the applicant performed a detailed update of the structural features (folds and faults) within the site region. The applicant concluded that the results of the information update on the structure features show that the general structural picture remains the same. Chapter 2 of SSAR Appendix B provides a description of each of the folds and faults surrounding the ESP site. Rather than attempting to characterize the seismic potential of these folds and faults, the applicant defined broad seismic source zones that encompass these structural features. Within a 200-mile radius of the site (or just beyond), the two major sources of potential earthquakes are the NMSZ and WVSZ. In addition to the NMSZ and WVSZ, evidence from recent paleoliquefaction studies indicates that significant earthquakes have occurred in the central Illinois basin, where there are no obvious folds or faults at the surface. Although the size, location, and recurrence of such events are not well constrained, the applicant developed a background source zone for this region, referred to as the central Illinois basin background source zone. The staff's evaluation of the applicant's characterization of these areal seismic sources for its PSHA is provided in SER Section 2.5.2.3.3.

In addition to evaluating regional structural folds and faults, the applicant also evaluated the regional tectonic setting for the ESP site using the most recent results from a GPS network in southern Illinois. The applicant reported that given the current level of error in individual GPS observations, an extended period of time will be required before these observations can fully characterize the regional strain field. The applicant also found that recent geodetic measurements in the NMSZ indicate that the rate of strain accumulation is below the current detection threshold; however, these observations are not inconsistent with a model of seismicity in intraplate regions occurring along weak zones in the crust.

The staff reviewed the applicant's description of the individual structural features (folds and faults) for completeness and accuracy. SER Section 2.5.1.3.1 provides the staff's review of the applicant's description. The staff concurs with the applicant's decision to use large areal seismic source zones rather than attempting to characterize the seismic potential of each of the regional structural features. Both the LLNL and EPRI PSHA seismic source models, endorsed by RG 1.165, use this approach. As described in SER Section 2.5.2.3.3, the applicant updated the EPRI-SOG source model for its PSHA for the ESP site.

2.5.2.3.3 Correlation of Earthquake Activity with Geologic Structure or Tectonic Province

The staff focused its review of SSAR Section 2.5.2.3 on the applicant's updating of the original EPRI-SOG seismic source and ground motion models for its PSHA for the ESP site. The applicant based its update on an evaluation of recent geological and seismological information. The specific areas that the applicant focused on for each of the three major seismic source zones (NMSZ, WVSZ, and central Illinois) are earthquake recurrence rates, maximum magnitudes, and ground motion attenuation.

Earthquake Recurrence Rates. The applicant compared the updated seismicity catalog with an additional 17 years of earthquake data to the original EPRI-SOG catalog and found that the recurrence rates used for the EPRI-SOG study are still valid. In addition to the smaller recorded events over the past 17 years, the applicant also added earthquakes that have occurred in the three source zones as revealed by paleoliquefaction studies. The applicant found that for the central Illinois basin and the WVSZ, the fit of earthquake recurrence relationships to the recorded seismicity envelops the rates of larger earthquakes estimated from paleoliquefaction data. However, for the NMSZ, the applicant found that recent paleoliquefaction data provide evidence that large-magnitude earthquakes have occurred on NMSZ faults more frequently than the seismicity rates specified in the EPRI-SOG source characterizations for NMSZ.

As described in SER Section 2.5.2.1.3, the applicant used the characteristic earthquake model for the occurrence of large earthquakes in the NMSZ. The characteristic earthquake model states that certain fault segments tend to move by approximately the same distance in each earthquake, implying that individual faults repeatedly generate earthquakes of similar size at or near their maximum magnitude. For the NMSZ, the three fault sources that the applicant modeled with the characteristic approach are the NS fault, NN fault, and RF. Based on the characteristic earthquake model, these three faults within the NMSZ have repeatedly generated similar sized earthquakes during each of the previous NMSZ earthquake sequences, including the most recent 1811–1812 sequence. The best constraints on recurrence of characteristic NMSZ events are from paleoliquefaction studies throughout the New Madrid seismic region and paleoseismic investigations of the RF scarp and associated fold. Based on these studies, researchers have found that NMSZ characteristic earthquake sequences have occurred around AD 1450 ± 150, AD 900 ± 100, AD 490 ± 50, AD 300 ± 200, and BC 1370 ± 970, in addition to the recent 1811–1812 sequence. The applicant fit the recurrence intervals between these dates with two recurrence models, a Poissonian model and a lognormal model, weighing each model equally. In addition, for each of these NMSZ earthquake sequences, the applicant determined, based on its review of the literature, that the RF has ruptured in each of the previous sequences but the NN and NS sources may not have produced large earthquakes in all three sequences. The applicant used these observations to set the relative frequency of event sequences in the NMSZ as (1) rupture of all three sources (NN, RF, and NS) one-third of the time, (2) rupture of NN and RF one-third of the time, and (3) rupture of NS and RF one-third of the time.

In RAI 2.5.2-5, the staff asked the applicant to justify its modeling of the relative frequency of event sequences in the NMSZ. Specifically, the staff noted that Tuttle et al. (2002) concluded that all three sources (RF, NN, and NS) ruptured in each of the three sequences, but that one-third of the time the NN rupture may have been smaller than for the 1811–1812 sequence, and one-third of the time NS may have been smaller than in 1811–1812. Tuttle et al. (2002) also concluded that these smaller earthquakes are at least magnitude 7 events. This result differs from the event sequence modeling used by the applicant for NMSZ, which does not include NN or NS for some of the event sequences. The applicant responded to RAI 2.5.2-5 by stating the following:

> For the seismic source model developed for the New Madrid characteristic earthquakes in Appendix B of the EGC ESP SSAR, Figure 6 of Tuttle et al. (2002) was used to infer that previous ruptures of the New Madrid North and New Madrid South faults may have been approximately one magnitude unit

> smaller than the estimated site of the 1811–1812 ruptures. The magnitudes for the 1811–1812 sequence shown on Figure 6 of Tuttle et al. (2002) were those developed by Johnston (1996). The information presented on Figure 6 of Tuttle et al. (2002) was used to infer the relative size of ruptures of the New Madrid North and New Madrid South faults in the 1450 and 900 sequences compared to the 1811–1812 ruptures. Thus, if the size of the 1811–1812 ruptures on these faults were in the low magnitude M 7 range (e.g., values estimated by Bakun and Hooper, 2003), then the size of previous ruptures would have been below magnitude M 7. These smaller ruptures, which would be considered dependent events, were not included in the hazard calculations as characteristic earthquakes. The rupture model developed for the New Madrid characteristic earthquake sources in the EGC ESP Application consisted of three possible sequences, each occurring with a relative frequency of 1/3. One sequence consisted of full ruptures of all three New Madrid faults; one sequence consisted of full rupture of the New Madrid North and Reelfoot thrust faults, with the rupture of the New Madrid South fault being approximately one magnitude unit smaller than the 1811 rupture (this smaller dependent event was not included in calculating the hazard); and one sequence consisted of the full rupture of the New Madrid South and Reelfoot thrust faults, with the rupture of the New Madrid North fault being approximately one magnitude unit smaller than the 1811 rupture (this smaller dependent event was not included in calculating the hazard).

For two of the three NMSZ earthquake sequence models, the applicant considered either the NN or NS a smaller dependent event and, as such, did not include this smaller event for its calculation of the hazard. Dependent events are generally considered to be aftershocks of the main event, and, although dependent events can cause significant damage, a PSHA is intended to evaluate the hazard from discrete, independent releases of seismic energy. Therefore, dependent events are removed from the seismicity database before calculating the final PSHA hazard curves. However, the difference in magnitude between the three earthquakes in the NMSZ sequences is uncertain; therefore, the applicant's decision to identify either the NN or NS as smaller dependent events (for two of the three sequences) and not include them in the hazard calculation is questionable. In its response to RAI 2.5.2-5, the applicant stated that it discussed its NMSZ event sequence modeling with Dr. Tuttle since the model is based on an interpretation of Figure 6 of Tuttle et al. (2002). The applicant stated the following regarding its discussion with Dr. Tuttle:

> In addition, recent discussions with Dr. Tuttle indicate that she considers that the difference between the size of the 1811–1812 earthquakes and those of the 900 and 1450 sequences are likely to be smaller than what was portrayed in Figure 6 of Tuttle et al. (2002). Consequently, a revised model for New Madrid sequences was developed consisting of two alternative models for earthquake sequences. In Model A, all ruptures are similar in size to the 1811–1812 earthquakes. Model B is similar to the model used in PSHA for the EGC ESP Application in that 1/3 of the sequences contain a smaller rupture of the New Madrid North fault and 1/3 of the sequences contain a smaller rupture of the New Madrid South fault. However, the difference in magnitude from the 1811–1812 ruptures was set to be no more than ½ magnitude unit, and no ruptures were allowed to be less than M 7. In addition, all three earthquakes were included in

> the hazard calculation in all rupture sequences. Model A (always full ruptures) was given a weight of 2/3 and Model B a weight of 1/3 based on Dr. Tuttle's expression of the difficulties in estimating the size of the pre 1811–1812 ruptures and her judgment that the difference between the rupture sizes was likely smaller than that proposed in Tuttle et al. (2002). The hazard resulting from this revised model for rupture sequences combined with the updated magnitude distribution (response to RAI 2.5.1-1) is shown on the curves labeled "Revised magnitudes and sequences" on Figure 2.5.2-5-1. These results produce approximately 9 to 10 percent higher ground motions at the mean 10^{-4} and mean 10^{-5} hazard levels.

The staff reviewed the Tuttle et al. (2002) paper and found that the authors' "preferred interpretation of prehistoric sand blows" is that "at least two earthquakes occurred in A.D. 1450 and A.D. 900 that were similar in size and location to the largest 1811–1812 earthquakes." Based on this statement, the staff concurs with the applicant's revised modeling as described above in response to RAI 2.5.2-5. The staff notes that the applicant found that the hazard resulting from this revised model for rupture sequences combined with the updated magnitude distribution (response to RAI 2.5.1-1) produce approximately 9 to 10 percent higher ground motions at the mean 10^{-4} and mean 10^{-5} hazard levels. In summary, regarding the updated information for the NMSZ (magnitude distribution for rupture sets and ruptures sequence models), the applicant stated the following in its response to RAI 2.5.2-5:

> The assessment of the size of the 1811–1812 earthquakes and the likely scenarios for future ruptures continues to be an area of active research, and thus it is possible that the assessments presented in the ESP Application will undergo future evolution. It is expected, however, that the effects of these changes will be on the order of those presented in the sensitivity analyses presented in this response, and the calculated 1-Hz ground motions corresponding to the mean hazard in the 10^{-4} and 10^{-5} range will vary from those presented in the ESP Application by plus or minus 10 percent or less. A revision to the EGC ESP Application, therefore, is not warranted at this time.

The staff considers the applicant's rationale for not updating its seismic hazard characterization of the NMSZ to be inadequate. In response to the staff's RAIs, the applicant has updated both the magnitudes for the NMSZ characteristic earthquake rupture sets (RAI 2.5.1-1) and rupture sequence modeling (RAI 2.5.2-5). However, for both updates, the applicant only performed limited sensitivity analyses and did not update either its PSHA or SSE. The staff considers both of these updates to the NMSZ characteristic earthquake modeling to be of sufficient importance to justify updating both the PSHA and SSE for the ESP site. In Open Item 2.5.1-1, the staff asked the applicant to incorporate this newer information into its PSHA or SSE and to update the SSAR to reflect the corrected magnitude estimates and rupture sequence modeling. In response, the applicant updated its source characterization of the New Madrid earthquakes, including both the magnitudes for the NMSZ characteristic earthquake rupture sets and rupture sequence modeling. These changes have been incorporated into Revision 1 of the ESP application. Therefore, the staff considers Open Item 2.5.1-1 to be resolved.

In conclusion, as described above, the staff concurs with the applicant's decision to incorporate the characteristic earthquake model for the large NMSZ earthquakes into the original

EPRI-SOG model. In addition, the staff concurs with the applicant's use of the most recent models for the NMSZ rupture sequences.

Maximum Magnitudes. The applicant focused on the maximum magnitude values for the NMSZ, WVSZ, and central Illinois background seismic source zone, since these three zones are the main contributors to the total seismic hazard at the ESP site. For the NMSZ, the applicant concluded that the maximum magnitudes used for the EPRI-SOG model (7.2 to 8.8) are consistent with the more recent maximum magnitude evaluations (7.4 to 8.2). For the WVSZ, the maximum magnitudes range from 5.0 to 8.0, while recently published maximum magnitudes range from 7.0 to 7.8. Similarly, for the central Illinois background source zone, the maximum magnitudes used for the EPRI-SOG model range from 4.3 to 7.6, while recently published maximum magnitudes range from 6.0 to 7.0. As a result, the applicant concluded that the maximum magnitude values for both the WVSZ and central Illinois source zone need to be increased to reflect the magnitudes implied by recent paleoliquefaction studies.

The staff reviewed the NMSZ, WVSZ, and central Illinois source zone maximum magnitudes used by the applicant for its PSHA for the ESP site. The staff concurs with the applicant's conclusion that the EPRI-SOG maximum magnitudes for the NMSZ adequately cover the range of magnitudes estimated from recent geologic investigations, as described above. For the WVSZ, the staff reviewed the revised maximum magnitude range used by the applicant to verify its consistency with recent paleoliquefaction studies. The magnitude of the largest paleoearthquake in the lower Wabash Valley (the Vincennes-Bridgeport earthquake), which occurred 6011 ± 200 years ago, was estimated to be between 7.2 to 7.8. The next largest earthquake in the WVSZ has an estimated magnitude of about 7.1 to 7.2 and occurred 12,000 ± 1,000 years ago. The applicant used the following maximum magnitude range for the Wabash Valley region—M 7.0 (0.1), M 7.3 (0.4), M 7.5 (0.4), and M 7.8 (0.1). Based on the magnitudes of these two paleoearthquakes, the staff considers that the applicant's maximum magnitude range and weighting are appropriate for the WVSZ.

For its update of the maximum magnitudes of the central Illinois basin/background source zone, the applicant used a 1994 EPRI study that specifically addresses the problem of defining a maximum magnitude for seismic source regions that are characterized by the rare occurrence of maximum earthquakes without well-defined seismicity patterns associated with seismic sources. The 1994 EPRI study developed worldwide databases that could be used for assessments of maximum magnitudes for seismic sources in the CEUS. Using the database and method found in the 1994 EPRI study, the applicant developed the following maximum magnitude range for earthquakes in the central Illinois source zone—M 6.2 (0.4), M 6.4 (0.3), M 6.6 (0.2), and M 6.8 (0.1). This range of maximum magnitudes is strongly influenced by the estimated M 6.2 to 6.8 Springfield earthquake, which occurred about 6000 years ago about 30 miles to the southwest of the ESP site. In RAI 2.5.2-4, the staff asked the applicant to provide further detail and justification regarding its use of the 1994 EPRI study and accompanying worldwide database of earthquakes. Specifically, the staff requested the applicant to explain why its maximum magnitude for central Illinois should not be set at 6.8 since the two largest SCR earthquakes from nonextended crust are the Accra, Ghana, earthquake of 1862 (M 6.75 ± 0.35) and the Meeberrie, Western Australia, earthquake of 1941 (M 6.78 ± 0.25). In its response to RAI 2.5.2-4, the applicant stated the following regarding its use of the 1994 EPRI study and its maximum magnitude for central Illinois:

The EPRI-SOG assessments of seismic source characteristics in the CEUS did not start with the assumption that maximum magnitude is the same throughout the region or even throughout regions with similar characteristics. The EPRI-SOG assessments of maximum magnitude for the central Illinois source zone needed to be updated because of new information—the discovery of the Springfield paleo-earthquake. This update could have been performed using the EPRI-SOG approach—expert elicitation, but this would require a major study comparable to the EPRI-SOG program. As an alternative, the Johnston et al. (1994) Bayesian approach [1994 EPRI study] was used. The Johnston et al. (1994) Bayesian approach was developed as part of a study specifically focused on the assessment of maximum magnitudes in Stable Continental Regions (SCR). It provides a quantitative approach based on evaluation of a worldwide database of SCR earthquakes and crustal domains. This approach provides a reasonable method for assessing the uncertainty in maximum magnitude.

The Bayesian approach for estimating maximum magnitude developed by Johnston et al. (1994) does not start from the assumption that all SCR domains have the same maximum magnitude. Instead it assumes that there are characteristics that control the maximum size of an earthquake that can occur in an individual SCR domain and these characteristics vary from domain to domain, just as the maximum size of earthquakes varies for other source types (e.g., plate-boundary faults, subduction zones). The statistical analysis presented in Chapter 5 of Johnston et al. (1994) explored the utility of using the characteristics of the SCR domains as predictors of maximum magnitude. The first step in the process was the development of “super domains” by “pooling” the data for domains that “cannot, with the information available, be considered different.” The primary objective of pooling was to increase the earthquake sample size for a given super domain to provide a more constrained estimate of maximum magnitude. The resulting super domains were distinguishable from each other using the tectonic, geologic, and seismologic information gathered as part of the project. The prior distribution from Johnston et al. (1994) used in the EGC ESP probabilistic seismic hazard analysis (PSHA) assessment of maximum magnitude for central Illinois was based on grouping all of the 15 non-extended crust super domains and estimating the statistics of the maximum magnitudes of that group of domains. These 15 super domains all had the common characteristic of non-extended crust, but differ in other characteristics that may or may not be related to differences in maximum magnitude, such as crustal age, state of stress, and orientation of stress relative to structure. The Johnston et al. (1994) analysis did not assume that all of the non-extended crust super domains are identical, and thus would have the same maximum magnitude.

Using the EPRI (1994) approach, the applicant developed the maximum magnitude distribution described above (M 6.2 (0.4), M 6.4 (0.3), M 6.6 (0.2), and M 6.8 (0.1)), with a mean maximum magnitude of 6.65. As requested by the staff in RAI 2.5.2-4, the applicant compared the 10-Hz spectral acceleration hazard curves for the ESP site using its maximum magnitude distribution for central Illinois versus a single fixed value of a maximum magnitude equal to 6.8. The applicant found that the two maximum magnitude distributions yield nearly the same hazard, with the single value of M 6.8 maximum magnitude producing approximately only 2 to 3 percent higher ground motions at the mean 10^{-4} and mean 10^{-5} hazard levels.

To determine the adequacy of the maximum magnitude distribution used by the applicant for the central Illinois seismic source zone, the staff reviewed the 1994 EPRI study and, specifically, the Bayesian analysis recommended by the study. The Bayesian approach to assessing maximum magnitude is derived from the statistical analysis of the SCR global earthquake database (prior distribution) in combination with local or regional earthquakes (e.g., the Springfield earthquake). The prior magnitude distribution, based on the global earthquake database, is combined with information (the sample likelihood function for maximum magnitude) specific to the regional seismic source of interest, and the final product is a probabilistic distribution (posterior distribution) of maximum magnitude that incorporates uncertainties in the assessment. The Bayesian analysis used by the applicant for the central Illinois maximum magnitude produces a posterior distribution of maximum magnitude having a modal value of M 6.5 and a mean of M 6.7. This mean maximum magnitude is close to the value (M 6.8) used by the USGS for its national hazard maps and also to the magnitudes of the two largest earthquakes globally observed (Ghana and Australia) in nonextended SCR domains, similar to the central Illinois source zone. The staff notes, as described above by the applicant, that the difference between these two maximum magnitudes (M 6.7 and 6.8) is insignificant, producing only 2 to 3 percent higher ground motions at the mean 10^{-4} and mean 10^{-5} hazard levels. The staff also notes, based on its review of the global earthquake database used by the 1994 EPRI study, that no nonextended SCR domain has had a historical earthquake of M 7.0 or larger. Although this observation from the historical record of SCR seismicity is based on a small time sample of one to a few centuries, the historical record includes all known SCR earthquakes. In addition, there are no tectonic processes that affect SCRs and operate fast enough to undercut the assumption that the SCR seismicity of a few centuries before the SCR historical record likely looks much like the historical record itself. As such, the 1994 EPRI global database for SCR earthquakes provides a first-order description of how SCR crust behaves seismically in the present millennium or so of the present plate-tectonic cycle. In summary, the staff concludes that the applicant's use of the global SCR earthquake database in combination with paleoliquefaction data for the central Illinois source zone results in an adequate characterization of the maximum magnitude distribution of the central Illinois seismic source zone.

In conclusion, as described above, the staff concurs with the applicant's decision to increase the maximum magnitude distributions of the WVSZ and central Illinois source zone.

Ground Motion Attenuation. As described in SSAR Section 2.5.2.3, the original EPRI-SOG study used three attenuation relationships, developed in the mid 1980s. Since the completion of the EPRI-SOG study, estimating ground motions in the CEUS has been the focus of considerable research. The applicant used the expert-elicitation guidance in NUREG/CR-6372 to characterize the distribution of ground motion prediction for the CEUS. This study and the resulting CEUS ground motion attenuation relationships are described in an EPRI 2003 publication. The EPRI study grouped the selected ground motion attenuation relationships into four clusters, in which each cluster represents a group of models based on a similar approach for ground motion modeling. After comparing the three attenuation models used for the EPRI-SOG study with the new EPRI ground motion study, the applicant concluded that the recent median ground motion models are generally consistent with two of the three older models. However, the estimates of uncertainty or variability about the median ground motion predictions are considerably higher for the recent ground motion attenuation relationships compiled by the recent EPRI study compared to the uncertainty in the ground motion used for the original EPRI-SOG study. Therefore, the applicant decided to use the updated attenuation models.

In RAI 2.5.2-3, the staff asked the applicant to describe how the recent EPRI ground motion study converted the distance measure used for each of the attenuation relationships to a common measure. Specifically, the 13 CEUS attenuation relationships selected by the EPRI ground motion experts each use one of two different distance measures. In response to RAI 2.5.2-3, the applicant provided a description of the method it used to convert the "point-source" distance measure to the more commonly used Joyner-Boore distance measure. In EPRI ground motion clusters 1, 2, and 4, all but two of the individual models (Frankel et al., 1996; and Atkinson and Boore, 1995) use the Joyner-Boore distance, which is the closest distance from the site to the surface projection of the fault rupture in kilometers. The other two ground model attenuation relationships use the hypocentral distance, which is the distance from the site to the earthquake focus in kilometers. To convert the point-source distance to the Joyner-Boore distance, the applicant described the following method:

> These two relationships [Frankel et al. (1996) and Atkinson and Boore (1995)] were converted to Joyner-Boore distance by simulating a data set in terms of moment magnitude and Joyner-Boore distance and fitting this simulated data set. At a given Joyner-Boore distance, earthquake point source depths were simulated for a range of magnitudes using the point-source depth distributions for the CEUS proposed by Silva et al. (2002). These consist of lognormal distributions with the parameters listed in the following table.
>
> Point-Source Depth Distribution Parameters (from Silva et al. 2002)
>
> | Magnitude | Minimum Depth | Median Depth | Maximum Depth | $\sigma_{ln(D)}$ |
> |---|---|---|---|---|
> | 4.5 | 2 km (1 mi) | 6 km (4 mi) | 15 km (9 mi) | 0.6 |
> | 5.0 | 2 km (1 mi) | 6 km (4 mi) | 15 km (9 mi) | 0.6 |
> | 5.5 | 2 km (1 mi) | 6 km (4 mi) | 15 km (9 mi) | 0.6 |
> | 6.0 | 3 km (2 mi) | 7 km (4 mi) | 17 km (11 mi) | 0.6 |
> | 6.5 | 4 km (2.5 mi) | 8 km (5 mi) | 20 km (12 mi) | 0.6 |
> | 7.0 | 4.5 km (2.8 mi) | 9 km (5.6 mi) | 20 km (12 mi) | 0.6 |
> | 7.5 | 5 km (3 mi) | 10 km (6 mi) | 20 km (12 mi) | 0.6 |
> | 8.0 | 5 km (3 mi) | 10 km (6 mi) | 20 km (12 mi) | 0.6 |
> | 8.5 | 5 km (3 mi) | 10 km (6 mi) | 20 km (12 mi) | 0.6 |
>
> For each simulation, the depth and the Joyner-Boore distance were used to compute the corresponding point source distance. The median ground motion for the given magnitude and point source distance were then computed using the Frankel et al. (1996) and Atkinson and Boore (1995) relationships. The resulting simulated data sets were then fit with an appropriate functional form to provide ground motion relationships in terms of moment magnitude and Joyner-Boore distance consistent with the other relationships in Clusters 1 and 2.

In Open Item 2.5.2-1, the staff requested further clarification regarding the EPRI study's distance conversion process. In response, the applicant provided a detailed description of the distance conversion process used in the EPRI CEUS ground motion model. Specifically, the staff asked for clarification on the process used to convert Joyner-Boore distance to hypocentral distance so that the two attenuation relationships based on hypocentral distance can be combined with the relationships based on Joyner-Boore distance. In response, the applicant provided a detailed description of the distance-conversion process for the two attenuation relationships (Atkinson and Boore, 1995; and Frankel et al., 1996). The staff's review of the distance-conversion process determined that the EPRI (2003) implementation process provides a smooth variation with distance and results in somewhat higher median ground motions only at very small values of Joyner-Boore distance. Therefore, the staff considers Open Item 2.5.2-1 to be resolved.

The ESP applicant for the North Anna, Virginia, site also used the EPRI 2003 ground motion study for its PSHA. Many of the staff's RAIs and the open item related to the updated EPRI CEUS ground motion modeling are described in Section 2.5.2 of the staff's final SER for North Anna (ADAMS Accession No. ML051610246). After reviewing the North Anna ESP applicant's responses to the staff's RAIs and open item, the staff concluded that Dominion had adequately resolved each of the staff's concerns with regard to the development by EPRI of new ground motion models for the CEUS.

2.5.2.3.4 Maximum Earthquake Potential

The staff focused its review of SSAR Section 2.5.2.4 on the ESP site controlling earthquakes determined by the applicant after completion of its PSHA. The applicant determined the low- and high-frequency controlling earthquakes by deaggregating the PSHA results at selected probability levels. Before determining the controlling earthquakes, the applicant updated the original EPRI-SOG PSHA using the seismic source zone adjustments and new ground motion modeling described above in the previous SER subsection.

PSHA Results. The applicant performed PSHA calculations for PGA and spectral acceleration at frequencies of 25, 10, 5, 2.5, 1, and 0.5 Hz. Following the guidance provided in RG 1.165, the PSHA calculations were performed assuming generic hard rock site conditions (i.e., an S-wave velocity of 9200 ft/s). The actual local site characteristics are incorporated in the calculation of the SSE spectrum, which uses the hard rock PSHA hazard results as the starting point.

Controlling Earthquakes. To determine the low- and high-frequency controlling earthquakes for the ESP site, the applicant followed the procedure outlined in Appendix C to RG 1.165. This procedure involves the deaggregation of the PSHA results at a target probability level to determine the controlling earthquake in terms of a magnitude and source-to-site distance. The applicant chose to perform the deaggregation of the mean 10^{-4} and 10^{-5} PSHA hazard results. The low- and high-frequency controlling earthquakes are shown above in Table 2.5.2-1 in SER Section 2.5.2.1.4. For the high-frequency mean 10^{-4} hazard, the controlling earthquake is a magnitude 6.5 event occurring at a distance of 83 km (52 mi), corresponding to an earthquake from the WVSZ. In contrast, for the high-frequency 10^{-5} hazard, the controlling earthquake has a magnitude of 6.2 at a distance of only 24 km (15 mi). This controlling earthquake corresponds to the Springfield earthquake from the central Illinois background source zone.

For the low-frequency mean 10^{-4} and 10^{-5} hazard, the controlling earthquake has a magnitude of 7.2 at a distance of 320 km (199 mi). This earthquake corresponds to an event in the NMSZ.

Based on its review of the ESP site controlling earthquake magnitudes and distances, the staff concludes that the applicant's PSHA adequately characterized the overall seismic hazard of the ESP site. The staff also concludes that the applicant's controlling earthquakes for the ESP site (magnitude of 6.2 at 24 km (15 mi), magnitude 6.5 at 83 km (52 mi), and magnitude of 7.2 at 320 km (199 mi)) are generally consistent with both the historical earthquake record and paleoliquefaction studies in the NMSZ, WVSZ, and central Illinois seismic source zone. In addition, the staff finds that the ground motions developed by the applicant from the controlling earthquakes (see SER Figure 2.5.2-2) are consistent with the most recent CEUS ground motion evaluations. Accordingly, the staff concludes that the applicant followed the guidance in RG 1.165 for evaluating the regional earthquake potential and determining the ground motion resulting from the controlling earthquakes.

2.5.2.3.5 Seismic Wave Transmission Characteristics of the Site

The staff focused its review of SSAR Section 2.5.2.4 on the method used by the applicant to develop the site free-field ground motion spectrum. The hazard curves from the PSHA are defined for generic hard rock conditions. According to the applicant, these hard rock conditions exist at the ESP site at a depth of several thousand feet or more below the ground surface. To determine the free-field ground motion, the applicant performed a site response analysis.

The staff reviewed the applicant's analysis to ensure that it accurately incorporates the local site properties and conditions as well as their uncertainties. The applicant developed 60 different randomized soil/rock columns in order to model the uncertainties in the soil/rock properties, such as S-wave velocity, density, shear modulus, and damping. The applicant determined these soil/rock properties through its field explorations and laboratory tests, which are described in SER Section 2.5.4.

Based on the large range in S-wave velocities for some of the soil layers (Table 5-2 of SSAR Appendix A) and the differences in SPT blowcount values for ESP borings B1 and B4 compared to those of B2 and B3, the staff in RAI 2.5.4-4 requested that the applicant justify the appropriateness of using a single "average" soil column for the site response analyses rather than including a number of different base-case soil columns. In response to RAI 2.5.4-4, the applicant stated that the variations in S-wave velocity and SPT blowcounts result from "changes in the depositional conditions during formation of the soil profile and the geologic history of the site following deposition." The applicant further stated that for the ESP site, the geologic history includes the advance and retreat of a substantial thickness of ice during the last ice age. This ice loaded the material located below approximately 50 ft, which led to very dense or hard soil conditions (i.e., overconsolidation) by the ice load. Because of the ice loading, the variability of the soil existing below 50 ft after initial formation has been reduced. In contrast, the applicant reported that the soil in the upper 50 ft was formed by fluvial (river) and aeolian (wind) processes, resulting in more variability both vertically and horizontally.

Regarding the modeling of this variability in soil properties, the applicant stated the following:

> In recognition of the natural variability of the soil, the standard approach for site response analyses is to account for the likely variation in soil layering and soil

> properties within a specific layer by considering different combinations of soil property and soil profile conditions that could exist at a site. One method for evaluating these variations is by manually creating independent soil columns, as suggested in the RAI. The alternative that was taken during the EGC ESP site ground motion response studies was to statistically create a large number of profiles, or realizations, and conduct the site response analyses using these profiles.

The applicant concluded its response to RAI 2.5.4-4 by stating that the randomization process used to develop the transfer functions at the ESP site allows the uncertainty in soil layering and soil properties to be considered during the evaluation of site response effects.

The staff reviewed the applicant's response and found that the large variability in strength and stiffness of the site soils, as demonstrated by the S-wave velocities and SPT blowcounts from the relatively few borings taken at the EGC ESP site, indicates a potentially large epistemic uncertainty in site profiles that cannot easily be captured directly by the randomization process. In Open Item 2.5.2-2, the staff asked the applicant to further justify using only a single site velocity model to account for the variability in strength and stiffness of the site soils. In response, the applicant indicated that the soils in the upper 60 ft of the site will be removed during plant construction and replaced by engineering fill. Since the fill material will be placed under consistent compaction and gradation controls, the variability in shear wave velocity of the engineered fill will be significantly lower than that of the in situ soils. As such, the staff considers Open Item 2.5.2-2 to be resolved.

To account for the variability in soil shear strain modulus and material damping ratio with shearing strain amplitude, the applicant randomized the shear modulus and damping curves used for the site response analysis. In RAI 2.5.4-7, the staff asked the applicant to explain how these curves were used in the randomization process with respect to both the different depth ranges and the soil types occurring within those depth ranges. For example, the soil boring logs indicated that some soils are clays and some soils are silty sands over the same particular depth range. In response to RAI 2.5.4-7, the applicant stated that the modulus and material damping curves are primarily dependent on the depth range and not on the material type. The applicant stated that this is consistent with the development of the EPRI modulus reductions and material damping curves (EPRI, 1993), in which the standardized curves are based only on depth interval, thereby avoiding the need to link the modulus reduction curves and damping curves to the soil boring log. The applicant further stated that the independence of the modulus reductions and material damping curves from the specific soil type is based on laboratory tests that show that the primary variable contributing to the variation in shape and absolute value of the modulus reduction and material damping curves is the depth of the soil below the ground surface, which is an indication of the effective confining pressure on the soil sample. With regard to other variables that may affect the shape and magnitude of the modulus reduction and material damping curves, the applicant stated the following:

> Since there is evidence that the type of soil also has some effect on the shape and magnitude of the modulus reduction and material damping curves—though it can be considered a secondary effect—a range of unique modulus reduction and material damping curves is computed within each depth interval (i.e., 0 to 20, 21 to 50, 51 to 120, etc.) through the randomization process. The computation performed for the EGC ESP project resulted in 60 modulus reduction curves and

> 60 material damping curves with each of the five depth intervals. The range represented by each of the 60 sets of curves is intended to cover the uncertainties in the shape and absolute value of the modulus reduction and material damping ratio curves resulting from a number of different effects, including the particular soil type, the stress history for the soil, sample disturbance associated with the laboratory testing of soil samples, and random variability that is typically observed in laboratory testing programs.

In summary, the applicant stated that the randomization process for modulus reduction and material damping curves, as well as the low-strain S-wave velocity and thickness profiles, results in combinations of soil stiffness and damping conditions that account for the possible variations in soil type, soil layer thickness, and dynamic soil properties for the EGC ESP site.

In RAI 2.5.4-7, the staff also asked the applicant to explain why it did not incorporate the 15-percent damping cutoff as recommended in SRP Section 3.7.2 and to provide clarification regarding its use of high strain values in the randomization process. In response, the applicant stated that the 15-percent damping in SRP Section 3.7.2 pertains to soil-structure interaction (SSI) problems and not to free-field, site response analyses. The applicant also stated that there is no evidence in laboratory testing programs that material damping should be capped at 15 percent. Regarding the effect of using a 15-percent damping cutoff for the ESP site, the applicant stated the following:

> For a stiff site such as occurs at the EGC ESP Site, the 15 percent cutoff is expected to have little effect except perhaps in the shallowest soil layers, where the shear modulus is lowest. Where soils are relatively stiff and peak ground acceleration only moderate, such as occurs at the EGC ESP Site, the equivalent shearing strains will often be low enough that damping ratios do not exceed 15 percent. Only the upper 50 feet or so of soil profile at the EGC ESP site, where the shear modulus is reduced, could the site response potentially be affected by the damping cutoff.
>
> However, to support the response to this RAI, a series of supplemental computer runs were conducted using the low-strain shear wave velocity profile, the SHAKE program, and modulus reduction curves as discussed in the EGC ESP SSAR. For these supplemental analyses, the material damping curves in the EPRI soil model were capped at 15 percent. The results of a representative set of these analyses were compared to the mean transfer functions shown in Figures 4.2-23 and 4.2-24 from Appendix B of the EGC ESP SSAR. This comparison indicated that the 15 percent damping cap results in no more that a 2 percent increase in the transfer function for the 10-5 hazard level motions and much less for the 10-4 hazard level motions for the EGC ESP Site. These effects are considered negligible.

In summary, in its response to RAI 2.5.4-7, the applicant indicated that using the EPRI 1993 shear modulus and material damping curves (EPRI TR-102293, “Guidelines for Determining Design Basis Ground Motions”) eliminates the need to associate particular laboratory results for individual soil layers in the response calculations. However, the staff notes, as indicated in the plots included in the SSAR, that the difference between nonlinear material models for sandy soils as compared to clayey soils can be significant for high strain levels. As a result, this

difference in soil type may result in more than just a secondary effect. The response calculations performed for the EGC ESP site only considered the material models associated with sandy soils. The potential existence of high-plasticity index clay soils at the site is not discussed to a significant extent in the applicant's response.

Regarding the issue related to the 15-percent damping cutoff, the applicant stated that the guideline of the 15-percent damping cutoff in SRP Section 3.7.2 pertains to the SSI problem, but not the site response calculation. This is not acceptable to the staff, because the 15-percent cutoff limit for hysteretic damping mentioned in the SRP is not restricted to SSI analyses only, but is associated with the one-dimensional free-field calculations typically performed before the SSI analyses. The purpose of this restriction acknowledges the fact that at these high strain levels associated with the laboratory tests, the assumption of steady-state behavior is questionable. Therefore, the staff's position has been that excessively high damping values are not appropriate for site response calculations. The applicant stated that the use of the 15-percent damping cutoff in the calculation causes the surface design motions to increase by about 2 percent.

In Open Item 2.5.2-3, the staff asked the applicant to address the impact of plastic clay soils at the site on the assumption of the independence of the modulus reductions and material damping curves from the specific soil type. In response, the applicant presented plots of Atterberg Limit data for the various soils of the site that demonstrate that these soils are silts and sandy silts of low plasticity. Since the applicant has demonstrated that the site soils have low plasticity, the staff concludes that this portion of Open Item 2.5.2-3 is resolved.

In Open Item 2.5.2-3, the staff also asked the applicant to implement the 15-percent damping cutoff in its free-field, site response analyses. In response, the applicant performed new site response calculations using the 15-percent damping cutoff and used these results for computation of the SSE. These changes have been incorporated into Revision 1 of the ESP application. Since the applicant has incorporated the 15 percent damping cutoff in its free-field, site response analyses, the staff considers this issue and Open Item 2.5.2-3 to be resolved.

To determine the ESP dynamic site response, the applicant developed appropriate ground motion or earthquake time histories for several (12) deaggregation earthquakes, which correspond to the low- and high-frequency controlling earthquakes shown above in Table 2.5.2-2. The applicant selected matching earthquake time histories for each of the deaggregation earthquakes from the CEUS time history library provided with NUREG/CR-6728. As part of its review of the applicant's site response analysis, the staff verified that the deaggregation earthquake magnitudes and distances adequately characterized the local and regional seismic hazard for the ESP site. The three deaggregation earthquakes corresponding to each controlling earthquake represent lower, middle, and higher magnitude earthquakes appropriate for the ESP site. Specifically, the lower magnitude deaggregation earthquake (M = 5.7–6.0 at R = 11–15 km (9 mi)) corresponds to a local earthquake occurring in the central Illinois source zone, the middle magnitude deaggregation earthquake (M = 6.7–6.9 at R = 140–166 km (103 mi)) corresponds to an earthquake in the Wabash Valley-southern Illinois region, and the upper magnitude deaggregation earthquake (M 7.2–7.4 at R = 375–381 km (237 mi)) corresponds to a New Madrid earthquake.

To determine the final site response, the applicant used the program SHAKE to compute the site amplification function for each of the deaggregation earthquakes. The applicant paired the

60 randomized velocity profiles with the 60 sets of randomized shear modulus and damping curves (i.e., one velocity profile with one set of modulus reduction and damping curves). To obtain a site amplification function, the applicant divided the response spectrum from the computed surface motion by the response spectrum from the input hard rock motion. The applicant then computed the arithmetic mean of these 60 individual response spectral ratios to define the mean amplification function for each deaggregation earthquake.

The results of the applicant's site response analysis show that the ESP site subsurface amplifies the input hard rock motion over the fairly wide frequency range of 0.5 to 10 Hz, with the maximum amplification of 3.3 at a frequency of 1.7 Hz. The final site amplification function for each controlling earthquake represents the weighted average of the amplification functions for the associated deaggregation earthquakes. The weights (see SER Table 2.5.2-2) represent the relative contribution of earthquakes represented by the deaggregation earthquakes to the hazard at the appropriate spectral frequency and hazard level. The applicant determined the final soil surface spectra for the ESP site by scaling the rock controlling earthquake spectra by the mean site amplification functions.

In summary, the staff concludes that based on its review of SSAR Section 2.5.2.5, as described above, the applicant's site response analysis adequately incorporates the effects of the local site properties and their uncertainties into the determination of the ESP free-field SSE, as required by 10 CFR 100.23.

2.5.2.3.6 Safe-Shutdown Earthquake

The staff focused its review of SSAR Section 2.5.2.6 on the method used by the applicant to determine the SSE ground motion spectra (horizontal and vertical) for the ESP site. Rather than developing the SSE as recommended by RG 1.165, the applicant used a new method called the performance-based approach. The performance-based approach, which is described in ASCE/SEI Standard 43-05, sets a target of a mean annual frequency of 10^{-5} of unacceptable performance of Category I nuclear SSCs as a result of seismically initiated events. This safety performance target, P_{FT}, is based on assuming (1) a target 10^{-4} mean annual risk of core damage from all accident initiators and (2) that seismic initiators contribute about 10 percent of the risk of core damage posed by all accident initiators. To determine the SSE that achieves the annual performance goal of 10^{-5}, the performance-based approach scales the site-specific mean 10^{-4} UHRS, determined in the previous section, by a DF. The equations for the SSE and DF are provided in SER Section 2.5.2.1.6. As shown previously in Table 2.5.2-3, a DF is determined for several spectral frequencies in order to create the final SSE.

In RAI 2.5.2-1(a), the staff asked the applicant to justify the selection of the site-specific mean 10^{-4} UHRS as the appropriate starting point for determining the final SSE. In response to RAI 2.5.2-1(a), the applicant stated the following:

> [The] design amplitude required to achieve the performance goal at each structural period can be calculated starting from the mean 10^{-4} annual probability level of the seismic hazard spectrum in the free field at the ground surface, or from the 10^{-5} annual probability level, or from any intermediate probability level. The design factor on the spectrum associated with each of these probability levels would be different, but they all would lead to the same SSE.

The applicant explained that it selected a 10^{-4} annual probability level as the starting point based on the precedent set in ASCE/SEI Standard 43-05. After reviewing the derivation of the equations used by the performance-based approach to achieve an SSE that meets the target performance goal (see SER Section 2.5.2.1.6.1), the staff was able to verify the applicant's assertion that using a 10^{-4} annual probability level as the starting point is an arbitrary choice.

In RAI 2.5.2-1(b), the staff asked the applicant to demonstrate that the SSE envelops the site-specific response spectra from the controlling earthquakes at the reference probability level (median 10^{-5} per year) recommended by RG 1.165 or to justify why this approach was not used to determine the SSE. In response to RAI 2.5.2-1(b), the applicant stated the following:

> The EGC ESP does not rely on the site-specific response spectra from the controlling earthquakes at the hazard reference probability level of median 10^{-5} per year to determine the site-specific SSE. Instead, the ASCE/SEI Standard 43-05 is implemented to determine the site-specific SSE. Application of the ASCE/SEI Standard results in site-specific ground motions that are risk-consistent with the median of the mean seismic-induced core damage frequencies ([S]CDFs) [1.2×10^{-5}] determined from probabilistic risk assessments (PRAs) of existing nuclear power plants, which the Commission has determined to be adequately safe.

Regarding the method recommended in RG 1.165 for determining the SSE, the applicant stated the following:

> Studies carried out in 2003 and 2004 during the ESP Application process have found that the current understanding of seismic sources and ground motion models within the central and eastern United States may result in a significant increase in seismic hazard at some sites. These changes in seismic hazard indicate a need to update the reference probability given in RG 1.165 to account for new ground motion models, new seismic source information, and better site response adjustments.
>
> After reviewing the alternatives, EGC has concluded that a re-evaluation of the hazard reference probability in Appendix B of RG 1.165 would not achieve the regulatory stability sought by RG 1.165 and necessary for EGC to proceed with their current ESP Application or any future ESP application(s). Relative to overall industry needs, a revision to the current reference probability based on seismic information available in 2004 would remain valid only until new information becomes available on seismic sources near one or more of the 29 sites, or when new information becomes available on ground motion attenuation models. On a site-specific basis, EGC does not support development of an SSE using a reference probability that is not based on the latest seismic hazard information. Moreover, advances in technologies for determining site-specific SSEs since the late 1980s together with advances in NRC's regulation implementation policies, specifically the implementation of the Commission's Risk-Informed Regulation Policy, support the need for updating the guidance contained in RG 1.165 to comply with the current state of the practice (e.g., ASCE SEI methodology). This generic action is outside the scope of the EGC ESP submittal.

The staff acknowledges that the reference probability currently recommended in RG 1.165 (median 10^{-5} per year), which is the average probability of exceeding the SSE ground motion at 5 Hz and 10 Hz using either the 1993 LLNL PSHA or the 1989 EPRI-SOG PSHA, needs to be updated to more adequately represent current seismic hazard information. RG 1.165 endorses both the original LLNL and EPRI-SOG PSHAs; however, it also recommends updating the seismic source characterizations and ground motion models if they differ significantly from the original LLNL or EPRI models. RG 1.165 also states that the staff will review proposals for revised reference probability values on a case-by-case basis. The most important criterion for evaluating the acceptability of either the RG 1.165 approach with a revised reference probability or a new approach, such as the performance-based approach, is the suitability, with respect to the geological and seismological setting of the specific site, of the final SSE ground motion spectra resulting from either approach. Specifically, as required by 10 CFR 100.23, the SSE must provide a design-basis ground motion that adequately reflects the seismic characteristics of the proposed site. As described below in Open Item 2.5.2-4, the staff has concluded that the SSE for the ESP site satisfies this requirement.

In RAI 2.5.2-1(c), the staff asked the applicant to justify using SSC seismic fragility information, before the selection of a reactor design, to determine the site SSE. In response to RAI 2.5.2-1(c), the applicant stated that the performance-based approach "combines a conservative characterization of equipment/structure performance with ground motion hazard to establish risk-consistent SSEs, rather than only hazard-consistent ground shaking, as occurs using the hazard reference probability approach in Appendix B of RG 1.165." As described in SER Section 2.5.2.1.6.1 in the derivation of the equations and assumptions underlying the performance-based approach, the two parameters used by the performance-based approach to model SSC seismic fragility are the *HCLPF* and variability β. Since the actual *HCLPF* seismic capacity varies for different SSCs, the performance-based approach quantifies this value in terms of the SSE ground motion level and a required seismic margin (Equation 2.5.2-11). Following the recommendations of ASCE/SEI 43-05, the applicant selected a value of one for the seismic margin. As shown by Equation 2.5.2-19 in SER Section 2.5.2.1.6.1, a margin (M_s) of unity is a conservative choice since larger margins would result in a smaller SSE value. A margin of one implies that *HCLPF* = SSE for each SSC. This is a conservative assumption since designers will typically be more cautious than to design the HCLPF seismic capacity to barely resist the SSE ground motion. Assuming a smaller seismic margin (i.e., of unity) is equivalent to assuming that the seismic design criteria are less stringent, and hence a larger (more conservative) SSE ground motion will be used. For the β value, which varies from 0.3 to 0.6, the applicant used 0.4. This assumed value for β is discussed below as part of Open Item 2.5.2-5.

2.5.2.3.6.1 Derivation of the Performance-Based Approach

In RAI 2.5.2-7(b), the staff asked the applicant to provide the details of the derivation of the DF that, when multiplied by the mean 10^{-4} UHRS, achieves an SSE that meets the target performance goal of 10^{-5}. In response to RAI 2.5.2-7(b) the applicant provided an explanation of the performance-based method, including the important assumptions and derivations (see SER Section 2.5.2.1.6.1 for the complete derivation). The staff's review of the underlying assumptions and equations used for the performance-based approach resulted in further questions concerning the following assumptions:

- the assumption of a linear hazard equation *H(a)* in logarithmic space and, specifically, the determination of the slope of the hazard equation, $-1/\log(A_R)$, between only the 10^{-4} and 10^{-5} interval

- the assumption that the seismic capacity variability β is 0.40

- the definition of unacceptable performance as the "onset of significant inelastic deformation" (OSID) or "exceedance of essentially elastic behavior"

- the stability of the target performance goal 10^{-5} since this value is from seismic PRAs that used the original EPRI-SOG source models and ground motion estimates

- the applicability of the target performance goal 10^{-5} for advanced reactor designs that may differ considerably from current light-water reactors (LWRs)

- the consistency between the seismic design criteria in NUREG-0800 and ASCE/SEI Standard 43-05

In Open Item 2.5.2-5, the staff requested clarification and further information from the applicant regarding each of the six issues outlined above. The applicant's response and the staff's evaluation are provided below.

Linear Hazard Equation. In Open Item 2.5.2-5(a), the staff asked the applicant to justify the assumption of a linear hazard curve in logarithmic space (see Equation 2.5.2-13 and Figure 2.5.2-7) and the appropriateness of solely using the 10^{-4} to 10^{-5} interval to determine the amplitude ratio A_R and, as such, the DF. In response, the applicant stated the following:

> In developing the design factor, DF, the seismic hazard curve was approximated by a power law which results in a linear hazard curve when plotted on a log-log plot. Seismic hazard curves are close to linear when plotted on a log-log plot. However, they are not perfectly linear. They always curve downward with decreasing hazard exceedance frequency. Thus A_R reduces as the hazard exceedance frequency is reduced. In other words, an A_R computed over the range of hazard exceedance frequencies from $1\text{x}10^{-4}$/yr to $1\text{x}10^{-5}$/yr will be larger than that computed over the $1\text{x}10^{-5}$/yr to $1\text{x}10^{-6}$/yr range.

In addition, the applicant stated that "based upon several hundred rigorous convolutions of hazard and fragility curves, it has been found that P_{FT} is dominated by the portion of the fragility curve between about the 1% failure probability capacity $C_{1\%}$ and the 70% failure probability capacity $C_{70\%}$" (see Figure 2.5.2-11 for an illustration of this portion of the fragility curve). The applicant also compared SSE values obtained by direct integration of the risk integral (Equation 2.5.2-9), which uses the entire hazard and fragility curves, versus the those obtained by using the risk equation (Equation 2.5.2-1), which assumes a linear hazard curve in log-log space between the exceedance frequencies of $1\text{x}10^{-4}$/yr to $1\text{x}10^{-5}$/yr. Comparing the two results, the applicant stated, "one can see that the use of the approximate power law hazard curve introduces a slight, but generally negligible, conservative bias for the computed P_{FT}."

To verify the acceptability of assuming a linear hazard curve in log-log space between the exceedance frequencies of $1x10^{-4}$/yr to $1x10^{-5}$/yr to determine the SSE via the risk equation as opposed to direct convolution of the risk integral, the staff requested four hazard curves from the applicant. Figure 2.5.2-7 above shows these four hazard curves (1 Hz, 2.5 Hz, 5 Hz, and 10 Hz). The staff then compared the SSE values using these two approaches (i.e., "direct integration" and "risk equation"), which are shown below in Table 2.5.2-4. For both approaches, the staff assumed β = 0.4 and a performance target of mean $1x10^{-5}$/yr.

Table 2.5.2-4 Comparison of Performance-Based SSE Values

Natural Frequency (Hz)	SSE	
	Risk Integral (g)	Risk Equation (g)
1.0	0.3366	0.3945
2.5	0.5737	0.6582
5.0	0.6043	0.6570
10.0	0.5591	0.5864

Since the seismic hazard curves have a slight downward curvature, as illustrated in Figure 2.5.2-7, assuming a linear fit results in slightly higher exceedance values and, as a result, slightly higher SSE values, as illustrated above in Table 2.5.2-4. Therefore, the staff concludes that the applicant's use of the approximate power law hazard curve is slightly conservative and therefore acceptable.

Seismic Capacity Standard Deviation. In Open Item 2.5.2-5(b), the staff asked the applicant to justify why a β value of 0.4 was used and show how the DF varies with different β values over the range of amplitude ratios (A_R). In response, the applicant stated that the developers of the performance-based approach considered β values between 0.3 and 0.6 and A_R values between 1.5 and 4.5 when developing Equation 2.5.2-1 for DF. Regarding β values, the applicant stated that "the results for β of 0.4 and 0.5 were weighted more heavily than those for β of 0.3 and 0.6 because the fragility β values are most likely in the 0.4 and 0.5 range and β of 0.3 and 0.6 are considered to be extreme low and high values, respectively."

As shown previously in Figure 2.5.2-14 in Section 2.5.2.1.6.1, the DF recommended in ASCE/SEI 43-05 (Equation 2.5.2-1) is slightly unconservative for β=0.3 and conservative for larger β of 0.4 to 0.6. To evaluate the significance of the range of β values on the DF, the staff determined the unacceptable performance frequency values (P_{FT}) for the performance-based SSE values for four natural frequency values 1, 2.5, 5, and 10 Hz. The applicant determined the four performance-based SSE values shown below in Table 2.5.2-5 using the performance-based approach as described in ASCE/SEI 43-05, which assumes a β value of 0.4 and a target performance goal of $1x10^{-5}$/yr. The staff used the four hazard curves provided by the applicant to determine P_{FT} via direct integration of the risk integral (Equation 2.5.2-9) for β ranging from 0.3 to 0.6. As shown below in Table 2.5.2-5, the P_{FT} values for β=0.3 are only slightly larger than the target value of $1x10^{-5}$/yr.

Table 2.5.2-5 Unacceptable Performance Frequency Values for β from 0.3 to 0.6

		P_{FT}*10^{-5}/yr			
Freq (Hz)	SSE (g)	β=0.3	β=0.4	β=0.5	β=0.6
1.0	0.3945	1.08	0.95	0.70	0.55
2.5	0.6582	1.05	0.97	0.73	0.59
5.0	0.6670	1.03	0.96	0.71	0.58
10.0	0.5864	1.02	0.91	0.65	0.52

Since the P_{FT} values for β=0.3 are only slightly larger than the target performance goal of 10^{-5}/yr and fragility β values of 0.3 are not common for SSCs, the staff concludes that the applicant's assumption that β=0.4 for determining the SSE is acceptable.

Onset of Significant Inelastic Deformation. In Open Item 2.5.2-5(c), the staff asked the applicant to clarify the meaning of "onset of significant inelastic deformation" (OSID), specifically the words "onset" and "significant," OSID with regard to the failure of SSCs and core damage, and the relationship of OSID to "essentially elastic" behavior. In response, the applicant stated that OSID means that "localized inelasticity might occur at stress concentrations, [but] the overall seismic response (deformations) will be essentially the same as those computed by [a] linear elastic demand analysis." The applicant also stated that in ASCE/SEI 43-05 essentially elastic behavior (or OSID) is achieved by requiring that the seismic demand computed by sufficiently conservative linear elastic analysis is less than the conservative code-specified allowable seismic capacity (without an "inelastic factor" by which the linear elastic demand can exceed the code capacity). Generally there is less than a 2 percent probability of large inelastic deformation if the actual demand reaches the code capacity (as discussed in the commentary of ASCE/SEI 43-05).

Based on the applicant's response, the staff has determined that OSID is just beyond the occurrence of insignificant (or localized) inelastic deformation, and in this way corresponds to "essentially elastic behavior." As such, OSID of an SSC can be expected to occur well before seismically induced core damage, resulting in much larger frequencies of OSID than SCDF values. In fact, as implied by the applicant's definition, OSID occurs before SSC "failure," where the term failure refers to impaired functionality. To further demonstrate that the frequency of OSID is larger than SCDF, the staff used the four EGC ESP hazard curves (1, 2.5, 5, and 10 Hz) to calculate SCDF values for each of the four performance-based SSE values. In performing this calculation of SCDF, the staff used the risk integral equation (Equation 2.5.2-9) with the complete range of expected β values (0.3 to 0.6) and assumed that the seismic margin (M_s) against core damage is 1.67 for new standard plant designs as specified in staff requirements memorandum (SRM), dated July 21, 1993, on SECY 93-087. As shown in Table 2.5.2-6 below, SCDF values for the four natural frequencies and β values vary from 0.08×10^{-5}/yr to 0.32×10^{-5}/yr.

Table 2.5.2-6 SCDF Values for Clinton Performance-Based SSE

		SCDF *10^{-5}/yr			
Freq (Hz)	SSE (g)	β=0.3	β=0.4	β=0.5	β=0.6
1.0	0.3945	0.32	0.28	0.20	0.16
2.5	0.6582	0.20	0.18	0.13	0.11
5.0	0.6570	0.16	0.15	0.11	0.10
10.0	0.5864	0.11	0.12	0.09	0.08

For comparison, NUREG-1742 shows, based on the results of seismic PRAs of 25 nuclear power plants, that the median value for the mean core damage frequency is 1.2x10^{-5}/yr. Therefore, by setting the target performance goal, P_{FT}, to be a FOSID value of 1x10^{-5}/yr, the resulting SSE computed using the ASCE/SEI 43-05 methodology provides SCDF values that are substantially lower than those for most of the 25 nuclear power plants provided in NUREG-1742. Figure 2.5.2-15 in SER Section 2.5.2.1.6.1 shows the results of the seismic PRAs from NUREG-1742 in terms of mean ground motion recurrence interval, which is the inverse of mean SCDF. Figure 2.5.2-17, below, shows these same results and adds the values computed above in Table 2.5.2-5 for the EGC ESP site. For the natural frequencies of 5 and 10 Hz and for β values of 0.4 and 0.5, SCDF is about 1x10^{-6}/yr for the EGC ESP performance-based SSE, which is about 10 times lower than the median of the mean SCDF for the 25 nuclear power plants in NUREG-1742.

In conclusion, the staff has determined that there is a significant difference between OSID, which is set at 10^{-5}/yr as the target performance goal, and seismic core damage. This result follows from assuming that the seismic margin against core damage is 1.67 as specified in SRM, dated July 21, 1993, on SECY 93-087.

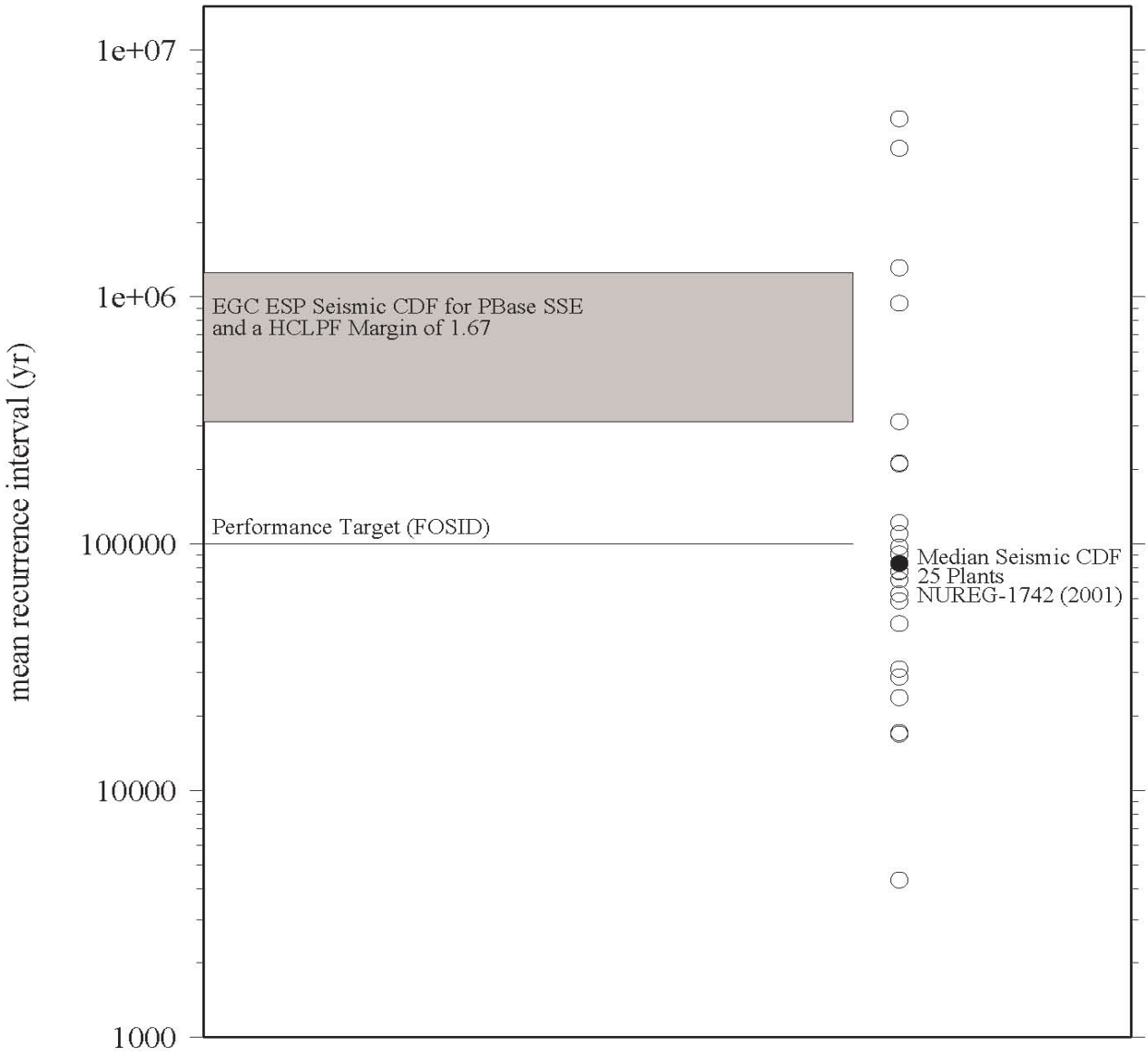

Figure 2.5.2-17 Seismic core damage in terms of mean ground motion recurrence interval for EGC ESP site and 25 nuclear power plants. For comparison, FOSID is also shown.

Stability of Target Performance Goal. In Open Item 2.5.2-5(d), the staff asked the applicant to justify the long-term stability of the target performance goal $1x10^{-5}$ in comparison to the hazard-based approach (reference probability) in RG 1.165, as both values are based on PSHAs for several CEUS nuclear sites. In response, the applicant stated the following:

> Although Regulatory Guide 1.165 was officially issued in early 1997, the guidance is based on late 1980s to early 1990s technologies. EGC recognized that the reference probability approach of Regulatory Guide 1.165 does not provide the regulatory stability that was originally intended and expected, as it is inherently unstable with the updating of the input parameters for PSHAs for CEUS sites. Updating the PSHAs at CEUS sites changes the basis upon which the reference probability was established and a new reference probability must be established. The performance-based criterion on the other hand, remains unchanged by updating the PSHAs, even though the site-specific SSE ground motion will reflect the updated PSHA results. The method provides uniform performance across sites and thus provides performance consistency and regulatory stability.

Although the target FOSID value of $1x10^{-5}$/yr is based on the mean SCDF of $1.2x10^{-5}$/yr from the seismic PRAs of 25 nuclear power plants, as described above and in NUREG-1742, the applicant stated that the performance-based criterion "remains unchanged by updating the PSHAs." Since the target performance criterion (i.e., the FOSID value of $1x10^{-5}$/yr) produces an SSE for the EGC ESP site that adequately reflects the regional and local seismic hazards (see Open Item 2.5.2-4 below) and this performance criterion will remain fixed, the staff finds that the performance-based approach is an adequately stable method.

Applicability of Target Performance Goal. In Open Item 2.5.2-5(e), the staff asked the applicant to justify the use of the target performance goal of $1x10^{-5}$/yr for advanced reactor designs, which may differ considerably from current LWRs. As described above in the applicant's response to RAI 2.5.2-7(a), the target performance goal is based on seismic PRAs for current LWRs. In its response, the applicant stated that the performance-based approach sets the target performance goal of $1x10^{-5}$/yr to be equal to the FOSID for SSCs. Furthermore, the applicant stated that the "onset of significant inelastic deformation of an SSC does not correspond to Seismic-Induced Core Damage particularly for an advanced reactor design with redundant safety features."

Regardless of the advanced reactor design, in SRM, dated July 21, 1993, on SECY 93-087, the Commission approved the use of 1.67 times the design basis SSE for a margin-type assessment of seismic events. Using this criterion, the staff calculated SCDF values for the EGC ESP SSE, as described above in Table 2.5.2-5, that range from 0.18 to $0.09x10^{-5}$/yr for natural frequencies 2.5, 5, and 10 Hz and β equal to 0.4 and 0.5. Based on these results, the staff concludes that the applicant's use of $1x10^{-5}$/yr as the target performance goal results in an SSE for the EGC ESP site that is adequately conservative.

Comparison of NUREG-0800 and ASCE/SEI 43-05. In Open Item 2.5.2-5(f), the staff asked the applicant to clarify how the design criteria in ASCE/SEI Standard 43-05 are similar enough to the seismic criteria in NUREG-0800 such that SSCs designed following NUREG-0800 would also achieve a 1 percent or lower probability of unacceptable performance. In response, the

applicant stated that the seismic design criteria in ASCE/SEI Standard 43-05 for Seismic Design Category SDC-5D are nearly identical to the NRC SRP (NUREG-0800), RGs, and professional design codes and standards referenced therein. The staff compared the two design standards and found that the differences between the seismic demand criteria in ASCE/SEI Standard 43-05 and the SRP are sufficiently small that SSCs designed following the SRP will also achieve a 1 percent or lower probability of unacceptable performance for the design-basis earthquake ground motion.

In conclusion, after extensive review, the staff finds that the performance-based approach is an advancement over the solely hazard-based reference probability approach recommended in RG 1.165. The performance-based approach uses not only the seismic hazard characterization of the site from the PSHA, but also basic seismic fragility SSC modeling in order to obtain an SSE that directly targets a structural performance frequency value. The staff concludes that the applicant targeted a sufficiently low value ($1x10^{-5}$/yr), which it set to be equivalent to FOSID, such that the resulting performance-based SSE achieves an SCDF that is about 10 times smaller ($1x10^{-6}$/yr) than the median of the mean SCDF for the 25 nuclear power plants in NUREG-1742. Therefore, the staff considers Open Item 2.5.2-5 to be resolved.

2.5.2.3.6.2 Target Annual Performance Goal

In RAI 2.5.2-7(a), the staff asked the applicant to justify the selection of the mean annual frequency of 10^{-5} as the safety performance target for the unacceptable performance of Category I SSCs as a result of seismically initiated events. In response to RAI 2.5.2-7(a), the applicant made the following four main points:

(1) The results from seismic PRAs, which were performed for 25 nuclear facilities, show an annual mean SCDF of 10^{-5} or higher for seismic core damage for 50 percent of the operating power plants.

(2) Setting the performance goal of 10^{-5} to be equivalent to the annual FOSID of SSCs is conservative since the seismic demand resulting in the onset of significant inelastic deformation is less than that for failure of the SSC.

(3) The target 10^{-5} annual performance goal is achieved so long as seismic demand and structural capacity evaluations have sufficient conservatism, which is inherent for plants reviewed and approved using the SRP guidelines.

(4) The target 10^{-5} annual performance goal results in a plant that is as safe as the plants currently operating, as shown by the seismic PRAs.

The primary basis for the target 10^{-5} annual performance goal is from the results of seismic PRAs of 25 nuclear power plants (NUREG-1742), which show the median value for the mean SCDF to be $1.2x10^{-5}$. The results of the seismic PRAs in terms of mean ground motion recurrence interval, which is the inverse of SCDF, are shown above in Figure 2.5.2-17. Since the target 10^{-5} annual performance goal and the accompanying performance-based approach for determining the SSE constitute a major departure from the hazard-based approach currently recommended by RG 1.165, in addition to focusing on the underlying assumptions of the performance-based approach (see Open Item 2.5.2-5 above) the staff also focused on the results of its application to the EGC ESP site. To determine the appropriateness of the target

10^{-5} annual performance goal and performance-based approach for the EGC ESP site, the staff reviewed the applicant's final SSE to ensure that it adequately reflects the regional and local seismic hazards surrounding the ESP site.

As shown previously in SER Section 2.5.2.1.6, the final SSE using the performance-based approach is calculated by multiplying the DF and 10^{-4} surface UHRS. Since, by definition, the DF is at least 1.0, the final SSE ground motion spectrum will be at least the 10^{-4} UHRS and higher, depending on the value of the amplitude ratio (A_R) for the 10^{-4} and 10^{-5} hazard curves. For the EGC ESP site, the DF values from 2.5 to 100 Hz are very close to 1.0, implying that the final SSE, while meeting the target 10^{-5} annual performance goal, is close to the 10^{-4} surface UHRS. This result is shown by Figure 2.5.2-6 in SER Section 2.5.2.1.6, which shows the 10^{-4} and 10^{-5} surface UHRS along with the final SSE.

The high-frequency and low-frequency controlling earthquakes that provide the largest contribution to these two hazard levels (10^{-4} and 10^{-5}) for the ESP site were shown previously in SER Section 2.5.2.1.4. This table is repeated below for convenience.

Table 2.5.2-7 High- and Low-Frequency Controlling Earthquakes

Hazard	Magnitude (m_b)	Distance
Mean 10^{-4} High Frequency (5 and 10 Hz)	6.5	83 km (52 mi)
Mean 10^{-4} Low Frequency (1 and 2.5 Hz)	7.2	320 km (199 mi)
Mean 10^{-5} High Frequency (5 and 10 Hz)	6.2	24 km (15 mi)
Mean 10^{-5} Low Frequency (1 and 2.5 Hz)	7.2	320 km (199 mi)

Because the performance-based SSE is close to the 10^{-4} surface UHRS, the corresponding controlling earthquakes for the ESP site are M_w 6.5 at 83 km (52 mi) (high frequency) and m_b 7.2 at 320 km (199 mi) (low frequency). These two earthquakes correspond to events in the WVSZ and NMSZ, respectively. Both of these events are somewhat distant from the ESP site. In contrast, the mean 10^{-5} high-frequency controlling earthquake (m_b 6.2 at 24 km (15 mi)) represents a local earthquake from the central Illinois seismic zone.

The seismic hazard for the central Illinois basin/background source zone, which encompasses the ESP site, is dominated by the Springfield earthquake. Paleoliquefaction studies in the area have found evidence that one or, more likely, two prehistoric earthquakes occurred 5900 to 7400 years ago near Springfield, Illinois, approximately 37 mi southwest of the ESP site (McNulty and Obermeier, 1999). These earthquakes were large enough to generate liquefaction features, with magnitude estimates ranging between 6.2 and 6.8 for the larger event and at least 5.5 for the second event. In addition to the Springfield events, geologists have discovered paleoliquefaction features further south near Shoal Creek. The estimated magnitude and date for this event is about 6.5 and 5700 years BP. In addition to the above

liquefaction features, the applicant also found smaller liquefaction features along the banks of streams closer to the ESP site. Finally, a magnitude 5.4 earthquake occurred in 1968 in the Illinois basin.

In Open Item 2.5.2-4, the staff asked the applicant to demonstrate that the SSE developed using the performance-based approach adequately reflects the local seismic hazard from the central Illinois basin/background source zone. In response, the applicant stated the following:

> The Springfield earthquake represents an event near the largest size expected to occur in the source zone [Central Illinois basin/background source zone] and at a relatively large distance (approximately 60 km epicentral distance). Because there is no concentration of seismicity at Springfield, there is no peak in the magnitude-distance distribution of earthquake frequencies at that distance, and earthquakes of comparable size can occur closer to the site. Because earthquakes smaller than the Springfield earthquake occur much more frequently, they have a larger contribution to the hazard. As a result, the procedure outlined in Regulatory Guide 1.165 would not identify the Springfield earthquake as a controlling earthquake. In addition, it would not appear as a peak (mode) in the magnitude-distance de-aggregation of the hazard.

In addition, the applicant directly compared the rock $UHRS_{10\text{-}4}$, which is slightly smaller than the SSE, and estimated ground motions for the Springfield event. Using the EPRI (2004) ground motion attenuation models, assuming the estimated energy center for the Springfield event to be the earthquake epicenter, and earthquake magnitudes and weights of M 6.2 (0.4), M 6.4 (0.3), M 6.6 (0.2), and M 6.8 (0.1), the applicant determined response spectra (median and 84th percentile) ground motion for comparison with the rock $UHRS_{10\text{-}4}$. The results of this comparison show that the rock $UHRS_{10\text{-}4}$ envelops both the median and 84th percentile ground motion from the Springfield earthquake at the ESP site. The scale factors to match the $UHRS_{10\text{-}4}$ at an average of 5 and 10 Hz spectral frequencies are 1.67 for the median and 1.20 for the 84th percentile.

The applicant also used the latest relationships for estimating the magnitude of prehistoric earthquakes based on the distribution of associated paleoliquefaction features to refine its magnitude estimates for the Springfield earthquake. The applicant used the relationship developed by Olson et al. (2005 in press) to estimate a magnitude of M 6.3 for the Springfield earthquake, which is consistent with the higher weight given to lower magnitudes in the distribution developed for the Springfield earthquake. The applicant then calculated ground motion response spectra from a magnitude 6.3 at 60 km for comparison with the $UHRS_{10\text{-}4}$. Figure 2.5.2-18, which is reproduced from Figure 2.5.2-4-12 from the applicant's response to Open Item 2.5.2-4, shows these comparisons of the ground motion estimates for the Springfield earthquake and the $UHRS_{10\text{-}4}$.

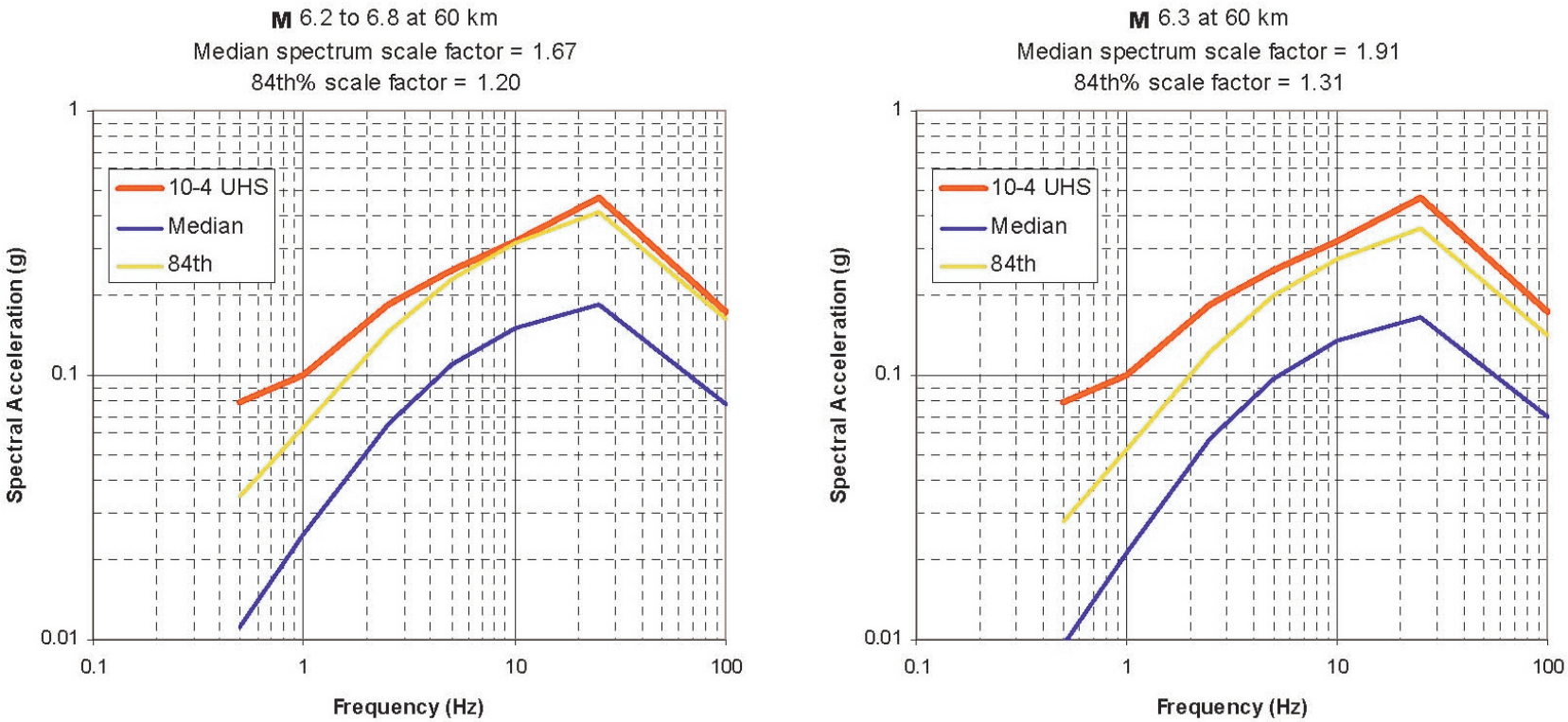

Figure 2.5.2-18 Comparison of $UHRS_{10\text{-}4}$ with estimated ground motion response spectra for the Springfield earthquake

To characterize the seismic hazards for the ESP site, including the controlling earthquake magnitudes and distances, the applicant used the guidance provided in RG 1.165. SER Sections 2.5.2.1 through 2.5.2.5 fully describe the results of this characterization. The applicant departed from RG 1.165 in the use of the performance-based approach for the ESP site to determine the final SSE. The staff has determined, as described above in Section 2.5.2.3.6.1, that the performance-based approach used by the applicant results in an SSE that is adequately conservative based on SCDF values of about $1x10^{-6}$/yr. In addition, based on its review of the applicant's response to Open Item 2.5.2-4, the staff concludes that the SSE adequately represents both the regional and local seismic hazards for the ESP site. This conclusion is based on the applicant's comparison of the estimated ground motion from the largest known prehistoric local event (Springfield earthquake) and the $UHRS_{10-4}$, which is slightly smaller than the SSE. This comparison shows that the SSE envelops the best estimates for the ground motion from the most severe local event. Therefore, the staff considers Open Item 2.5.2-4 to be resolved.

2.5.2.3.6.3 Vertical Safe-Shutdown Earthquake

To compute the vertical SSE, the applicant used the V/H response spectral ratios provided in NUREG/CR-6728. The V/H response spectral ratios given in NUREG/CR-6728 are CEUS hard rock site conditions and depend on the PGA value of the horizontal SSE spectrum. For the ESP site, the V/H ratios used by the applicant are based on having a PGA less than 0.5g. The vertical SSE spectrum is given by multiplying the horizontal SSE spectrum by the V/H ratios. The applicant also considered the effects of the ESP site soil conditions on the vertical ground motions by using ground motion models that provide vertical motions for soil conditions. The applicant used a magnitude 6.4 earthquake at source-to-site distance of 15 km (9 mi) as input to the ground motion models. This magnitude and distance roughly correspond to the high-frequency controlling earthquake.

To verify the adequacy of the V/H SSE ratios used by the applicant, the staff evaluated both the V/H ratios provided in NUREG/CR-6728 and the applicant's consideration of the local site effects on the vertical ground motions. The V/H ratios provided in NUREG/CR-6728 take into account the effects of magnitude, source distance, and local site conditions and are based on earthquake strong motion data. Previous regulatory guidance (RG 1.60 and NUREG/CR-0098) recommended that the V/H ratio be fixed at 2/3 independent of ground motion frequency, earthquake magnitude, distance, and local site conditions. To incorporate the effect of the local site conditions on the vertical ground motions, the applicant used a magnitude 6.4 at a source-to-site distance of 15 km. Based on its review of the V/H ratios provided in NUREG/CR-6728 and the applicant's use of a representative local controlling earthquake, the staff concludes that the V/H ratios used by the applicant are adequate for the EGC ESP site. The staff notes that for higher frequencies (20 Hz and above), the vertical SSE is larger than the horizontal SSE.

2.5.2.3.6.4 Design Response Spectrum

In SSAR Section 3.4.1.4.3, the applicant compared the horizontal performance-based SSE for the ESP site with the RG 1.60 DRS anchored to a PGA of 0.3g at 33 Hz, which is the DRS used by many of the current reactor designs. The applicant noted that the ESP SSE is lower than the RG 1.60 DRS except at frequencies between 15 and 65 Hz. However, after applying the high-frequency reduction factors recommended in a 1993 EPRI study, the ESP SSE is completely enveloped by the RG 1.60 DRS. The applicant concluded by stating that the high-

frequency exceedances by the ESP SSE in relation to the RG 1.60 DRS are not significant, which indicates that the "EGC ESP site is suitable for any design based on the RG 1.60 DRS." Regarding the applicant's above conclusion, the staff has determined that its evaluation of ESP applications will not include a comparison of the site-specific SSE with generic DRS, which may or may not be used by the COL applicant. The staff's review of the acceptance of the final SSE is based on whether the SSE ground motion adequately reflects the local and regional seismic hazard and not on a comparison of the SSE with DRS. In addition, the staff is currently discussing the suitability of high-frequency ground motion reduction factors, similar to those in EPRI 1993, with industry representatives. Therefore, the staff rejects the applicant's conclusion that the ESP site, after the application of the high-frequency reduction factors, is suitable for any design based on the RG 1.60 DRS.

2.5.2.4 Conclusions

As set forth above, the staff reviewed the seismological information submitted by the applicant in SSAR Section 2.5.2. On the basis of its review of SSAR Section 2.5.2 and the applicant's responses to the RAIs, the staff finds that the applicant has provided a thorough characterization of the seismic sources surrounding the site, as required by 10 CFR 100.23. In addition, the staff finds that the applicant has adequately addressed the uncertainties inherent in the characterization of these seismic sources through a PSHA, and that this PSHA follows the guidance provided in RG 1.165. The staff concludes that the controlling earthquakes and associated ground motion derived from the applicant's PSHA are consistent with the seismogenic region surrounding the ESP site. In addition, the staff finds that the applicant's SSE, which was developed using the performance-based approach, adequately represents the regional and local seismic hazards and accurately includes the effects of the local ESP subsurface properties. After extensive review, the staff concludes that the performance-based approach is an advancement over the solely hazard-based reference probability approach recommended in RG 1.165. The performance-based approach uses not only the seismic hazard characterization of the site from the PSHA but also basic seismic fragility SSC modeling in order to obtain an SSE that directly targets a structural performance frequency value. The staff concludes that the proposed ESP site is acceptable from a geologic and seismologic standpoint and meets the requirements of 10 CFR 100.23.

2.5.3 Surface Faulting

SSAR Section 2.5.3 describes the potential for surface faulting at the ESP site. The information presented by the applicant in SSAR Section 2.5.3 is supplemented in Chapter 5 of SSAR Appendix B.

2.5.3.1 Technical Information in the Application

2.5.3.1.1 Surface Faulting Investigations

Geologic Evidence for Surface Deformation. To investigate the potential for surface faulting or fold deformation at the ESP site, the applicant constructed a site-specific geologic cross section based on the site borehole data. The applicant found that irregularities in the upper units of glacial till are not reflected in the older, underlying bedrock units. In particular, the contact between the top of bedrock (300 ft below ground surface) and the overlying glacial till is flat-

lying across the entire site. As a result, the applicant concluded that there is no potential for surface faulting or fold deformation at the ESP site.

Earthquakes Associated with Capable Tectonic Sources. As a result of its geologic investigations, the applicant concluded that there have been no historically reported earthquakes within 25 miles of the site that can reasonably be associated with a local geologic structure. At greater distances from the ESP site, historical earthquakes have been postulated to be associated with geologic faults. At approximately 50 miles from the ESP site, a group of small earthquakes has been postulated for the northern part of the Peru monocline. Other seismic activity within the WVSZ, over 100 miles from the ESP site, has been correlated with the CGL. In addition, the applicant noted that a spatial association of seismicity has been attributed to the Du Quoin monocline and Centralia fault zone in south-central Illinois. Each of these geologic structures is described in SER Section 2.5.1.1.1. Rather than characterizing the seismic potential of each of the above regional geologic structures, the applicant used the EPRI-SOG seismic hazard study, which groups these potential sources into large areal seismic sources zones.

Ages of Most Recent Deformation. To search for evidence of nearby prehistoric earthquakes, the applicant conducted extensive paleoliquefaction investigations along the banks of several streams near the ESP site. The applicant stated that the results of these investigations suggest that no repeated moderate to large events (comparable to the postulated M 6.2 to 6.8 Springfield earthquake) occurred in the site vicinity since the late Pleistocene (2 mya) that would indicate a capable tectonic structure within 25 miles of the ESP site. The applicant found only a small number of paleoliquefaction features and concluded that there was not sufficient information to estimate an earthquake location or magnitude. Although the applicant was unable to attribute these local paleoliquefaction features to a specific earthquake or geologic structure, the seismic activity of the area was characterized as a background areal seismic source zone, referred to as the central Illinois basin/background source. The central Illinois basin/background source encompasses the ESP site area and is modeled as part of the applicant's PSHA. The applicant's paleoliquefaction investigations and the central Illinois basin/background source are further described in SER Section 2.5.1.1.1.

Relationship of Tectonic Structures in the Site Area to Regional Tectonic Structures. Within a 25-mi radius of the ESP site, the applicant found no evidence of geologic faults. Based on its search of the geologic literature, the applicant noted that folds within the La Salle anticlinorium (series of anticlines) do lie within the 25-mile radius. However, the applicant stated that there is no evidence for tectonic surface deformation that is associated with this series of anticlines within 25 miles of the site.

Characterization of Capable Tectonic Sources. The applicant stated that it found no capable tectonic sources within 25 miles of the site.

Designation of Zones of Quaternary Deformation in Site Region. The applicant stated that the licensee's previous geologic investigations for the CPS site found no evidence of capable faulting. For the ESP application, the applicant conducted paleoliquefaction investigations along the banks of local streams, as described above and in SER Section 2.5.1.1.1. The applicant stated that the results of these paleoliquefaction investigations revealed evidence for possible seismic ground shaking associated with prehistoric earthquakes. However, the applicant found no evidence for tectonic Quaternary faulting or surface deformation during its

field reconnaissance along the selected rivers. In addition, the applicant found no evidence for Quaternary deformation in the site region in the recent geologic literature.

Potential for Surface Tectonic Deformation. The applicant stated that the original investigations for the CPS site as well as its own investigations for the ESP site found no evidence for surface faulting or deformation that would pose a hazard to the ESP site.

2.5.3.2 Regulatory Evaluation

SSAR Section 2.5.3 describes the applicant's evaluation of the potential for surface deformation that could affect the site. The applicant did not state which regulations SSAR Section 2.5.3 addressed; however, in response to RAI 1.5-1, the applicant stated that it complied with all of the regulations listed in RS-002. This statement by the applicant implies that SSAR Section 2.5.3 conforms to the requirements of GDC 2 of Appendix A to 10 CFR Part 50, Appendix S to 10 CFR Part 50, and 10 CFR 100.23. In SSAR Table 1.5-1, the applicant stated that it developed the geological, seismological, and geophysical information used to evaluate the potential for surface deformation in accordance with the guidance presented in RG 1.165. The staff reviewed this portion of the application for conformance with the regulatory requirements and guidance applicable to determining the potential for near-surface tectonic and nontectonic deformation, as identified below. The staff notes that application of Appendix S in this portion of an ESP review, as referenced in 10 CFR 100.23(d), is limited to characterizing the potential for surface deformation as a basis for design.

In its review of the application, the staff considered the regulatory requirements in 10 CFR 100.23(d)(2), which state that an applicant for an ESP must determine the potential for surface tectonic and nontectonic deformations. SRP Section 2.5.3 and RG 1.165 provide specific guidance concerning the evaluation of information characterizing the potential for surface deformation, including the geological, seismological, and geophysical data that the applicant needs to provide to establish the potential for surface deformation.

2.5.3.3 Technical Evaluation

This section of the SER provides the staff's evaluation of the seismological, geological, and geophysical investigations carried out by the applicant to address the potential for surface deformation that could affect the site. The technical information presented in SSAR Section 2.5.3 resulted from the applicant's surface and subsurface investigations performed in progressively greater detail as they moved closer to the ESP site. Through its review, the staff determined whether the applicant complied with the applicable regulations and whether the applicant conducted its investigations with an appropriate level of thoroughness.

In order to thoroughly evaluate the surface faulting investigations performed by the applicant, the staff sought the assistance of USGS. The staff and its USGS advisors visited the ESP site and met with the applicant to assist in confirming the interpretations, assumptions, and conclusions presented by the applicant concerning potential surface deformation. Specific areas of review during the staff's site visit included the applicant's geological investigations, with an emphasis on the applicant's paleoliquefaction reconnaissance of local streams. In addition, the staff reviewed the applicant's conclusions concerning the association of earthquakes with capable tectonic sources, the ages of most deformation, the relationship of local area tectonic structures to regional tectonic structures, the characterization of capable tectonic sources, the

designation of zones of Quaternary deformation, and the potential for surface tectonic deformation.

As a result of its geologic investigations, the applicant found no potential for surface faulting or fold deformation at the ESP site. In addition, the applicant was unable to associate any of the historically reported earthquakes within 25 miles of the site with local geologic structures. Rather than characterizing the seismic potential of the known geologic folds and faults in the region, the applicant used the EPRI-SOG seismic hazard study, which groups these potential sources into large areal seismic source zones. The EPRI-SOG seismic hazard study is endorsed by RG 1.165 as an acceptable method for evaluating the seismic hazard for CEUS sites. The staff concurs with the applicant's characterization of the regional and local seismic sources as broad areal source zones. Within these source zones, earthquakes are modeled as occurring over a large area as part of the applicant's PSHA. The ESP site is located within the Illinois basin/background seismic source zone.

To search for evidence of nearby prehistoric earthquakes, the applicant conducted extensive paleoliquefaction investigations along the banks of several streams near the ESP site. The applicant found only a small number of paleoliquefaction features and concluded that there is insufficient information to estimate a location or magnitude for the prehistoric earthquake which caused these features. The staff concurs with the applicant's conclusion that the results of these paleoliquefaction investigations imply that no repeated moderate to large earthquakes comparable to the Springfield earthquake (M 6.2 to 6.8) occurred in the site vicinity during the past 6,700 to 7,000 years.

Based on its review of SSAR Section 2.5.3, as well as the supporting information in Chapter 5 of SSAR Appendix B, the staff concludes that the applicant adequately investigated the potential for surface faulting in the site area as required by 10 CFR 100.23. The staff concludes that the applicant performed extensive field investigations and concurs with the applicant's conclusion that there are no capable faults within the site area. The applicant noted that folds within the La Salle anticlinorium do lie within 25 miles of the site; however, the staff concurs with the applicant's statement that there is no evidence for tectonic surface deformation that is associated with this series of anticlines. Based on its site visit and its review of SSAR Section 2.5.3, as set forth above, the staff concurs with the applicant's conclusion that there are no capable tectonic sources within 25 miles of the site that would cause surface deformation in the site area.

2.5.3.4 Conclusions

In its review of the geological and seismological aspects of the ESP site, the staff considered the pertinent information gathered by the applicant during the regional and site-specific geological, seismological, and geophysical investigations. As a result of this review, described above, the staff concludes that the applicant performed its investigations in accordance with 10 CFR 100.23 and RG 1.165 and provided an adequate basis to establish that no capable tectonic sources exist in the site vicinity that would cause surface deformation in the site area. The staff concludes that the site is suitable from the perspective of tectonic surface deformation and meets the requirements of 10 CFR 100.23.

2.5.4 Stability of Subsurface Materials and Foundations

SSAR Section 2.5.4 presents the applicant's evaluation of the stability of subsurface materials that underlie the ESP site. Section 2.5.4.1, "Geologic Features," presents a brief description of the subsurface geology; Section 2.5.4.2, "Properties of Subsurface Materials," describes the engineering properties of the subsurface materials; Section 2.5.4.3, "Explorations," describes the subsurface explorations performed by the applicant; and Section 2.5.4.4, "Geophysical Surveys," describes the geophysical surveys performed by the applicant to determine the S-wave velocity of the soil and rock beneath the ESP site. Section 2.5.4.5, "Excavation and Backfill," describes the excavation and backfill work for the CPS site; Section 2.5.4.6, "Groundwater Conditions," describes the local ground water conditions; Section 2.5.4.7, "Response of Soil and Rock to Dynamic Loading," defers the evaluation of SSI to the COL stage; Section 2.5.4.8, "Liquefaction Potential," describes the applicant's evaluation of liquefaction potential; and Section 2.5.4.9 describes the applicant's use of the new performance-based approach for determining the SSE. Sections 2.5.4.10, "Static Stability," through 2.5.4.14, "Construction Notes," describe analyses and evaluations that the applicant has deferred to the COL stage.

2.5.4.1 Technical Information in the Application

2.5.4.1.1 Geologic Features

SSAR Section 2.5.4.1 states that the geologic features at the ESP site and CPS site are very similar. The subsurface geology at the ESP site consists of nearly 300 ft of hard or dense soil overlying rock. Other than the uppermost 50 feet, the soils have been overridden during past glaciations. As shown in Figure 2.5.4-1, reproduced from Figure 5.1-1 in SSAR Appendix B, there are seven primary soil layers at the ESP site.

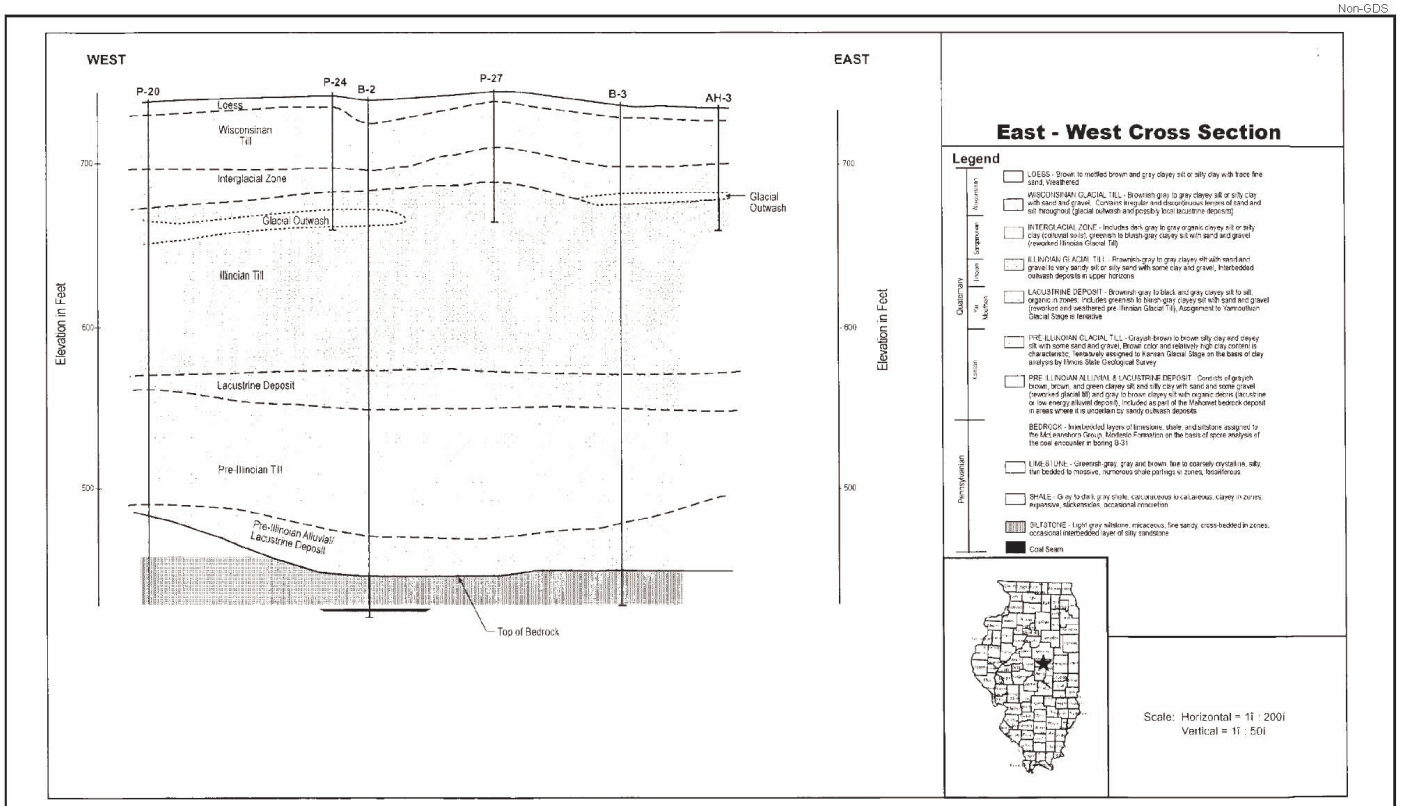

Seismic Hazards Report for the EGC ESP Site
Site-Specific Geologic Cross Section (from SSAR, Appendix A, 2003)

Figure
5.1-1

Figure 2.5.4-1 Site-specific geologic cross section

Each of these soil layers is mainly composed of silts and clays with some sand and gravel. The applicant stated that the boundaries between each of the soil layers is relatively horizontal and each layer is consistent in its thickness and contents. The ground water table beneath the ESP site is located approximately 30 ft below the surface, and the applicant stated that there are no geologic hazards such as karst terrain or underground mine openings underlying the site. SSAR Sections 2.5.1.1 and 2.5.1.2 provide a complete description of the regional and site geologic features for the ESP site. These two SSAR sections are supplemented by additional background information in SSAR Appendices A and B. Section 2.5.1.3 of this SER contains the staff's technical evaluation of the applicant's description and characterization of the regional and site geology.

2.5.4.1.2 Properties of Subsurface Materials

SSAR Section 2.5.4.2 states that the applicant established the engineering properties of the subsurface materials at the ESP site through field and laboratory measurements and by drawing upon the extensive database of information that was developed for the CPS site. The properties measured by the applicant include strength, consolidation, dynamic/cyclic, and other physical test results from soil samples recovered from the ESP site. The applicant stated that it determined these properties from the ground surface to the top of rock, located nearly 300 ft below the ground surface. Based on its field and laboratory measurements, the applicant reached the following conclusions regarding the properties of subsurface materials existing at the ESP site:

- The physical property tests indicate that the soil profile consists primarily of low-plasticity silts and clays. Sands and occasionally gravels are found in the predominantly fine-grained soil profile.

- Results of the compressibility and strength tests indicate that the soil has low compressibility and very high strength. Unconfined compressive strengths vary from 1 to 15 tons per square ft (tsf), unconsolidated undrained strengths vary from 2 to 9 tsf, and the effective strength friction angle from a consolidated undrained triaxial test is 32.6 degrees.

- The modulus and damping properties of soil from resonant column/cyclic torsion shear tests indicate that the low-strain S-wave velocity of samples ranges from approximately 800 ft per second (fps) to over 2000 fps, depending on the specific layer from which the soil sample was obtained. Low-strain material damping ratios for the same samples vary from approximately 5 percent to less than 1 percent. The changes in shear modulus and material damping ratios with the level of shearing strain are consistent with published modulus and damping characteristics of low-plasticity soils.

The applicant stated that the purpose of the ESP site laboratory testing program was to show that the properties of the ESP site are similar to those reported in the CPS USAR. By showing the similarity between the two sites, the applicant was able to utilize the extensive soil properties database in the CPS USAR to augment the information it collected for the ESP site. The scope of the soil testing reported in the CPS USAR includes (1) strength tests on soil and rock, (2) dynamic tests on soil samples such as cyclic triaxial and resonant column tests, (3) tests to determine soil type, settlement potential, and dewatering requirements, (4) chemical tests on ground water samples, (5) strength tests on excavated soils, and (6) liquefaction tests.

The applicant compared the soil classification, strength, and consolidation test results from the ESP and CPS sites and concluded that soil conditions at the two sites are consistent. Specifically, the applicant obtained similar average values of water content, density, strength, and compressibility from soil sampled at similar depths from each site. In RAI 2.5.4-1, the staff asked the applicant to describe its criteria for assessing whether the differences in the soil properties for the ESP and CPS sites were significant enough to warrant additional soil exploration. In response to RAI 2.5.4-1, the applicant stated that it used both visual and quantitative criteria to assess the similarity between the soils underlying the two sites. The applicant stated that it would have conducted additional explorations if it had encountered significant differences in the soil properties between the two sites. SER Section 2.5.4.3.2 provides a complete description of the applicant's response to RAI 2.5.4-1 as well as the staff's evaluation of this response.

The applicant conducted cyclic testing of the ESP site soils to determine the variation in shear modulus and material damping ratio with shearing strain amplitude. These dynamic properties are necessary to construct shear modulus and damping curves in order to determine the response of the site to the SSE ground motion. The applicant was unable to make a comparison between its cyclic test results for the ESP and CPS sites because significant advances in resonant column/cyclic torsional shear tests have occurred since the licensee conducted cyclic tests on soils from the CPS site. Since it had conducted only six sets of resonant column/cyclic torsional shear tests, the applicant decided to use the EPRI shear modulus and damping curves (EPRI 1993) for its site response analyses. As justification for this approach, the applicant stated the following:

> The rationale for using the EPRI curves rather than the EGC ESP Site data was that a much larger database was used to develop the EPRI curves and, therefore, average EPRI results are expected to be representative of conditions at the EGC ESP Site if an extensive dynamic testing program had been conducted. It is important to note that the dynamic test results for the EGC ESP Site are very consistent with the EPRI curves, indicating that use of the EPRI curves is acceptable.

Figures 2.5.4-2 and 2.5.4-3, reproduced from Figures 5-20 and 5-21 in SSAR Appendix A, show a comparison of the EPRI and ESP site cyclic test results.

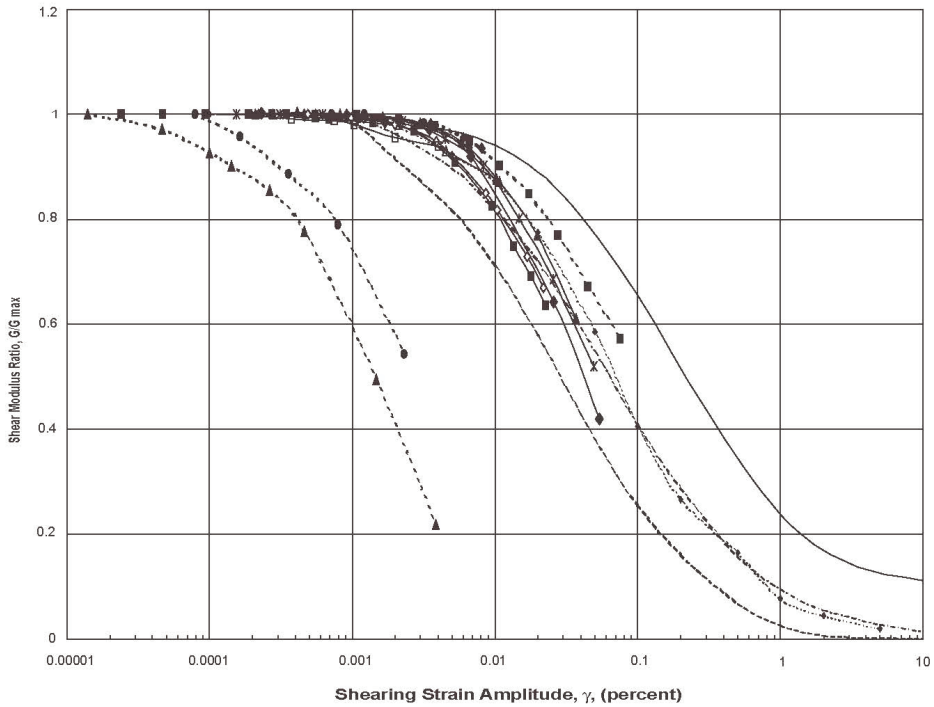

Geotechnical Report for the EGC Early Site Permit

Figure 5-20
G/Gmax Plot
Resonant Column and
Cyclic Torsion Test Results

Legend

- V & D for PI = 0 (Vucetic and Dobry, 1991)
- V & D for PI = 15 (Vucetic and Dobry, 1991)
- Clay - PI = 10-20 (Sun et al., 1988)
- Clay (Seed and Sun, 1989)
- Sample A -- 33 ft depth -- Resonant Column
- Sample A -- 33 ft depth -- Cyclic Torsion
- Sample B -- 41.5 ft depth -- Resonant Column
- Sample B -- 41.5 ft depth -- Cyclic Torsion
- Sample C -- 171 ft depth -- Cyclic Torsion
- Sample C -- 171 ft depth -- Resonant Column
- Sample D -- 115 ft depth -- Resonant Column
- Sample D -- 115 ft depth -- Cyclic Torsion
- Sample E -- 208 ft depth -- Resonant Column
- Sample E -- 208 ft depth -- Cyclic Torsion
- Sample F -- 242 ft depth --Resonant Column
- Sample F -- 242 ft depth -- Cyclic Torsion

Note:
PI for EGC ESP soils typically 10

Figure 2.5.4-2 G/G_{max} plot resonant column and cyclic torsion test results

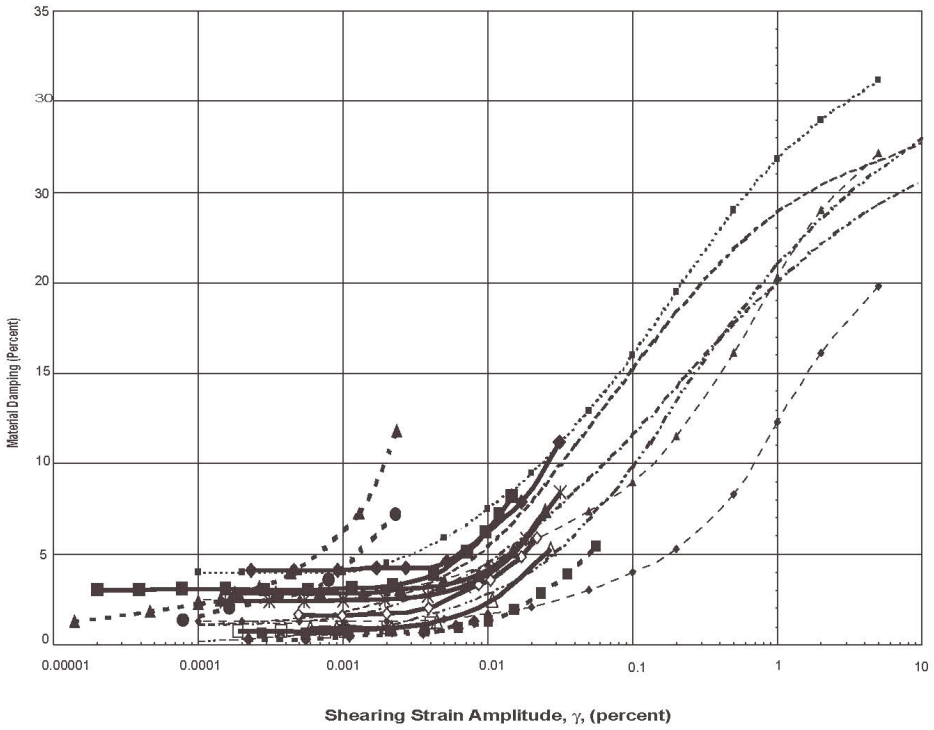

Geotechnical Report for the EGC Early Site Permit

Figure 5-21
Material Damping Plot
Resonant Column and Cyclic Torsion Test Results

Legend

- V & D for PI = 0 (Vucetic and Dobry, 1991)
- V & D for PI = 15 (Vucetic and Dobry, 1991)
- Clay - Lower Bound (Sun et al., 1988)
- Clay - Average Bound (Sun et al., 1988)
- Clay - Upper Bound (Sun et al., 1988)
- Clay (Idriss, 1990)
- Sample A -- 33 ft depth -- Resonant Column
- Sample A -- 33 ft depth -- Cyclic Torsion
- Sample B -- 41.5 ft depth --Resonant Column
- Sample B -- 41.5 ft depth -- Cyclic Torsion
- Sample C -- 171 ft depth -- Cyclic Torsion
- Sample D -- 115 ft depth --Resonant Column
- Sample D -- 115 ft depth -- Cyclic Torsion
- Sample E -- 208 ft depth --Resonant Column
- Sample E -- 208 ft depth -- Cyclic Torsion
- Sample F -- 242 ft depth --Resonant Column
- Sample F -- 242 ft depth -- Cyclic Torsion

Note:
PI for EGC ESP soils typically 10

Figure 2.5.4-3 Material damping plot resonant column and cyclic torsion test results

In RAI 2.5.4-2, the staff asked the applicant to justify its use of the EPRI curves and to further explain its basis for concluding that the ESP site soils are consistent with those used to develop the EPRI curves. In response to RAI 2.5.4-2, the applicant stated that the EPRI curves it used represent soils in the general range of gravelly sands to low-plasticity silty or sandy clays and that soils at the ESP site fall within this category of soils. SER Section 2.5.4.3.2 provides a complete description of the applicant's response to RAI 2.5.4-2 and the staff's evaluation of this response.

In RAI 2.5.4-5, the staff asked the applicant to explain the difference between soil S-wave velocities measured directly in the field and in the laboratory using soil samples. For two of the soil samples, taken at depths of 208 and 242 ft, the laboratory measurement of S-wave velocity is 68 and 76 percent, respectively, of the field-measured test results for similar depths. In response to RAI 2.5.4-5, the applicant stated that the low values are an indication of the accumulated disturbance that occurs to soil samples when they are removed from the ground, transported to the laboratory, and tested in equipment that may not replicate the in situ stress state and loading conditions. SER Section 2.5.4.3.2 provides a complete description of the applicant's response to RAI 2.5.4-2 and the staff's evaluation of this response.

2.5.4.1.3 Explorations

To characterize the ESP site, the applicant conducted a subsurface exploration program that consisted of drilling and sampling four boreholes and conducting four cone penetrometer tests (CPT) with pore pressure measurements. The applicant stated that the purpose of the exploration work was to establish the location and consistency of the soil layers, to collect soil samples for laboratory testing (see SER Section 2.5.4.1.2), and to install piezometers for ground water monitoring. For guidance, the applicant stated that it used RG 1.132, "Site Investigations for Foundations of Nuclear Power Plants," with the exception of the number and depth of explorations. The applicant stated that fewer explorations were justified because of the similarity of soil conditions at the ESP and CPS sites. Specifically, the applicant stated in Section 3.1.1 of SSAR Appendix A that its rationale for the reduced number of explorations was as follows:

- Over 10 explorations had been previously drilled, sampled, and tested within the general EGC ESP Site footprint area during the investigation for the CPS Site. A careful review of this existing information determined that the methods used for drilling and sampling, soil classification, and laboratory testing of soils from these explorations was of sufficient quality to allow re-use of the data for the EGC ESP Site work.

- The work being carried out for the EGC ESP was being done before the reactor plant design had been selected. Therefore, some of the spacing and depth requirements given in Appendix C of RG 1.132 could not be established. Once a reactor plant design is selected, then the requirements in Appendix C of RG 1.132 will be reviewed again during the COL stage, along with the design requirements of the reactor plant design, to determine whether additional drilling and sampling is needed.

In addition, the applicant stated that if it had encountered any significant soil property variations during its drilling and sampling program, it would have added more explorations to resolve the observed differences.

The applicant used mud rotary drilling methods for the four explorations that it drilled at the ESP site. Figure 2.5.4-4, reproduced from Figure 3-1 in SSAR Appendix A, shows the locations of each of the four boreholes.

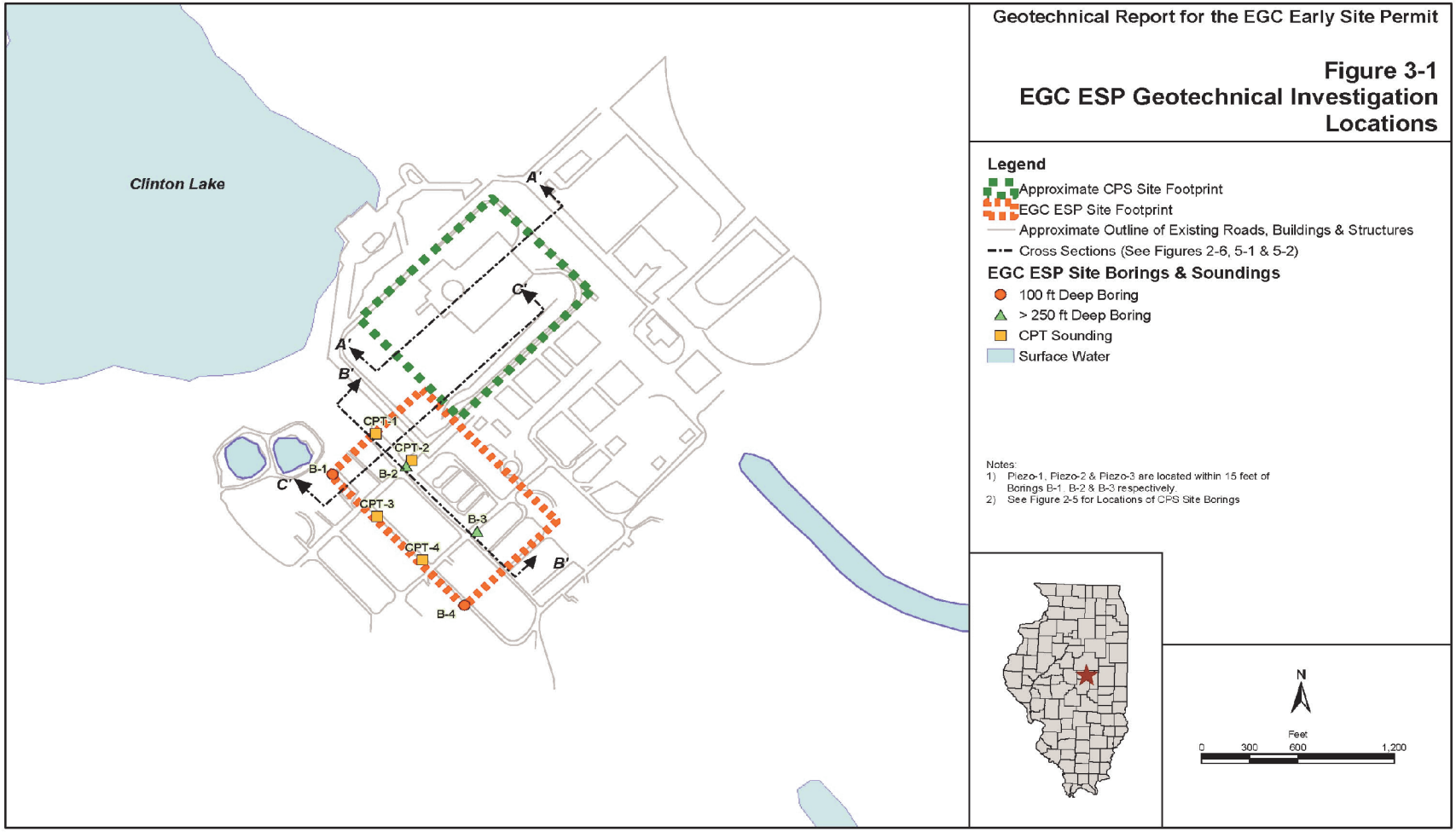

Figure 2.5.4-4 EGC ESP geotechnical investigation locations

Two of the explorations extended to 100 ft below the ground surface, and the other two extended 20 to 30 ft into rock at nearly 300 ft below the ground surface. The applicant used SPT, Shelby, and Pitcher tube sampling methods to collect representative soil samples. For each borehole, the applicant obtained SPT blowcounts and also calibrated the SPT hammer system in one of the boreholes. At depths shallower than 100 ft, the applicant collected soil samples at 5 ft intervals using ASTM D 1586-99, "Standard Test Method for Penetration Resistance and Split Barrel Sampling of Soils," for guidance. At each major change in stratigraphy, the applicant also collected undisturbed soil samples following the methods given in ASTM D 1587-00, "Standard Practice for Thin-Walled Tube Sampling of Soils for Geotechnical Purposes." At depths between 100 and 150 ft (at boreholes B-2 and B-3), the applicant increased its soil sampling interval to 10 ft, and at depths greater than 150 ft, the applicant used a sampling interval of 15 ft. For the two boreholes that extended down into rock, the applicant collected continuous rock-core samples for classification using ASTM D 2113-99, "Standard Practice for Rock Core Drilling and Sampling of Rock for Site Investigations."

The applicant also conducted a CPT program at the ESP site. The locations of the CPT soundings are shown above in Figure 2.5.4-4. The applicant used the results of the CPT soundings to evaluate the consistency of the soils in the upper 50 to 80 ft of soil in the ESP site area. The CPT soundings included pore water pressure measurements, and during two of the soundings, the applicant obtained S-wave velocity data. The total depths of the soundings at CPT-1, CPT-2, CPT-3, and CPT-4 were 78.1, 55.7, 54.0, and 76.9 ft, respectively. For the seismic tests, the applicant generated an S-wave at the ground surface by horizontally striking a board at the surface using a sledge hammer. The applicant measured the travel time of the resulting S-waves with a velocity-sensitive geophone located at the tip of the CPT assembly. The applicant made measurements of S-wave travel times at 3-ft depth intervals from the ground surface until it could no longer advance the CPT assembly into the ground.

The applicant used its four ESP boreholes and CPT soundings to augment the results of similar programs conducted at the CPS site. The licensee conducted an extensive drilling and sampling program during work on the CPS site, which consisted of 76 boreholes. The applicant stated that some of these boreholes were drilled within or adjacent to the footprint of the ESP site and a number of the boreholes extended into rock. Concerning its comparison of the results between the ESP and CPS site boreholes, the applicant stated the following:

> Results of these comparisons show that both sites consist of over 250 feet of predominantly silts and clays overlying rock. The silts and clays are very stiff to hard in consistency—as a result of past glaciations. Rock is slightly deeper at the EGC ESP Site (specifically, nearly 250 ft below ground surface at the CPS Site versus over 280 ft at the EGC ESP Site); however, rock descriptions and quality are consistent between the sites. It was concluded from this comparison that the engineering characteristics of the two sites are consistent; therefore, the database from the CPS Site can be used in evaluating site response to gravity and seismic loading at the EGC ESP Site.

2.5.4.1.4 Geophysical Surveys

The applicant conducted geophysical surveys at the ESP site in order to determine the S-wave velocity of the soil and upper layer of rock. The applicant stated that it would use this information to determine the response of the site to seismic ground motion propagating up from

the rock to the ground surface. In addition, the applicant stated that it may use the results of the geophysical surveys during the COL stage of design to evaluate SSI.

The applicant used two types of geophysical seismic tests. The first test was a P- and S-wave suspension logging test in one of the boreholes, and the second test used the CPT assembly, which was described above in SER Section 2.5.4.1.3. The applicant conducted the P-S suspension logging test at approximately 1.5-ft depth intervals to within approximately 20 ft into the top of rock. The applicant performed the test by lowering the logging probe into the open borehole filled with drilling fluid. Each measurement recorded the average P- and S-wave velocity of the subsurface material between the two receivers located near the top of the probe. The applicant stated that the quality of the test results was influenced by the integrity of the borehole sidewalls and by the consistency of the drilling mud. Therefore, in order to optimize the quality of the measurements, the applicant performed the test on the same day as the completion of the rock coring at borehole B-2 and mixed the bentonite drilling fluid immediately before the start of the test. Figure 2.5.4-5, reproduced from Figure 5-19 in SSAR Appendix A, shows the P- and S-wave velocities for each of the different soil units to a depth of about 300 ft below the ground surface.

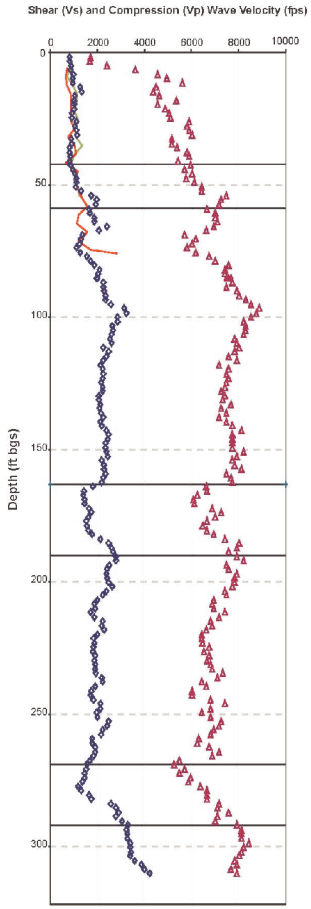

Unit	Depth (ft. bgs)	Soil Properties - EGC ESP Site *(and CPS Site)*[1] Moist Unit Wt. (pcf)	Moist. Cont. (%)	LL	PL	PI	Comments
Loess & Wisconsinan Till	0 - 42	131 *(131)*	16 *(16)*	35 *(25)*	14 *(14)*	14 *(11)*	Perched water table at ~5 ft bgs
Interglacial	42 - 59	116 *(132)*	39 *(17)*	40 *(26)*	26 *(13)*	14 *(13)*	
Illinoian Till	59 - 163	148 *(147)*	8 *(9)*	18 *(18)*	9 *(11)*	9 *(7)*	
Lacustrine	163-190	133 *(140)*	13 *(11)*	28 *(19)*	11 *(12)*	17 *(7)*	
Pre-Illinoian Till	190 - 269	138 *(137)*	14 *(14)*	29 *(27)*	14 *(14)*	15 *(13)*	
Pre-Illinoian Alluvial/ Lacustrine	269 - 292	N.A. *(N.A.)*	23 *(N.A.)*	48 *(N.A.)*	17 *(N.A.)*	29 *(N.A.)*	
Bedrock	292-322	N.A. *(N.A.)*	N.A. *(N.A.)*	N.A. *(N.A.)*	N.A. *(N.A.)*	N.A. *(N.A.)*	Weathered rock contact at 292 ft bgs

Geotechnical Report for the EGC Early Site Permit

Figure 5-19

Shear and Compressional Wave Velocities and Other Soil Properties

Legend

- Vs at B-2
- Vp at B-2
- Vs at CPT-02
- Vs at CPT-04

Notes:

1 Soil properties shown are the arithmetic mean values for all available soil sample results for each stratigraphic unit. Top number is the mean value of applicable EGC ESP Site investigation data.

(Italic) = Mean value of applicable data from CPS Site P-Series Soil Samples, as reported in Section 2.5 of CPS, 2002

N.A. = Results not available

Figure 2.5.4-5 S- and P-wave velocities and other soil properties

Based on its geophysical surveys, the applicant established the following minimum site characteristic S-wave velocities in its plant parameter envelope (PPE) table (SSAR Table 1.5-1):

- 820 ft/s in the upper 50 ft of soil
- 1090 ft/s to nearly 3000 ft/s at depths of 50 ft to the top of rock
- 2580 ft/s in the upper 20 ft of rock

The applicant found that its comparison of the velocities between the CPS and ESP sites showed very similar average conditions. The applicant used a much smaller depth interval for its velocity measurements during the ESP site tests, and, therefore, the ESP site velocity results provided a much better indication of the variation in velocity within each of the prominent stratigraphic units.

2.5.4.1.5 Excavation and Backfill

SSAR Section 2.5.4.5 states that construction of the facilities at the ESP site would likely require excavations to a depth of approximately 55 to 60 ft below the ground surface to avoid potential settlement and liquefaction concerns. The applicant stated that during original excavations at the CPS site, the following conditions were observed:

- The excavation work at the CPS site shows that the drilling and sampling program provided a good description of the soil conditions in the upper 56 ft at the site, confirming that the boreholes completed within the EGC ESP site footprint for both the CPS and EGC ESP sites will be representative of conditions in the upper 56 ft of soil profile.

- Seepage into the construction excavation was very limited at the CPS site. This observation indicates that dewatering requirements within the upper 56 ft at the EGC ESP site will be minimal because of the similarity in ground water location and soil types.

- Some localized pockets of sand were encountered at the base of the excavation at a depth of 56 ft. These pockets were either compacted or removed and replaced with a flyash-backfill mixture. Similar conditions could be encountered at the EGC ESP site.

The applicant found that nothing discussed within Section 2.5.4.5 of the CPS USAR indicates a condition that would significantly affect the construction or operation of a new generating facility at the ESP site.

2.5.4.1.6 Ground Water Conditions

The applicant installed three piezometers during its ESP site exploration to obtain more specific information about ground water conditions at the ESP site. The applicant's ground water measurements indicate that the static ground water table within the Illinoian till is approximately 30 ft below the ground surface, but that there are shallower perched ground water layers closer to the surface. The applicant found similar ground water conditions at both the ESP and CPS sites. SSAR Section 2.5.4.6 provides a complete description of the ESP site ground water conditions.

2.5.4.1.7 Response of Soil and Rock to Dynamic Loading

SSAR Section 2.5.4.7 defers the analyses of soil-rock-structure interaction for the ESP site to the COL stage. Specifically, the applicant stated that these analyses will depend on the geometry and weight of the selected power generating system, and on the method that it will use during the COL stage to evaluate SSI. Since some of the soil and rock dynamic tests used by the licensee for the CPS site in the mid-to-late 1970s are no longer used, the applicant stated that before adopting any of the dynamic soil and rock properties given in the CPS USAR, it will re-derive these dynamic properties based on the results of field and laboratory information collected during the ESP site program (see SER Section 2.5.4.1.2) and future programs. Section 2.5.2.3.5 of this SER presents the staff's evaluation of the applicant's free-field site response analysis, including an evaluation of the applicant's responses to RAIs 2.5.4-4 and 2.5.4-7. The applicant's decision to defer the SSI analyses to the COL stage is **COL Action Item 2.5.4-1.**

2.5.4.1.8 Liquefaction Potential

To evaluate the liquefaction potential of the soils at the ESP site, the applicant used an empirical blowcount procedure, which is described in RG 1.198, "Procedures and Criteria for Assessing Seismic Soil Liquefaction at Nuclear Power Plants," issued November 2003. This approach uses correlations between blowcounts recorded during SPT tests and observed liquefaction at sites that did or did not liquefy. The empirical method calculates a factor of safety (FOS) based on the expected soil shearing resistance and the expected maximum seismically induced shearing stresses in a soil layer. The soil shearing resistance is quantified by the cyclic resistance ratio (CRR), which is determined from the SPT blowcount values, with modifications for depth and SPT driving conditions. The shearing stresses induced by seismic loading are quantified by the cyclic stress ratio (CSR), which is proportional to the PGA for the specified seismic loading. In addition, the method uses a magnitude scaling factor (MSF), which is based on the specified earthquake M_w that is expected to generate the specified PGA. The FOS against liquefaction is calculated as:

$$FOS = \frac{CRR}{CSR}(MSF)$$

The MSF is smaller for larger magnitude earthquakes (reducing the FOS) to account for the longer duration of shaking and lower frequency vibrations typical of larger events. The applicant calculated the FOS against liquefaction for soil conditions at regular depth intervals to obtain a profile of FOS with depth.

To implement the above liquefaction procedure for the ESP site, the applicant used a PGA of 0.3g, which represents the peak acceptable value for the plant that forms the basis for the PPE. The applicant also used a range of earthquake magnitudes (M = 5.5, 6.5, and 8.0) that are consistent with the range of source mechanisms that have the potential to cause ground shaking at the ESP site. To estimate the shearing resistance of the ESP site soils, the applicant used the SPT blowcount values from its four boreholes (B-1, B-2, B-3, and B-4). The applicant found that the FOS is greater than 1.1 for the soil layers below a depth of 60 ft below the ground surface. Above 60 ft, the applicant found several layers where the FOS is less than 1.1, indicating that these layers are susceptible to liquefaction. RG 1.198 states that soil

elements with an FOS less than or equal to 1.1 “would achieve conditions wherein soil liquefaction should be considered to have been triggered.” However, the applicant stated that these soils (susceptible to liquefaction) will “need to be excavated and replaced or improved for settlement considerations, thereby mitigating any liquefaction potential.” Therefore, the applicant concluded that liquefaction is not a design consideration for the ESP site.

In RAI 2.5.4-6, the staff asked the applicant to provide a sample liquefaction analysis from one of its four borehole locations and to clearly show how it determined the FOS for the different soil layers. In addition, the staff asked the applicant to describe the methods that it might use to mitigate the potential for liquefaction and to describe the extent of the liquefiable soils over the ESP site area. In response to RAI 2.5.4-6, the applicant provided a sample calculation for borehole B-1 at the 38.5-ft depth interval. In addition, the applicant described the methods (other than removal and replacement) that it may use to mitigate the potential for liquefaction. The applicant stated that it encountered noncohesive soils in its soil borings, but that not all of these noncohesive soils are considered liquefiable. SER Section 2.5.4.3.8 provides a complete description of the applicant’s response to RAI 2.5.4-6 and the staff’s evaluation of this response.

For the CPS site, the licensee used a different method to assess the potential for liquefaction. Instead of using the empirical blowcount procedure, the licensee used cyclic triaxial testing to determine the soil shearing resistance. To determine the shearing stresses induced by seismic loading, the licensee used the SSE ground motion. Using this method, the licensee found an FOS greater than 2.0, and, therefore, liquefaction was not an issue for the CPS site.

2.5.4.1.9 Earthquake Design Basis

SSAR Section 2.5.4 describes the development of the SSE ground motion for which the applicant used the performance-based approach, described in ASCE/SEI Standard 43-05. Section 2.5.2.1.6 of this SER describes the applicant’s use of the performance-based approach to develop the SSE response spectrum for the ESP site.

2.5.4.1.10 Static Stability

The applicant did not estimate the bearing capacity, settlement, or lateral earth pressures for the ESP site, since it has not selected a nuclear power plant design. The applicant stated that each generating system has different footprint sizes, depths of embedment, and effective weights, and these variables will affect the determination of bearing pressures, settlement, and lateral earth pressures. For this reason, the applicant deferred the determination of static stability to the COL stage.

Using the licensee’s evaluation of static stability for the CPS site, the applicant stated that it expected high allowable bearing values and low compressibility for the ESP site because of the similarity in soil conditions between the two sites. Based on the bearing capacity values given in the CPS USAR, which range from 39.9 to 60.6 tsf, the applicant established the minimum site characteristic value for bearing pressures at the ESP site at 25 tsf. Net foundation pressures for the Category I structures at the CPS site are less than 2.5 tsf.

In RAI 2.5.4-3, the staff asked the applicant to provide further detail regarding the criteria that it used to establish the minimum static bearing capacity of 25 tsf for the ESP site. In response to

RAI 2.5.4-3, the applicant stated that the methods used by the licensee for the calculation of the bearing capacities were conventional methods that assume a local shear failure condition. The applicant stated that the combination of foundation depth below the ground surface and the heavily overconsolidated state of the Illinoian till result in the high bearing capacities given in the CPS USAR. Comparing the minimum bearing capacity value chosen by the applicant (25 tsf) with the lower value in the range of bearing capacities for the CPS site (39.9) provides an FOS greater than 1.5. SER Section 2.5.4.3.10 provides a complete description of the applicant's response to RAI 2.5.4-3 and the staff's evaluation of this response.

2.5.4.1.11 Design Criteria

SSAR Section 2.5.4.11, "Design Criteria," states that the design criteria for the ESP site Category I structures will be established during the COL stage when the physical characteristics of the operating system are known. The applicant stated that it would use the CPS USAR as a starting point for developing design criteria for the ESP site.

2.5.4.1.12 Techniques to Improve Subsurface Conditions

SSAR Section 2.5.4.12, "Techniques to Improve Subsurface Conditions," states that until the power generating system is selected, the need for ground improvement for the ESP site is unknown. The applicant stated that systems that are founded at depths of 55 ft or above could require ground improvement and that decisions regarding the need for and type of ground improvement will be made during the COL stage. For the CPS site, the licensee encountered localized areas and pockets of loose granular material at the base of excavations for the CPS Category I structures (about 55 ft below the ground surface) during construction at the CPS site. These materials were either compacted or removed and replaced with a flyash-backfill material.

2.5.4.1.13 Subsurface Instrumentation

SSAR Section 2.5.4.13, "Subsurface Instrumentation," states that the settlement measurements made by the licensee for the CPS plant structures will be used for future settlement predictions at the ESP site. Because of the similar soil conditions between the two sites, and assuming the new facilities are similar in size, load, and foundation level to those constructed at the CPS site, the applicant stated that it will be able to use conventional settlement prediction methods and rely on the previous settlement measurements.

2.5.4.1.14 Construction Notes

SSAR Section 2.5.4.14 states that the CPS USAR provides valuable information from the construction of the CPS facilities and that this information will be used during the COL stage of the project. The applicant stated the following:

> Any future excavation associated with the construction of a new generating system will be mapped to confirm that soil types and consistency are in general accord with the conditions identified during previous construction at the site and that have been interpreted from the field explorations carried out at the EGC ESP Site. This field mapping will involve inspecting excavated slopes for the presence of previously unknown fault offsets.

The applicant also committed to (1) “notify the NRC staff immediately if previously unknown geologic features that could represent a hazard to the plant are encountered during excavation,” and (2) “notify the NRC staff when the excavations are open for examination and evaluation.”

2.5.4.2 Regulatory Evaluation

SSAR Section 2.5.4 describes the applicant’s evaluation of the stability of the subsurface materials and foundations at the ESP site. In SSAR Section 1.5, the applicant stated that it developed the geological, geophysical, and geotechnical information used to evaluate the stability of the subsurface materials in accordance with the requirements of 10 CFR 100.23. The applicant applied the guidance of RS-002, RG 1.70, DG-1105 (which has been superseded by RG 1.198 since the applicant submitted the SSAR), RG 1.132, and RG 1.138, “Laboratory Investigations of Soils for Engineering Analysis and Design of Nuclear Power Plants.” The staff reviewed SSAR Section 2.5.4 for conformance with the regulatory requirements and guidance applicable to the characterization of the stability of subsurface materials, as identified below.

In its review of SSAR Section 2.5.4, the staff considered the regulatory requirements in 10 CFR 100.23(c) and 10 CFR 100.23(d)(4). According to 10 CFR 100.23(c), applicants must investigate the engineering characteristics of a site and its environs in sufficient scope and detail to permit an adequate evaluation of the proposed site. Pursuant to 10 CFR 100.23(d)(4), applicants must evaluate siting factors such as soil and rock stability, liquefaction potential, and natural and artificial slope stability. Section 2.5.4 of RS-002 provides specific guidance concerning the evaluation of information characterizing the stability of subsurface materials, including the need for geotechnical field and laboratory tests as well as geophysical investigations.

2.5.4.3 Technical Evaluation

This section provides the staff’s evaluation of the geophysical and geotechnical investigations carried out by the applicant to determine the static and dynamic engineering properties of the materials that underlie the ESP site. The technical information presented in SSAR Section 2.5.4 resulted from the applicant’s field and laboratory investigations performed for the ESP. The applicant intended its ESP field and laboratory field investigations to confirm the large volume of geotechnical data developed by the licensee for the existing CPS units, located adjacent to the ESP site. The applicant used the subsurface material properties from its field and laboratory investigations to evaluate the response of the site to dynamic loading (SSE ground motion), including liquefaction potential. The applicant deferred the determination of static stability to the COL stage.

Through its review of SSAR Section 2.5.4, the staff determined whether the applicant adequately sampled the subsurface materials underlying the ESP site in order to characterize the engineering properties as well as the response of the site to dynamic and static loading. The staff also reviewed the applicant’s field and laboratory investigations used to determine the geotechnical engineering properties of the soil and rock underlying the ESP site. In addition, the staff observed some of the applicant’s onsite borings and field explorations, performed August 7–8, 2002, to determine whether the applicant followed the guidance in RG 1.132.

2.5.4.3.1 Geologic Features

SSAR Section 2.5.4.1 references SSAR Section 2.5.1 for a description of the regional and site geology. Section 2.5.1.3 of this SER presents the staff's evaluation of the regional and site geology.

2.5.4.3.2 Properties of Subsurface Materials

The staff focused its review of SSAR Sections 2.5.4.2 (properties of subsurface materials) and 2.5.4.3 (explorations) on the applicant's description of (1) subsurface materials, (2) field investigations, (3) laboratory testing, and (4) static and dynamic engineering properties of the ESP site subsurface materials.

Normally, an applicant performs a complete field investigation and sampling program to evaluate the engineering properties and stability of the soil and rock underlying the site. However, since the applicant relied on the licensee's previous field and laboratory investigations for the existing CPS units, the applicant's ESP investigations were used to confirm previously established soil and rock properties. As such, the applicant conducted a subsurface exploration program that consisted of drilling and sampling four boreholes and conducting four CPTs. In RAI 2.5.4-1, the staff asked the applicant to describe its criteria for assessing whether the differences in the soil properties for the ESP and CPS sites were significant enough to warrant additional soil exploration. In addition, the staff asked the applicant to provide tables showing a comparison between the static and dynamic soil properties for the two sites. In response to RAI 2.5.4.1, the applicant stated that it would have conducted additional explorations if it had encountered significant differences in the soil properties between the two sites. The applicant stated that the geologic information it reviewed indicated that the regional processes that formed the site profile at the two sites were the same. In addition, the applicant stated that the sampling program for the CPS site included a number of explorations within and beyond the ESP site. Since the geologic formation and stratigraphy for the two sites were essentially the same, the applicant expected to encounter only small local variations in soil properties during its ESP site exploration. During its ESP site exploration, the applicant visually monitored the soil it retrieved during drilling and sampling to see if the soil color and texture were consistent with the soil profile described in the CPS site USAR. In addition, the applicant also compared the SPT blowcount values that it obtained from the ESP boreholes to those from the CPS site boreholes. The applicant used the combination of consistency, color, and texture to decide whether the material was essentially the same. As an example of its evaluation process, the applicant stated the following:

> For example, if the blowcount reported in the USAR was significantly different (e.g., an order of magnitude greater) than what was recorded during the EGC ESP Site exploration program and the texture of the material was fine-grained rather than a sand, the field task leader for the EGC ESP Site explorations was prepared to take additional soil samples to investigate this difference.

Once the applicant completed its fieldwork, it made the following comparisons during its laboratory testing program:

- It compared visual-manual field descriptions of the soil samples collected during the EGC ESP site investigation with each other and with CPS site data. These comparisons

were performed to evaluate whether each stratigraphic unit encountered at the CPS site was present or absent at the EGC ESP site, and to identify similarities and/or differences in thickness of and contact elevations between these units. Soil descriptions compared include apparent soil gradation, plasticity, presence of inclusions and bedding, color, consistency (soft to hard, loose to dense), and moisture condition. This comparison differed from that done in the field from the standpoint that all the information was available for review, rather than the individual comparisons done in the field as the boring was drilled and sampled. Details of these comparisons are presented in Sections 5.2.1 and 5.2.2 of SSAR Appendix A. As described, the same stratigraphic units were identified between each EGC ESP site investigation location and the CPS site, with moderate variations in contact elevations and unit thicknesses.

- It compared data from laboratory tests performed on samples from the EGC ESP site with each other and with CPS site test data. These comparisons were performed to identify similarities and/or differences in engineering properties of the stratigraphic units between the two sites, and within the EGC ESP site. Test results compared include Atterberg Limits, in situ dry density, moisture content, undrained shear strength, and consolidation properties. Results of these comparisons are presented in Sections 5.2.2 and 5.2.3 of SSAR Appendix A. SPT blowcounts at the two sites were also compared, as summarized in Section 5.2.1 of SSAR Appendix A. S- and P-wave velocity data from the seismic CPT and suspension logging tests were also compared with applicable data from the CPS site (from downhole and uphole logging tests), as described in Section 5.2.4 of SSAR Appendix A.

After making the comparisons as described above, the applicant developed qualitative and quantitative criteria to determine the similarity between soil stratigraphic units and the engineering properties within each stratigraphic unit. The applicant's qualitative criteria consisted of observing the similarities of the soil descriptions between the sites. These descriptions included soil color, texture, and consistency in terms of denseness or hardness as indicated by SPT blowcounts. The applicant's quantitative criteria consisted of comparing plots and tables of the engineering property data for similarity. The applicant's comparison focused on the typical range of properties within a stratigraphic unit recorded at the CPS site versus the range in the same properties recorded at the ESP site. The applicant stated that it did not use "hard numerical acceptance criteria" for this comparison of engineering properties; however, the applicant observed that the ESP site data generally fell within the range of CPS site results for each stratigraphic unit. In conclusion, the applicant stated that there were some variations, but that these variations were not considered significant enough to alter the conclusion that subsurface conditions are similar between the sites and within the ESP site.

The staff reviewed the applicant's comparison of the soil properties between the two sites in Section 5.2 of SSAR Appendix A. The staff's review included a comparison between SPT blowcount values, in situ dry density, moisture content, Atterberg limits, compressibility and strength characteristics, P- and S-wave velocities, and modulus and damping properties. In addition, the staff also reviewed the tabulated statistical summaries of the geotechnical test results that the applicant provided in response to RAI 2.5.4-1. Figures 5-7 through 5-18 in SSAR Appendix A provide an excellent visual comparison of the engineering properties between the CPS and ESP sites. While there are some outliers, for the most part the staff concurs with the applicant's conclusion that the subsurface conditions are similar between the two sites. As such, the staff concludes that the applicant has sufficiently sampled the ESP site

subsurface in order to establish the similarity between the CPS and ESP sites. The staff notes that 76 locations were drilled and sampled by the licensee for the CPS site investigation and that some of these locations (10) overlapped with the ESP site area. Regarding future subsurface investigations for the ESP site, the applicant stated the following:

> The work being carried out for the EGC ESP was being done before reactor plant design had been selected. Therefore, some of the spacing and depth requirements given in Appendix C of Regulatory Guide 1.132 could not be established. Once a reactor plant design is selected, then the requirements in Appendix C of Regulatory Guide 1.132 will be reviewed again during the COL stage, along with the design requirements of the reactor plant design, to determine whether additional drilling and sampling is needed.

Concerning the appropriate spacing of borings or soundings, RG 1.132 states that for favorable uniform geologic conditions, at least one boring should be made at the location of every safety-related structure. Where variable conditions occur, RG 1.132 states that the spacing between borings should be smaller. For larger, heavier structures, such as the containment and auxiliary buildings, RG 1.132 recommends a boring spacing of at least 100 ft with a number of additional borings along the periphery, at corners, and other selected locations. Regarding the appropriate depth for borings, RG 1.132 states that all borings should extend at least 33 ft below the lowest part of the foundation. With regard to these recommendations in RG 1.132, the staff cannot accept the applicant's concluding statement to review RG 1.132 at the COL stage to "determine whether additional drilling and sampling is needed" as sufficient. While the staff's review of the applicant's geotechnical field and laboratory test results confirmed the similarity between the CPS and ESP subsurface soil layers and properties, this similarity does not eliminate the need for further soil borings during the COL stage. There are enough variations in the soil properties within the ESP site itself to necessitate further exploration at the COL stage. Examples include variations in SPT blowcount values, S-wave velocities, and other static and dynamic properties, which may indicate localized areas of variable subsurface material.

In Open Item 2.5.4-1, the staff asked the applicant to clarify its intentions with respect to the need for additional field drilling and sampling of soil at the ESP site during the COL stage. In response, the applicant stated that the original wording in the ESP application indicates that the need for additional explorations will be determined during the COL stage. The applicant stated that this wording will be revised to indicate that additional exploration work is expected consistent with the following information:

> If this site is selected in the future for a COL application, additional explorations will be conducted by the COL contractor for the final design of the selected reactor system. This additional exploration work will include a sufficient amount of drilling and sampling to characterize soil conditions and collect soil samples for laboratory testing necessary for the final design of the foundations for the structures. The numbers and locations of the additional explorations will depend on the depth and plan view area of the foundation for the selected reactor system, the net weight of the various components of the reactor system, and the sensitivity of the selected system to settlement. These explorations would be required to meet the standard of practice for foundation design of a large structure. Additional explorations will also be required for the new intake

> alignment, and could be required to assess construction methods. Examples of exploration carried out for construction evaluations could include groundwater pump tests for dewatering evaluations or collections of samples from selected areas for material re-use studies.
>
> The COL application will consider and address Regulatory Guide 1.132 when determining the number, location, depth, and type of explorations. The specific scope of final explorations will also consider the design requirements of the structure and the uniformity of conditions encountered during the COL explorations relative to previous information and relative to design requirements such that appropriate and sufficient information is available for final design of the selected reactor system.

Since the applicant has clarified its intentions to perform further drilling and sampling during the COL stage and to address the guidance recommended by RG 1.132, the staff considers Open Item 2.5.4-1 to be resolved. The applicant's commitment to address the guidance in RG 1.132 regarding drilling and sampling during the COL stage is **COL Action Item 2.5.4-2.**

To determine the variation in shear modulus and material damping ratio with shearing strain amplitude, the applicant conducted cyclic testing of the ESP site soils. These dynamic properties are necessary to construct shear modulus and damping curves in order to determine the response of the site to the SSE ground motion. The applicant was unable to make a comparison between its cyclic test results for the ESP and CPS sites, since significant advances in resonant column/cyclic torsional shear tests have occurred since the licensee conducted cyclic tests on soils from the CPS site. Since the applicant conducted only six sets of resonant column/cyclic torsional shear tests, the applicant decided to use the EPRI shear modulus and damping curves (EPRI, 1993) for its site response analyses. The EPRI curves are based on a much larger cyclic testing data set than that gathered by the applicant for the ESP site. In RAI 2.5.4-2, the staff asked the applicant to justify its use of the EPRI curves and to further explain its basis for concluding that the ESP site soils are consistent with those used to develop the EPRI curves. In addition, the staff asked the applicant to explain why the material damping values from the ESP laboratory tests, shown in Figures 5-21 and 5-24 of SSAR Appendix A, are higher than the EPRI damping curves. In response to RAI 2.5.4-2, the applicant stated that the EPRI curves represent soils in the "general range of gravelly sands to low plasticity silty and sandy clays." The EPRI curves are based on a hyperbolic model of the nonlinear change in soil shear modulus and material damping with shearing strain. This model was developed in the late 1960s and early 1970s through laboratory testing programs and developed for use in generic site response studies in eastern North America. Subsequent to the development of the EPRI curves, the applicant stated that regression analyses of recorded ground motions "were conducted to confirm that use of the curves in site response analyses produces reasonable ground response predictions." The applicant stated that information in Section 5.2 of SSAR Appendix A indicates that soils at the ESP site fall within the range of gravelly sands to low-plasticity silty or sandy clays. In response to the staff's observation that the ESP laboratory testing data for hysteric damping appear to be relatively high at low strain compared to the generic data from the EPRI report, the applicant stated the following:

> The information in Figure 5-21 (SSAR Appendix A) does indeed suggest that the hysteric damping from the laboratory tests was higher than the EPRI curves.

The same conclusion can be made from the information in Figure 5-24. However, the curves that are above the EPRI damping curves are related to the resonant column tests. The fact that the resonant column data shown in Figures 5-21 and 5-24 are solid, bold lines masks the response from the torsional shear tests—suggesting that all the damping values are too high at low shearing strain amplitudes. However, material damping values from the torsional shear tests are consistent with the EPRI damping curves, as shown in Figures 4.2-2 through 4.2-6 of Appendix B to the EGC ESP SSAR.

The higher damping from the resonant column tests has been recognized for a number of years, and was noted in the EPRI (1993) set of reports. It is attributed to rate of loading effects. Typical frequencies of loading for the resonant column test range from 100 to 200 Hz for these soils. As the frequency increases from the torsional shear testing (frequencies of 0.1 to 10 Hz) to resonant column (frequencies of 100 to 200 Hz), the absolute value of damping increases by several percent. This trend is shown in Figures B.15, C.15, D.15, E.15, and G.15 of Attachment A-7 to the Appendix A report. The observed frequency effect on damping is the reason combined resonant column/torsional shear (RC/TS) tests are conducted. The frequency of loading for the torsional shear tests ranges from 0.1 to 10 Hz and therefore is much more consistent with predominant frequencies of earthquake loading.

In order to verify the applicant's classification of the ESP soils as "gravelly sands to low plasticity silty and sandy clays," the staff reviewed Section 5.2.2 of SSAR Appendix A. Section 5.2.2 provides a general description of each of the soil layers underlying the ESP site and includes information on plasticity, water content, and dry density. The staff concludes from its review that the applicant's characterization of the ESP site soils is appropriate. In addition, the staff concludes that the applicant's use of the EPRI curves is justified since these curves are based on a much larger database of properties from similar soils (gravelly sands) than those obtained by the applicant for the ESP site from its four soil borings. Although the fit between the EPRI curves and the resonant column tests on the ESP site soils is weak, the staff notes that the torsional shear test data do fit the EPRI curves. The frequency of loading for the torsional shear tests ranges from 0.1 to 10 Hz, which is consistent with the predominant frequencies of earthquake ground motion. Figure 2.5.4-6, which reproduces Figure 4.2-2 from

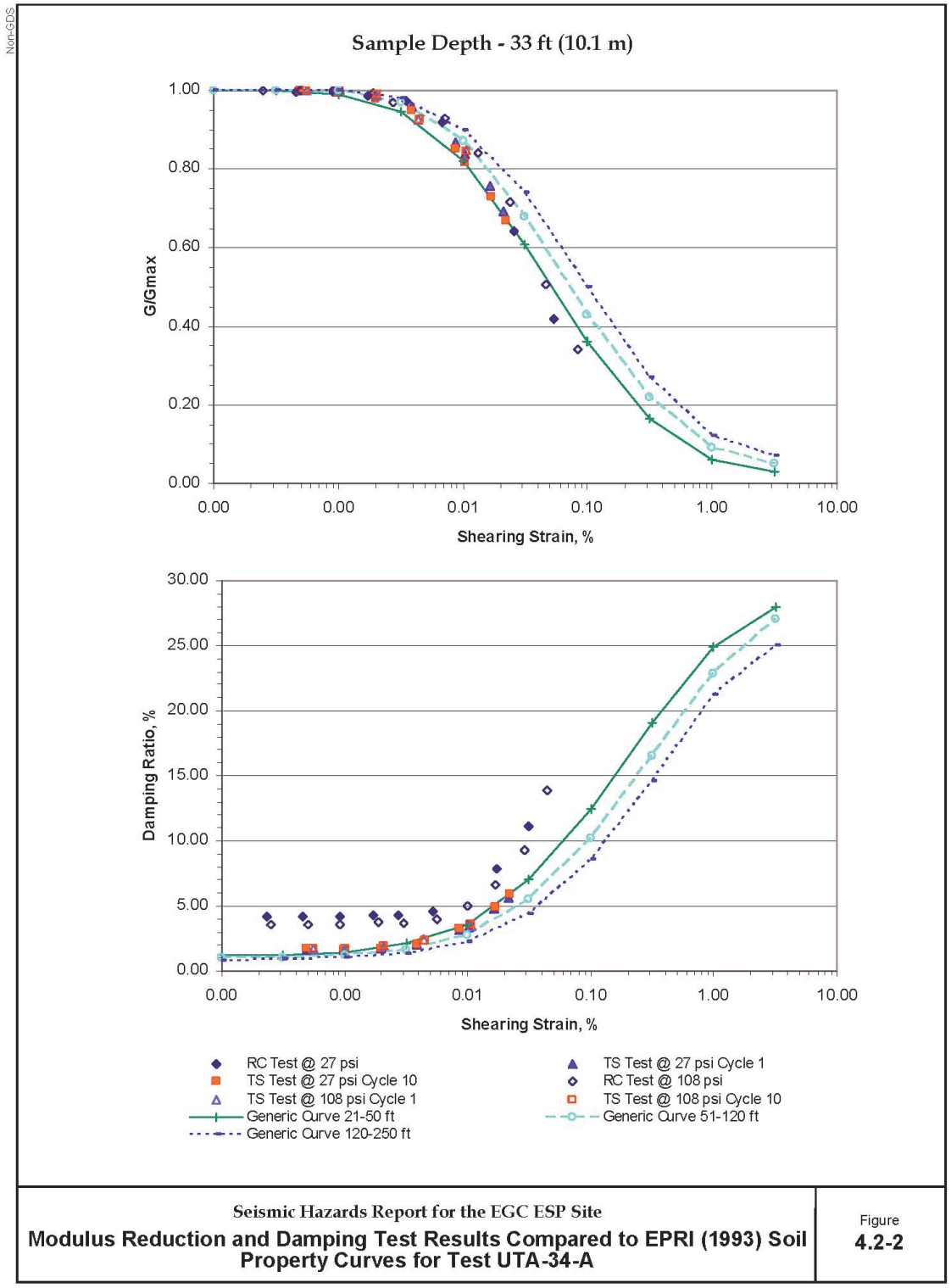

Figure 2.5.4-6 Modulus reduction and damping test results compared to EPRI (1993) soil property curves for test UTA-34-A

SSAR Appendix B, shows the fit between the ESP site data from the resonant column and torsional shear tests compared to the EPRI (1993) generic curves for gravelly sands to low-plasticity silty or sand clays.

Based on its review of the applicant's soil classifications and the fit between the ESP site soil torsional shear test data and the EPRI (1993) generic curves, described above, the staff concludes that the applicant's use of the EPRI shear modulus and damping curves is appropriate.

In addition to its field measurements (CPT and suspension logging) of the soil S-wave velocities, the applicant also made laboratory measurements of S-wave velocity using the six resonant column tests on ESP site samples taken over a range of depths. For the first four laboratory samples (from depths of 33, 41.5, 115, and 171 ft below the surface), the applicant's S-wave velocity results closely match the field suspension logging test results. As shown in Table 5-3 of SSAR Appendix A, the ratio of laboratory- to field-measured S-wave velocity is between 86 to 95 percent for each of these samples. For the deepest two soil samples at depths of 208 and 242 ft, the ratio decreased to 68 and 76 percent, respectively. Since the difference between S-wave velocities (field and laboratory) is caused primarily by sample disturbance associated with the laboratory testing process, the staff asked the applicant in RAI 2.5.4-5 to justify these low ratios. In response to RAI 2.5.4-5, the applicant stated that the low ratios are an indication of the accumulated disturbance that occurs to soil samples when they are removed from the ground, transported to the laboratory, set up in the laboratory, and tested in equipment that may not replicate the stress state and loading conditions in situ during a seismic event. For the soil sample with the lowest ratio (0.68), the applicant stated that this was an obviously disturbed sample as shown by its modulus and damping ratio curves, which are shown in Figures 5-20 and 5-21 in SSAR Appendix A (Sample E). For the deepest sample at 242 ft below the surface, the applicant attributed its low ratio (0.76) to the large, unavoidable stress relief as the applicant brought the sample to the surface. Since these two deeper soil samples showed evidence of disturbance, the applicant used only the shallower soil samples to determine the shear modulus and damping ratio to justify its use of the EPRI (1993) generic curves.

Since the applicant was able to use its shallower laboratory test results to show a fit to the EPRI (1993) generic shear modulus and damping ratio curves (see RAI 2.5.4-2 above), the staff concludes that the low laboratory- to field-measured S-wave velocity ratios are not significant. The applicant used the EPRI (1993) generic curves to determine the site response to the SSE ground motion.

The staff concludes, based on its review of SSAR Sections 2.5.4.2 and 2.5.4.3 and the applicant's responses to its RAIs and open item, that the applicant adequately determined the engineering properties of the soil and rock underlying the ESP site through its field and laboratory investigations. In addition, the applicant used the latest field and laboratory methods, in accordance with RGs 1.132 and 1.138, to determine these properties. The staff concludes that the applicant performed sufficient field investigation and laboratory testing to establish the similarity between the CPS and ESP sites and, as such, the overall subsurface profile as well as the material properties underlying the ESP site. The staff notes that in response to Open Item 2.5.4-1 the applicant committed to perform additional investigations (soil borings) once it has selected the building locations, as recommended in RG 1.132 (see Open

Item 2.5.4-1 above). The COL (or construction permit (CP)) applicant will need to describe these additional investigations in its COL (or CP) application. See COL Action Item 2.5.4-2.

2.5.4.3.3 Relationship of Foundations and Underlying Materials

Section 2.5.4.3 of RS-002 directs the staff to compare the applicant's plot plans and the profiles of all seismic Category I facilities with the subsurface profile and material properties. Based on this comparison, the staff can determine if (1) the applicant performed sufficient exploration of the subsurface and (2) the applicant's foundation design assumptions contain adequate margins of safety. The applicant decided to provide this information as part of its COL submittal. Submission of the applicant's plot plans and the profiles of all seismic Category I facilities for comparison with the subsurface profile and material properties is **COL Action Item 2.5.4-3.**

2.5.4.3.4 Geophysical Surveys

The staff focused its review of SSAR Section 2.5.4.3 on the adequacy of the applicant's geophysical investigations to determine the soil and rock dynamic properties. The applicant conducted four CPT soundings and, during two of the soundings, obtained S-wave velocity data. To measure the S-wave velocity of the soil, the applicant generated an S-wave at the ground surface by horizontally striking a board at the surface using a sledge hammer. The applicant measured the travel time of the resulting S-waves with a velocity-sensitive geophone located at the tip of the CPT assembly. In addition to the CPT soundings, the applicant also conducted P- and S-wave suspension logging tests in one of its four soil borings. The applicant performed the suspension logging test at approximately 1.5-ft depth intervals to within approximately 20 ft into the top of rock. In addition to these two seismic tests, the applicant also measured the S-wave velocity of the soil samples in the laboratory as part of its cyclic testing.

The staff reviewed the applicant's description of the suspension logging test and the CPT. In addition, the staff reviewed the applicant's test reports, prepared by its two contractors, in Attachments A-4 and A-5 to SSAR Appendix A. Attachment A-4 provides the details of the applicant's CPT soundings and includes a number of seismograms, which show the S-wave arrivals at the tip of the CPT assembly. In addition, the staff reviewed the applicant's computation of the S-wave velocities, which were based on S-wave travel times and the seismic receiver (geophone) depth. Attachment A-5 provides the details of the applicant's suspension logging tests and includes a few sample seismograms, a P- and S-wave velocity depth profile, and the measured P- and S-wave velocity values. For the 280 ft of soil, the S-wave velocity gradually increased from about 800 ft/s to nearly 3000 ft/s. The staff noted that there are fairly significant oscillations in the S-wave velocity profile with depth, which the applicant captured in its dynamic site response analyses (see Section 2.5.2.1.5 of this SER). The S-wave velocity results from the CPT soundings, which covered the upper soil layers to a depth of about 55 and 76 ft, are consistent with those from the suspension logging tests. In addition, the older CPS site S-wave velocity results are consistent with the ESP site results.

The staff has determined that the applicant used the latest geophysical and geotechnical measurement methods and equipment in accordance with the recommendations of RGs 1.132 and 1.138 to determine the dynamic properties of the soil and rock underlying the site. Based

on its review of SSAR Section 2.5.4.4, the staff concludes that the applicant adequately determined the soil and rock dynamic properties through its geophysical survey of the ESP site.

2.5.4.3.5 Excavation and Backfill

In SSAR Section 2.5.4.5, the applicant stated that the construction of the facilities at the ESP site would likely require excavations to a depth of approximately 55 to 60 ft below the ground surface to avoid potential settlement and liquefaction concerns. The applicant also described some of the licensee's findings during its excavations for the CPS site. The most important finding is that the licensee encountered some localized pockets of sand at the base of the excavation at a depth of 56 ft. The licensee either compacted these sand pockets or removed and replaced them with a flyash-backfill mixture.

Since the applicant has not selected a reactor design or location within the ESP site, it did not provide detailed excavation and backfill plans or plot plans and profiles as outlined in Section 2.5.4 of RS-002. Therefore, the staff could not adequately evaluate the applicant's excavation and backfill plans and will await future submittal of these plans as part of the COL or CP application. This is **COL Action Item 2.5.4-4**.

The applicant also included SSAR Sections 2.5.4.13 and 2.5.4.14 in its application. The ESP review standard RS-002 covers these two subsections under Section 2.5.4.5.

SSAR Section 2.5.4.13 states that the applicant will perform settlement analyses at the COL stage and will be able to use previous settlement measurements made by the licensee for the CPS plant structures. The applicant's assertion is based on the assumption of similar soil conditions between the two sites and that the new facilities will be similar in size, load, and foundation level to those constructed at the CPS site. The need for the COL or CP applicant to perform settlement analyses is covered below in SER Section 2.5.4.3.10.

SSAR Section 2.5.4.14 states that the applicant will map any future excavation associated with the construction of a new nuclear power plant to confirm that the soil types and consistency are in agreement with the conditions identified and interpreted from the ESP field explorations. The applicant stated that this field mapping will involve inspecting excavated slopes for the presence of previously unknown fault offsets. The applicant also committed to inform the NRC staff (1) if it encounters previously unknown geologic features that could represent a hazard to the plant and (2) when site excavations are open for examination and evaluation. These commitments comprise **COL Action Item 2.5.4-5.**

2.5.4.3.6 Ground Water Conditions

In SSAR Section 2.5.4.6, the applicant briefly described its installation of three piezometers during its ESP site exploration to obtain more specific information about ground water conditions at the ESP site. The applicant found that the static ground water table is approximately 30 ft below the ground surface and that the ground water conditions are similar at the ESP and CPS sites.

Since the applicant has not selected a reactor design or location within the ESP site, it did not provide an evaluation of ground water conditions as they affect foundation stability or detailed

dewatering plans as outlined in Section 2.5.4 of RS-002. Therefore, the staff could not evaluate the ground water conditions as they affect the loading and stability of foundation materials or the applicant's dewatering plans during construction as well as ground water control throughout the life of the plant. As such, the staff will await the future submittal of these evaluations and plans as part of the COL or CP application. The need to evaluate ground water conditions as they affect foundation stability or detailed dewatering plans is **COL Action Item 2.5.4-6.**

2.5.4.3.7 Response of Soil and Rock to Dynamic Loading

In SSAR Section 2.5.4.7, the applicant stated that it deferred the analyses of the SSI for the ESP site to the COL stage. Since the SSI analyses will depend on the geometry and weight of the selected power generating system and the ESP applicant has not selected a reactor design or location within the ESP site, it did not perform SSI analyses. The staff concurs with the applicant's decision to defer the SSI analyses to the COL stage; however, the staff expected to review the applicant's determination of the free-field site amplification response in SSAR Section 2.5.4.7. Instead of providing the ESP site free-field site amplification in SSAR Section 2.5.4.7, the applicant provided the site amplification in SSAR Section 2.5.2.5 and a description of the soil dynamic properties in SSAR Section 2.5.4.2. Section 2.5.2.3.5 of this SER contains the staff's evaluation of the applicant's site response analyses, and SER Section 2.5.4.3.2 provides the staff's evaluation of the ESP site dynamic soil properties.

2.5.4.3.8 Liquefaction Potential

In its review of SSAR Section 2.5.4.8, the staff evaluated the applicant's liquefaction analyses. The staff's review focused on the applicant's conclusion that, based on its liquefaction evaluations, liquefaction is not a design consideration for the ESP site. The applicant found that, above 60 ft below the ground surface, there are several soil layers for which the FOS against liquefaction is less than 1.1, indicating that these layers are susceptible to liquefaction. However, the applicant stated that "potentially liquefiable soils in the upper 60 ft at the EGC ESP Site will likely have to be removed to meet settlement requirements." The applicant stated that it would select fill material (heavily compacted granular fill) that is stronger than the removed soil, which would increase the FOS against liquefaction to be greater than 1.1.

Concerning the applicant's liquefaction analyses, the staff reviewed the empirical blowcount procedure used by the applicant, which is described in RG 1.198. The empirical method calculates an FOS based on the expected soil shearing resistance and the expected maximum seismically induced shearing stresses in a soil layer. In RAI 2.5.4-6, the staff asked the applicant to provide a sample liquefaction analysis from one of the four borehole locations and to clearly show how it determined the FOS for the different soil layers. In addition, the staff asked the applicant to describe the methods that it may use to mitigate the potential for liquefaction and to describe the extent of the liquefiable (noncohesive) soils over the ESP site area.

In response to RAI 2.5.4-6, the applicant provided a sample calculation for borehole B-1 at the 38.5-ft depth interval. In addition, the applicant described the methods (other than removal and replacement) that it may use to mitigate the potential for liquefaction. The four ground improvement methods described by the applicant are (1) use of vibro-densification methods, (2) use of stone columns, (3) use of in-place soil cement mixing, and (4) use of earthquake

drains. For each of these improvement methods, the applicant provided a brief description and an assurance that most of these methods have been tested in severe earthquakes and have successfully controlled the potential for and consequences of liquefaction. With regard to the third part of RAI 2.5.4-6, the applicant provided the following description of the extent of the noncohesive (silts and sands) soils over the ESP site area:

> The extent of the non-cohesive soils at the EGC ESP site is generally limited to outwash intervals in the Wisconsinan till, interglacial zone, and upper 15 feet of the Illinoian till. Interbedded silt and sand layers were encountered from 62 to 72 feet bgs [below ground surface] at Borehole B-2, sand was encountered from 43 to 60 feet bgs at Borehole B-3, and clayey sand was encountered from 49 to 59 feet bgs at Borehole B-4. Additional thinner layers of non-cohesive sands and silts were observed in shallower intervals in B-1 and B-2.

The applicant added that not all of these noncohesive soils are considered liquefiable for the design considerations.

The staff reviewed the sample liquefaction analysis provided by the applicant for borehole B-1 to verify that the applicant used the method recommended by RG 1.198 for determining the FOS against liquefaction. The applicant used the Youd (2001) procedure, which evaluates soil strength against liquefaction based on SPT blowcount values and the induced cyclic stresses based on earthquake PGA and magnitude values. The applicant evaluated three earthquakes with magnitudes of 5.5, 6.5, and 8.0 and a constant PGA of 0.3g for each earthquake. The applicant selected these three earthquake magnitudes based on its deaggregation of the PSHA results for the controlling earthquakes for the ESP site. The M 5.5 earthquake represents a local source mechanism, the M 6.5 earthquake represents an earthquake from the Wabash Valley source zone, and the M 8.0 earthquake represents an earthquake from the New Madrid seismic source zone. The applicant used a constant PGA value of 0.3g since this is the PPE value it selected for the ESP site. The peak acceleration value of 0.3g exceeds the peak acceleration value (at 100 Hz) of the ESP site SSE, which is 0.26g. For each of the three magnitudes, some of the soil layers had FOSs less than 1.1. The applicant also varied the peak acceleration values to determine the sensitivity of the calculated FOS to changes in magnitude and peak acceleration. The applicant found that a reduction in PGA from 0.35 to 0.25 increases the FOS by approximately 50 percent for each depth interval. Based on its review of the sample liquefaction analysis, the staff concludes that the applicant used the latest empirical method and adequately varied the significant soil and seismic input parameters in accordance with the guidance provided in RG 1.198. Therefore, the applicant's liquefaction analyses are acceptable.

In addition to the applicant's sample liquefaction analysis, the staff also reviewed the applicant's descriptions of potential soil improvement methods and its description of the extent of the potentially liquefiable soils over the ESP site. From the applicant's above description, the staff concludes that noncohesive soils are fairly extensive over the area of the ESP site.

Based on its review of SSAR Section 2.5.4.8 and the applicant's response to RAI 2.5.4-6, described above, the staff concludes that the applicant has employed an acceptable methodology to determine the liquefaction potential of the soil underlying the ESP site. Because portions of the upper 60 ft of soil are susceptible to liquefaction, the applicant stated

that these soils would be either removed or replaced or improved to reduce any liquefaction potential. This is **Permit Condition 6**.

2.5.4.3.9 Earthquake Design Basis

SSAR Section 2.5.4.9 describes the performance-based approach used by the applicant to determine the SSE. This approach is also described in SSAR Section 2.5.2.6 and in more detail in Section 4.3 of SSAR Appendix B. Section 2.5.2.3.6 of this SER provides the staff's evaluation of the SSE, including the performance-based approach.

2.5.4.3.10 Static Stability

SSAR Section 2.5.4.10 states that the applicant deferred the determination of static stability to the COL stage. The applicant stated that since it has not selected a nuclear power plant design, it did not estimate the bearing capacity, settlement, or lateral earth pressures for the ESP site. These analyses depend on factors such as building footprint size, depth of embedment, and effective weight. The applicant did establish an ESP site characteristic value for minimum static stability at 25 tsf. This value is based on the licensee's evaluation of static stability for the CPS site and the assumption that similar-sized structures will be built on the ESP site. Bearing capacities in the CPS USAR range from about 40 to 60 tsf.

In RAI 2.5.4-3, the staff asked the applicant to provide further detail regarding the criteria that it used to establish the minimum static bearing capacity of 25 tsf for the ESP site. In response to RAI 2.5.4-3, the applicant stated that the methods used by the licensee for the calculation of the bearing capacities were conventional methods that assume a local shear failure condition. The range in bearing capacity values for the Category I structures at the CPS site range from 39.9 to 60.6 tsf and correspond to CPS building foundation elevations ranging from 35 to 40 ft below the ground surface. The applicant stated that during the construction of the CPS facility, the soil was excavated to a depth of approximately 55 ft below the ground surface to remove soils that could be compressible. The licensee then placed approximately 20 ft of highly compacted granular backfill between the base of the excavation and the foundation level for the CPS facility foundations. The values given by the licensee for the bearing capacity represent, therefore, a condition in which the foundations were placed on approximately 20 ft of highly compacted granular fill over the highly overconsolidated Illinoian till soil unit. The applicant stated that the combination of depth below the ground surface and the heavily overconsolidated state of the Illinoian till results in the high bearing capacities given in the CPS USAR. Comparing the minimum bearing capacity value chosen by the applicant (25 tsf) with the lower value in the range of bearing capacities for the CPS site (39.9) provides an FOS greater than 1.5.

Since, as the applicant points out, the minimum bearing capacity value established by the applicant provides an FOS greater than 1.5 compared to the minimum calculated bearing capacity for the CPS Category I structures, the staff finds that this value is appropriate as a PPE for the ESP site. This finding is based on the applicant's commitment to excavate approximately 55 ft below the ground surface and to backfill with highly compacted granular fill. In addition, the average undrained shear strength of the Illinoian till must be similar to that underlying the CPS site. The applicant stated that the actual foundation depth, size, and shape, structure locations, and settlement limits "will be considered to confirm the final ultimate

bearing capacity at COL." The need for the COL or CP applicant to perform a complete static stability assessment (including bearing capacities, settlement analyses, and lateral load assessment) and to ensure that the bearing capacities meet the minimum value of 25 tsf comprises **COL Action Item 2.5.4-7.**

2.5.4.3.11 Design Criteria

SSAR Section 2.5.4.11 states that the design criteria for the ESP site Category I structures will be established during the COL stage. Since the applicant has not selected a reactor design or location within the ESP site, its deferral of a description of the design criteria to the COL stage is acceptable to the staff. The need for the COL or CP applicant to describe the design criteria and methods, including the FOSs from the design analyses, is **COL Action Item 2.5.4-8.**

2.5.4.3.12 Techniques to Improve Subsurface Conditions

SSAR Section 2.5.4.12 states that until the power generating system is selected, the need for ground improvement for the ESP site is unknown. The applicant stated that structures that are founded at depths of 55 ft or above could require ground improvement, and that "decisions regarding the need for and type of ground improvement will be made during the COL stage." Based on the applicant's liquefaction analyses, which showed that portions of the upper 60 ft of soil are susceptible to liquefaction (FOS $\leq$ 1.1), the staff considers the improvement (i.e., removal and replacement or compaction) of the upper 55 ft of soil beneath the ESP site to be necessary. The improvement of the upper soil layers beneath the site will also be necessary to ensure that the minimum bearing capacity value of 25 tsf is met. In addition, the licensee encountered localized pockets of loose granular material at the base of the excavations for the CPS Category I structures during construction at the CPS site. The licensee either compacted these loose granular pockets of soil or removed and replaced them with backfill material. The need to employ ground improvement for the ESP site is also discussed above in conjunction with Permit Condition 6.

2.5.4.4 Conclusions

Based on its review of SSAR Section 2.5.4 and the applicant's responses to the associated RAIs and open item, the staff concludes that the applicant has adequately determined the engineering properties of the soil and rock underlying the ESP site through its field and laboratory investigations. In addition, the applicant used the latest field and laboratory methods, in accordance with RGs 1.132, 1.138, and 1.198, to determine these properties. Accordingly, the staff concludes that the applicant performed sufficient field investigations and laboratory testing to determine the overall subsurface profile, the properties of the soil and rock underlying the site, and the similarity between the CPS and ESP subsurface profiles and properties. Specifically, the staff concludes that the applicant adequately determined (1) the soil and rock dynamic properties through its field investigations and laboratory tests and (2) the liquefaction potential of the soils. The applicant covered the response of the soil and rock to dynamic loading in SSAR Section 2.5.2.

In SSAR Sections 2.5.4.5, 2.5.4.6, 2.5.4.10, 2.5.4.11, and 2.5.4.12, the applicant did not provide sufficient information for the staff to perform a complete evaluation. In addition, the applicant did not provide any information on the relationship of the foundation and underlying

materials (Section 2.5.4.3 in RS-002). The staff reviewed SSAR Sections 2.5.4.13 and 2.5.4.14 as part of its review of SSAR Section 2.5.4.5. Each of these topics depends on specific information related to building location and design and will be needed as part of any COL or CP application.

In SSAR Table 1.4-1, the applicant identified three subsurface material properties as ESP site characteristic values. The first site characteristic specifies that there is no liquefaction below 60 ft below the ground surface. The applicant demonstrated, in SSAR Section 2.5.4.8, that any liquefaction at the ESP site would be limited to the upper 60 ft of soil. SSAR Table 1.4-1 states that "soils above 60 ft bgs to be replaced or improved"; however, in SSAR Section 2.5.4.12 the applicant stated, "decisions regarding the need for and type of ground improvement will be made during the COL stage." An unequivocal commitment by the applicant to improve or replace and remove the soils above 60 ft below the ground surface is Permit Condition 6. The second site characteristic value specifies a minimum bearing capacity of 25 tsf. This value is based on the CPS site soil properties and not the ESP site properties, since the applicant deferred the determination of bearing capacity values to the COL stage. Finally, the third design parameter specifies minimum S-wave velocities for the three depth intervals 0–50 ft, 50–285 ft, and 285–310 ft as 820 ft/s, 1090 ft/s, and 2580 ft/s, respectively. These S-wave velocity values are based on the applicant's field geophysical surveys. The staff has reviewed the applicant's suggested site characteristics related to SSAR Section 2.5.4 for inclusion in an ESP, should the NRC issue one to the applicant. For the reasons set forth above, the staff agrees with the applicant's site characteristics and the values for those characteristics.

2.5.5 Stability of Slopes

SSAR Section 2.5.5 describes the applicant's plans for future slope stability analyses. The applicant did not carry out slope stability analyses for the ESP application.

2.5.5.1 Technical Information in the Application

The applicant stated that it did not perform a slope stability analysis for the ESP site application. If a new intake structure into Clinton Lake is required for a future design, the applicant stated that it would perform an additional assessment of the slope stability at the point of entry into the lake. The applicant further stated that the slopes for the existing CPS Unit 2 facility are approximately 30 ft deep and are located over 500 ft from the ESP site, and therefore do not pose a hazard. In addition to slopes associated with the potential future intake structure, the applicant stated that it will analyze the slopes associated with the construction of the power block or the outfall at the COL stage. Currently, the foundation depth of the new generating system is unknown, and the applicant stated that these depths are necessary to assess the potential height of slopes required for construction.

The applicant stated that the starting point for future slope stability analyses will be the information in the CPS USAR. The applicant stated that the licensee performed an extensive evaluation of slope stability during design work for the CPS site. The licensee evaluated the stability of the slopes associated with the Clinton Lake main dam and the CPS UHS under both static and dynamic loading conditions. However, since the Clinton Lake dam is not considered a Category I structure, the licensee only evaluated the CPS UHS for the SSE ground motion. The applicant concluded from its review of the CPS USAR that potential future issues

associated with slope stability will not result in any unusual construction requirements or constraints.

2.5.5.2 Regulatory Evaluation

SSAR Section 2.5.5 states that the applicant did not perform a slope stability analysis for the ESP site application. As such, the applicant did not list any regulatory guidance or cite any regulations as applicable to SSAR Section 2.5.5.

2.5.5.3 Technical Evaluation

In SSAR Section 2.5.5, the applicant provided a general description of its plan for future slope stability analyses at the COL stage. Although the general description was useful to the staff in performing a complete review, the COL or CP applicant will need to provide detailed slope stability analyses. This is **COL Action Item 2.5.5-1**.

2.5.5.4 Conclusions

SSAR Section 2.5.5 states that the applicant will provide slope stability analyses at the COL stage. As such, at this time the staff is unable to reach any conclusions regarding the stability of slopes that have not been designed or constructed.

2.5.6 Embankments and Dams

SSAR Section 2.5.6 describes the applicant's assessment of (1) the Clinton Lake main dam and the CPS UHS as they relate to a potential future nuclear facility on the ESP site and (2) the potential for seismically induced floods and water waves.

2.5.6.1 Technical Information in the Application

2.5.6.1.1 Design of Main Dam and CPS Ultimate Heat Sink

SSAR Section 2.5.6.1, "Design of Main Dam and CPS UHS," states that there are no plans to modify or rely on the Clinton Lake main dam for emergency cooling water for potential future nuclear facilities on the ESP site. The applicant stated that the ESP facility will use cooling towers for cooling, with Clinton Lake being used to provide makeup water to the cooling towers. Since the ESP facility will use the CPS UHS to supply makeup water to the cooling towers, the applicant stated that it would perform evaluations (if appropriate) at the COL stage to assess the performance of the submerged dam forming the UHS under the ESP SSE ground motion. The applicant stated that the starting point for its COL assessment of the CPS UHS will be the CPS USAR. SSAR Section 2.4.8, "Cooling Water Canals and Reservoirs," provides the main description of the applicant's plans to use the CPS UHS to supply shutdown cooling water for the existing CPS facility as well as makeup water to the ESP facility cooling towers.

2.5.6.1.2 Seismically Induced Floods and Water Waves

SSAR Section 2.5.6.2, "Seismically Induced Floods and Water Waves," describes the potential for seismically induced floods and water waves. Since there are no dams located upstream of

the ESP site and no large water-retaining structures in proximity to the existing facilities, the applicant stated that the potential for seismically induced floods and water waves at the ESP site is negligible. In addition, the applicant stated that the potential for flooding from a seiche is also negligible because of the configuration of Clinton Lake and the relative elevation difference between the lake and the plant site grade. The ground surface at the ESP site is at an approximate elevation of 730 ft msl. In contrast, Clinton Lake is at an elevation of approximately 690 ft. In addition, the ESP site is also about 800 ft from the shoreline of Clinton Lake. The applicant stated that any seiche caused by an SSE would be too small to reach the ESP site because of the distance (800 ft) and the height difference (40 ft). SSAR Section 2.4.5, "Probable Maximum Surge and Seiche Flooding," provides additional discussion of the maximum surge and seiche flooding.

2.5.6.2 Regulatory Evaluation

The applicant did not state which regulations SSAR Section 2.5.6 addressed; however, in response to RAI 1.5-1, the applicant stated that it complied with all of the regulations listed in RS-002. RS-002 does not contain a specific section on embankments and dams; however, these topics are covered in RS-002 Sections 2.4.4 and 2.5.5. In SSAR Table 1.5-1, the applicant stated that it used RG 1.70 for general guidance on format and content. Section 2.5.6 of RG 1.70 describes the necessary information and analysis related to the investigation, engineering design, proposed construction, and performance of all embankments used for plant flood protection or for impounding cooling water.

Since the applicant decided to defer the analyses of dam failure and slope stability until the COL stage, the staff did not evaluate the regulatory compliance of SER Section 2.5.6. SER Section 2.4.5 presents the staff's regulatory evaluation concerning the potential for seiche flooding.

2.5.6.3 Technical Evaluation

SSAR Section 2.5.6 states that the ESP facility will use cooling towers for cooling, with Clinton Lake being used to provide makeup water to the cooling towers. Since the ESP facility will use the CPS UHS to supply makeup water to the cooling towers, the applicant stated that it would perform evaluations (if appropriate) at the COL stage to assess the performance of the submerged dam forming the UHS under the ESP SSE ground motion. The applicant's decision to delay this evaluation until the COL stage is acceptable to the staff. This is **COL Action Item 2.5.6-1**.

Concerning seismically induced floods and water waves, SSAR Section 2.5.6 states that since there are no dams located upstream of the ESP site and no large water-retaining structures in proximity to the existing facilities, the potential for seismically induced floods and water waves at the ESP site is negligible. In addition, the applicant stated that the potential for flooding from a seiche is also negligible because of the configuration of Clinton Lake and the relative elevation difference between the lake and the plant site grade. Since the ground surface at the ESP site is approximately 40 ft higher than Clinton Lake and about 800 ft from the shoreline of Clinton Lake, the staff concurs with the applicant's conclusion that any seiche caused by an SSE would be too small to reach the ESP site. SER Section 2.4.5 provides additional evaluation of the potential for seiche flooding.

2.5.6.4 Conclusions

Sections 2.4.4, 2.4.5, and 2.5.5 of this SER present the staff's conclusions regarding dam failures, seiche flooding, and slope stability, respectively.